CA1
DTC 801
86
D27
c.2

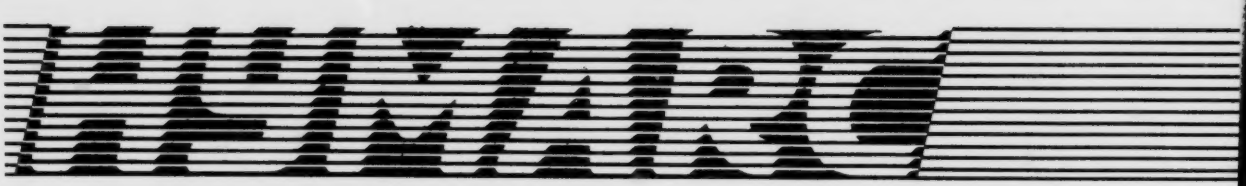

Library and Information Centre / Centre de documentation (GSLA)
RECU LE
JUL 18 1986
Transport Canada

TP 7653E

DEVELOPMENT & TESTING OF A COMPUTER SIMULATION OF CRANE DYNAMIC LOADING WITH MOTION COMPENSATION FOR AT-SEA LIFTING OPERATIONS

Prepared for:
Transportation Development Centre,
Transport Canada.

by
Mr. Andrew J. Fraser
Mr. Alex F. Tulai
HYMARC Engineering Ltd., Ottawa, Canada.

15 April 1986

DISCLAIMER

The contents of this report reflect the views of A.J. Fraser and A.F. Tulai, HYMARC Engineering Ltd., and not necessarily the official view or opinions of the Transportation Development Centre of Transport Canada.

Un sommaire en français de ce rapport est inclus avant la Table des matières.

PROJECT TEAM

Mr. Andrew J. Fraser, P.Eng., M.A.Sc.

Mr. Alex F. Tulai, B.Sc.

HYMARC Engineering Ltd.
P.O. Box 5127, Station F,
OTTAWA, Ontario.
K2C 3H4

Office: 66 Colonnade Road,
Nepean, Ontario.
K2E 7K7

(This page intentionally left blank.)

Transport Canada / Transports Canada
Development / Développement

REPORT DOCUMENTATION FORM

1. Transport Canada Report No.	2. TDC Project No.	3. Recipient's Catalogue No.
TP 7653E	6423	

4. Title and Subtitle
Development & Testing of Computer Simulation of Crane Dynamic Loading With Motion Compensation for At-Sea Lifting Operations

5. Report Date
15 April 1986

6. Performing Organization Report No.
8425-R2

7. Author(s)
A.J. Fraser; A.F. Tulai

8. Transport Canada File No.
D1460-223

9. Performing Organization Name and Address
Hymarc Engineering Ltd
P.O. Box 5127, Station F
Ottawa, Ontario K2C 3H4

10. DSS File No.
14SD.T8200-4-4587

11. DSS or Transport Canada Contract No.
1SD85-00026

12. Sponsoring Agency Name and Address
Transportation Development Centre (TDC)
200 Dorchester Blvd. West
West Tower, 6th floor
Montreal, Quebec H2Z 1X4

13. Type of Report and Period Covered
Final Report

14. Sponsoring Agency Code

15. Supplementary Notes

16. TDC Project Officer
C.A. Versailles

17. Abstract

The development and application of a computer program which simulates at-sea lifting operations in real time is described. The program allows the user to select a sea state and use response amplitude operators either from the program library, or of his own choosing, to model vessel response. Crane component characteristics are also specified by the user. A human operator controlling the winch is modelled, mathematically allowing the user to examine dynamic load magnification induced by the operator, in addition to that caused by vessel motions.

Several motion compensating control algorithms are tested and the operator's performance with and without compensation is analyzed.

18. Key Words
Cranes, At sea, Lifting, Motion compensation, Operator performance, Computer Simulation, Ship, Marine.

19. Distribution Statement
Limited number of copies available on request from the Transportation Development Centre

20. Security Classification (of this report)	21. Security Classification (of this page)	22. No. of Pages	23. Price
unclassified	Unclassified	193	-

Canada

Transports Canada / Transport Canada

Développement / Development

FORMULE DOCUMENTAIRE DU RAPPORT

1. N° du rapport Transports Canada	2. N° de l'étude — CDT	3. N° de catalogue du destinataire
TP7653E	6423	

4. Titre et sous-titre	5. Date du rapport
Development & Testing of Computer Simulation of Crane Dynamic Loading with Motion Compensation for At-Sea Lifting Operations	Le 15 avril 1986
	6. N° du rapport de l'organisme exécutant: 8425-R2
7. Auteur(s): A.J. Fraser; A.F. Tulai	8. N° de dossier Transports Canada: D1460-223
9. Nom et adresse de l'organisme exécutant: Hymarc Engineering Ltd, P.B. 5127, Succursale F, Ottawa, Ontario K2C 3H4	10. N° de dossier — ASC: 14SD.T8200-4-4587
	11. N° de contrat — ASC ou Transports Canada: 1SD85-00026
12. Nom et adresse de l'organisme parrain: Centre de développement des transports (CDT), 200 boul. Dorchester ouest, Tour ouest, 6ième étage, Montréal, Québec H2Z 1X4	13. Genre de rapport et période visée: Final
	14. Code de l'organisme parrain:
15. Remarques additionnelles:	16. Agent de projet — CDT: C.A. Versailles

17. Résumé

Ce rapport rend compte de la recherche sur un programme informatique permettant de simuler en temps réel les opérations de manutention en mer. Ce programme permet à l'utilisateur de figurer le comportement du navire porte-grue en fonction d'un état de mer donné et d'une gamme de temps de réaction qu'il pourra choisir dans une programmathèque, ou qu'il a établis d'après ses besoins particuliers. L'utilisateur pourra également préciser les caractéristiques mécaniques de la grue. Par la simulation des commandes, il pourra en outre, déterminer l'amplitude des charges dynamiques dues aux manoeuvres du grutier qui s'ajoutent aux charges attribuables aux mouvements oscillatoires du navire.

Un certain nombre d'algorithmes sur la compensation de ces mouvements ont été éprouvés, ainsi que le rendement du grutier avec et sans compensation automatique des commandes.

18. Mots-clés	19. Diffusion
Grues, manutention en mer, compensation, mouvements, rendement, grutier, simulation, navire, marine.	Le CDT dispose d'un nombre limité d'exemplaires.

20. Classification de sécurité (de ce rapport)	21. Classification de sécurité (de cette page)	22. Nombre de pages	23. Prix
non-classifié	non-classifiée	193	-

CDT/TDC 79-005 Rev 86

Canada

ACKNOWLEDGEMENTS

The authors wish to thank the Departments of Transport, Fisheries and Oceans, National Defence and Supply and Services whose support through the Unsolicited Proposal Fund, made this project possible.

(This page intentionally left blank.)

SUMMARY

Cranes find extensive application in the marine environment not just in the transfer of loads between vessels, or from vessels to platforms, but also for the overboarding and retrieving of buoys, towed arrays, and submersibles. The motions of these vessels or objects involved in at-sea lifting (or towing) operations, substantially alter the crane loading when compared with similar land-based lifts. Operator effectiveness is reduced and both efficiency and safety decline, leading to accidents with consequent material damage, personal injury, and sometimes death.

A computer program has been developed to permit the real-time simulation of lifting operations. It allows the user to model various sea states, to compute the response of two vessels as a function of sea state, to model a typical crane and its machinery, and to model a human operator engaged in lifting operations.

The program was used to measure the performance that could be expected of an operator over a range of sea states and loads. Results showed that as the operator attempts to maintain either constant load height or constant closure rate between the load and the deck onto which it is to be placed, he induces a dynamic load in the crane components. His performance was also found to deteriorate under conditions of a low natural frequency of the load and cable combination.

As a means of improving the performance of an operator, compensating the load height for the vessel's motions was considered. First, adjusting cable length in response to the vertical position of the crane-carrying vessel was modelled. Without operator input, the load ideally appears fixed in space, making the operator's task similar to lifting with a platform mounted crane.

Second, cable length was further modified to take account of the motions of the second vessel. By compensating in this way for the relative motion between vessels, the load appears at a fixed height above the second vessel, subject of course to machinery lags and limitations.

Both algorithms offered significant improvement in lifting performance. Operator activity or workload was reduced, induced dynamic loads decreased, and tracking errors were smaller.

Compensation also extended the performance capability of the system studied into higher sea states by imposing corrections without the time delay or lag associated with a human operator.

The program also models the pendulous action of the load in the horizontal plane. Compensation was not attempted in the horizontal plane but the simulation may be used to design and/or evaluate load stabilizing concepts, an example of which is a tag-line system.

SOMMAIRE

Les grues flottantes ou de bord servent non seulement aux opérations de transbordement ou de chargement/déchargement de navires, mais aussi pour la mise à l'eau ou hors eau des bouées, réseaux sonar remorqués et autres objets flottants ou submersibles, Or, les mouvements oscillatoires du navire porte-grue ou des objets devant être manutentionnés peuvent être tels que les caractéristiques de charge de la grue en sont considérablement altérées, par rapport à une manutention faite à partir d'une base stable. De plus, l'efficacité du grutier baisse, tandis que diminue le niveau de la sécurité dont les conséquences prévisibles sont les dommages matériels et corporels, voire des accidents mortels.

Dans le but de représenter en temps réel les opérations de manutention dans le cas des grues flottantes ou de bord, un programme informatique a été élaboré; il permet les simulations suivantes: états de mer, réaction de deux navires en fonction des états de mer, contraintes sur une grue type et ses organes et, enfin, commandes du grutier lui-même.

Ce programme a servi à chiffrer les rendements pouvant être attendus d'un grutier, en fonction de la charge et de l'état de mer. La simulation a montré que la manoeuvre fait naître dans la grue et ses organes des charges dynamiques supplémentaires, quelle que soit la technique adoptée par le grutier: hauteur de charge constante ou vitesse d'approche constante. Elle a aussi montré que le rendement du grutier se détériorait dans le cas d'ensembles câble-charge ayant une basse fréquence naturelle de vibration.

Un des moyens possibles de relever ce rendement est de régler automatiquement la hauteur de la charge suivant les mouvements oscillatoires du navire porte-grue. Pour cela, il a fallu modéliser les variations dans la longueur du câble en fonction de ces mouvements, de manière que la charge demeure théoriquement fixe par rapport à l'horizon, tant que le grutier n'aurait pas manoeuvré. Tout se passerait comme si la manutention se faisait avec un appareil sur plate-forme fixe.

Ensuite, on a voulu modéliser les variations dans la longueur du câble en fonction des mouvements oscillatoires de l'autre navire, celui vers ou depuis lequel la manutention se fait. Par compensation des mouvements relatifs des deux navires, on obtient que la charge paraisse aux yeux du grutier comme si elle se trouvait à hauteur fixe par rapport au point de chute ou de prise, sous réserve des temps de réaction inévitables.

Ces deux modèles ont permis d'améliorer sensiblement les rendements: la tension sur la grutier diminuée, charges dynamiques réduites et erreurs d'alignement amenuisées.

Il est également apparu que la compensation permet de poursuivre les manutentions par états de mer plus agités, du fait que le programme informatique permet de rattraper les retards et les décalages dans le temps inhérents à la lenteur relative des réactions du grutier.

Ce programme informatique permet aussi de figurer les balancements de la charge, mais non de les compenser. La simulation a néanmoins permis d'étudier et d'évaluer diverses techniques de stabilisation de la charge, comme, par exemple, l'utilisation de câbles de manoeuvre.

TABLE OF CONTENTS

		PAGE
1.0	INTRODUCTION	1
2.0	MODEL OVERVIEW	4
3.0	PROGRAM ORGANIZATION	7
4.0	DIGITAL MODULES	11
	4.1 Sea Model	11
	4.1.1 Background	11
	4.1.2 Sea Model Digital Implementation	14
	4.2 The Axes System	22
	4.3 Axes Transformations	29
	4.4 Moment Calculations	31
	4.5 RAO Method	34
5.0	ANALOG MODULES	36
	5.1 Crane Boom Model	36
	5.2 Crane Cable and Load Model	41
	5.2.1 Vertical Dynamics	41
	5.2.2 Pendulous Motion	45
	5.3 Human Operator	49
	5.3.1 Background	49
	5.4 Winch Model	58
6.0	EVALUATION	60
	6.1 Input Data	60
	6.1.1 Sea State	60
	6.1.2 Response Amplitude Operators	67
	6.1.3 Crane Data	71
	6.1.4 Vessel 2	78
	6.1.5 Human Operator	84
	6.1.6 Compensation	86
	6.2 Performance Evaluation Results	90
	6.2.1 Position Control Performance	90
	6.2.2 Rate Control Performance	103
	6.2.3 Roll Compensation Performance	108
7.0	CONCLUSIONS	114

TABLE OF CONTENTS

	PAGE
REFERENCES	117
BIBLIOGRAPHY - With Brief Abstracts	118
APPENDIX A - Analog Diagrams	
APPENDIX B - Program Listings	

VARIABLE DEFINITION LIST

COMPUTER VARIABLE	VARIABLE NAME	UNITS	DESCRIPTION
RVGAMA	γ	rad	angle between wave direction and ship direction
RVA	**A**	-	matrix of Euler transformation elements
RVCT(j)	${}_cT(j)$	m	rigid boom tip coordinate for j^{th} axis in C-frame
RVOT(j)	${}_oT(j)$	m	rigid boom tip coordinate for j^{th} axis in o-frame
RVDER(i)	$\frac{d}{dt}\,{}_oG(i)$	m/s or rad/s	first derivative of the vessel's motion in the i^{th} degree of freedom
RVADER(i)	$\frac{d}{dt}[\mathbf{A}]$		first derivative of the Eulerian transformation matrix
RVOTV(j)	${}_oT_v(j)$	m/s	speed of rigid boom tip in j^{th} direction of o-frame
RVTIME	t	s	current time
RV0D2(j)	${}_oD_2(j)$	m	Deck 2 coordinate for j^{th} axis in o-frame
RVOD2V(j)	${}_oD_{2v}(j)$	m/s	speed of Deck 2 in j^{th} direction of o-frame
RVFSC	F_{SC}	N	cable tension
RVFSCX	F_{SCX}	N	X- component of cable tension
RVFSCY	F_{SCY}	N	Y- component of cable tension
RVFSCZ	F_{SCZ}	N	Z- component of cable tension
RVTLX	$T_{LX}, \Delta x$	m	load displacement in x-direction from rigid boom tip
RVTLY	$T_{LY}, \Delta y$	m	load displacement in y-direction from rigid boom tip
RVSC	S_C	m	cable length
RVSCV	$\dot{S}_C$	m/s	cable winching rate
RVPC	P_C	W	winching power
RVEH	e_H	m	height error - error between load height above deck 2 and set point height
RVEH2	e_H^2	m^2	square of height error
RVEHS	e_H^*	m	disturbance height error -departure of height of rigid boom tip above Deck 2 from 'at-rest' value
RVEHS2	e_H^{*2}	m^2	square of disturbance height error

COMPUTER VARIABLE	VARIABLE NAME	UNITS	DESCRIPTION
RVEV	e_V	m/s	closing rate error - error between rigid boom tip to Deck 2 closing rate and set point closing rate
RVEV2	e_V^2	m^2/s^2	square of closing rate error
RVEVS	e_V^*	m/s	disturbance closing rate - closing rate between rigid boom tip and Deck 2
RVEVS2	e_V^{*2}	m^2/s^2	square of disturbance closing rate
RVEVXS	e_{VX}^*	m/s	x- direction disturbance error -departure of rigid boom tip to Deck 2 x-distance from nominal
RVEVYS	e_{VY}^*	m/s	y- direction disturbance error -departure of rigid boom tip to Deck 2 y-distance from nominal
RVMRO	M_{RO}	Nm	crane rolling moment
RVMOT	M_{OT}	Nm	crane overturning moment
RVMSL	M_{SL}	Nm	crane slewing moment
RVQH(i)	$Q^{H(i)}$	m	motion of vessel 2 in its i^{th} degree of freedom
RVTPC(1)	r	m	extended boom length
RVTPC(2)	α	rad	boom elevation - negative above the horizon
RVTPC(3)	β	rad	boom slewing angle or azimuth - 0 in forward direction, positive clockwise
RVOD1(j)	${}_oD_1(j)$	m	load deck coordinate for j^{th} axis in 0-frame on vessel 1
RVOD1V(j)	${}_oD_{1V}(j)$	m/s	speed of load deck on vessel 1 in j^{th} direction of o-frame
RVOQ(j)	${}_oQ(j)$	m	vessel 2 mean C of G coordinate for j^{th} axis in 0-frame
RVV2	V_2	m/s	speed of vessel 2
RVV1	V_1	m/s	speed of vessel 1
RVV	V_1 or V_2	m/s	vessel speed
RVH	ζ	m	significant wave height
RVDTIM	Δt	s	elapsed time between calls
RVOLL3	${}_oL_L(3)$	m	load coordinate for Z-axis in o-frame
RVBUMP			load and Deck 2 contact signal
RVWH	h	m	wave amplitude

1.0 INTRODUCTION

The overboarding and retrieving of buoys, towed arrays, and submersibles, or the transfer of loads between vessels in other than calm seas presents a very complex problem of two major aspects. The first of these is operator control, and the second is the dynamic loading and performance requirements of the lifting system components.

During land-based operations, a crane operator does not begin lifting until the lifting line is directly over the load. The load is then picked up gradually, resulting in near-static loading conditions on the crane. Lifting speeds are dictated by efficiency and available power, rather than any special dynamic requirements. Likewise, when placing a load, the load is first positioned over the desired spot before lowering begins. As the contact distance decreases, speed is reduced, giving a smooth deceleration and hopefully, a gentle stop.

In the case of a load transfer at sea, however, the crane operator may have to devote considerable effort to positioning the lifting line over the load, as both the mother ship (or vessel upon which the crane is mounted), and the tender (the vessel with the load), may not be able to maintain stations very accurately, depending on sea state, vessel motion characteristics, and forward speed. When a load is being transferred from the tender to the mother ship, a very abrupt load pickup may occur once the line is secured to the load if the tender should drop away suddenly. After the load becomes suspended, it must be lifted away from the tender at a speed that ensures the tender cannot be driven up into the load by the next wave, thus dictating minimum crane performance requirements. Should the mother ship be heaved upward by the seas, the loading on the crane would be greater than the static loading by a factor equal to its vertical acceleration. Off lead-line pulls, resulting from deviations in station keeping, can produce substantial lateral loading on the crane structure, and the pendulous action of the load as it leaves the tender can pose a serious hazard to both tender and crew.

Numerous accidents, some involving fatalities, have resulted both from the overloading of cranes and from improper lifting of loads under difficult conditions (Ref. 1). Guidelines have been established (Ref. 2) for derating cranes as a function of sea state for oil rig installations. Additional research has proven the need to account for the dynamic response of the crane components themselves in platform installations. These analyses are restricted in their applicability to fixed-base cranes as they do not provide for the motion of the crane-carrying vessel. To date, little work has been done to address the problem of derating cranes, or establishing their

minimum performance requirements in situations where both the vessel carrying the crane and the vessel with the load are moving independently of each other. Cases involving the lifting of buoys, towed arrays, and submersibles are extensions of the preceding example wherein the 'load' has its own sea-keeping characteristics as a vessel prior to its being lifted by the mother ship.

Even less work has been done to date in establishing how the crane operator performs in the 3-dimensional tracking problem with which he is faced. To place a load on a second vessel, the operator must first position the load over the desired spot in spite of fore and aft, and sideways relative ship motions. A pendulating load may further complicate this problem. He must also control the height of the load above the second vessel or the rate of closure between the load and tender as both vessels heave out of phase with each other, while judging the moment to lower the load so as to minimize vertical impact speed and lateral sliding-contact speed. All this must be accomplished without inducing excessive dynamic loading or exceeding the structural or power limitations of the crane.

This project was undertaken for the purpose of developing a computer simulation that would allow the modelling of an irregular sea, the vessel response characteristics of two vessels engaged in at-sea lifting operations, a typical crane and its machinery, and a human operator.

It was hypothesized that crane operations would benefit by the addition of a motion compensating system capable of damping out motions of the vessel upon which the crane was mounted. This compensation would lower the dynamic loading on the crane, thus reducing structural stresses and power requirements, and allowing greater loads to be carried in a given sea state. In addition, the hook or sling would appear to the operator to be 'fixed' in space, allowing him to concentrate on correcting for the motions of the tender only. This simplification of the operator's tracking task should improve both the safety and the efficiency of crane operations.

It was further hypothesized that a second level of compensation to remove the relative motion of the tender would offer even greater simplification of the operator's task, as he would now see the hook fixed relative to the tender. The motions of both vessels would be transparent to the operator, and in this idealized situation, lifting at sea would be similar to lifting on land. This second level of compensation would, however, result in an increase in the power requirements and loading on the crane as the crane must now overcome the dynamic motion of the tender. Second level compensation is close to automatic control but the operator remains in the loop with full override authority.

The following sections describe the development and application of the computer simulation. Motion compensating algorithms are presented and evaluated, and the performance of a simulated human operator compared with and without compensation.

2.0 MODEL OVERVIEW

Shown in Figure 2.1 is a block diagram of the model simulated on the hybrid computer. An average ship speed and a significant wave height are specified to define the wave spectrum to be used. This spectrum is comprised of a number of discrete sinusoidal waves of different frequency and amplitude, which when summed together, yield a continuous time-varying irregular sea surface.

The dynamic characteristics of the ship bearing the crane (vessel 1), and the ship onto which the load is to be placed (vessel 2) are specified in terms of their response amplitude operators (RAO). These take the form of a series of non-dimensionalized motion response amplitudes as a function of frequency of encounter for each degree of freedom and for each vessel. Frequency of encounter is wave frequency modified by ship speed.

From the family of RAO's and with the discrete sinusoids defining the irregular sea, the vessel rotations (roll, pitch, and yaw) and translations (surge, sway, and heave) about their respective centres of gravity are computed and summed, providing a continuous description of vessel motion as a function of time.

When the crane is not co-located with the centre of gravity of the vessel, as is almost always the case, the crane experiences not just the translations corresponding to the translations of the vessel centre of gravity, but also translations brought about by the vessel rotations. In order to compute the position of the crane boom tip, the location of the crane on the ship must be specified. Using current values of the actuator inputs for crane slew angle, boom elevation, and boom extension (if applicable), the boom tip position as a function of vessel displacement and orientation is calculated with matrix transformations. The position so calculated is that of a "rigid" or inelastic boom.

When the deck onto which the load is to be placed is not located at the centre of gravity of vessel 2, a similar transformation is made to determine its position.

The boom tip position of the rigid boom is modified by the static and dynamic deflections of a second order, lightly damped, spring-mass model approximating a flexible crane boom.

The loading on the boom is a result of the external forces applied through the crane cable and its own internal dynamic forces. The cable and load are also modelled as a second order, lightly damped, spring-mass system. The position of

the load is determined by ship motion, cable length, boom deflection, and cable stretch.

In real load transfer operations, a human operator serves as the controlling element that forces the load to follow a desired trajectory. The performance of a human operator in a tracking situation is characterized by a time delay, neuromuscular lag, and adaptive terms that allow him to adjust in part to the characteristics of the system he is controlling. In the simulation, the model of the human operator embodies these functions, and compares either load height or closing rate, to a desired position or rate, in order to command corrective action through a winching rate demand.

The winching rate demand is modified by motion compensating signals, and this modified signal is passed to the winch model. Power limits, rate limits, and tension limits are incorporated in the model of the cable winch ensuring that the winching rate conforms to the limitations of real systems. The changing cable length, computed from the integrated winching rate, modifies the load position, completing the loop.

The pendulous motions of the load depend on cable length, cable tension and the coordinate position of the rigid boom tip. Aerodynamic and cable damping forces are also considered. The XY load coordinates computed from the three independent variables describe the load motion in inertial space. No load restraining devices nor pendulous motion damping controls were simulated in this phase of the program.

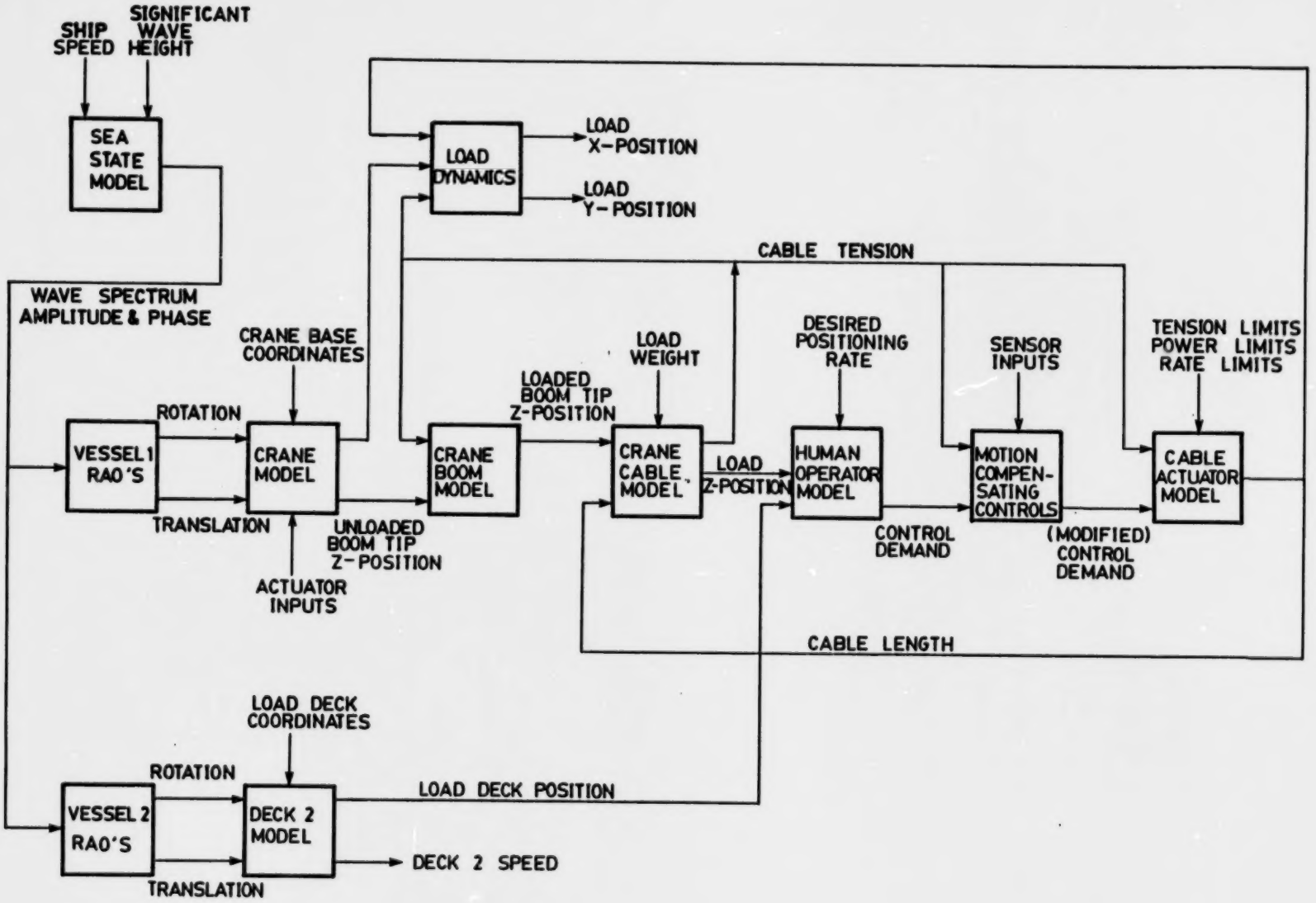

Figure 2.1 Information Flow, Crane Dynamics Model

3.0 PROGRAM ORGANIZATION

The concept of hybrid computation combines a digital computer and an analog computer to offer the advantages of each, and the benefits of parallel processing.

The analog computer uses electrical voltage to simulate the problem variables. For example, the analog computer may be "scaled" so that the problem variable of load height above the ship's deck has a maximum value of 20 metres when the computer voltage reaches 10 volts. A 5 volt reading means the load is positioned 10 metres above the deck.

Through combinations of resistors, capacitors, and operational amplifiers, the analog computer performs integrations, multiplications, divisions, etc. Numerous equations can be programmed or 'patched' on the analog board for simultaneous solution. This parallel solution of equations is particularly valuable when integrations and feedbacks are involved. The complex integration techniques often necessary in digital programming are avoided, as are the complications of sequential computation.

The continuous display of problem variables on strip chart recorders is also accomplished through the analog computer. What is sometimes regarded as one of the major advantages of the analog computer, is the ease with which control systems may be modelled, and the similarity of components on the analog board to those ultimately used in a control system implementation.

The digital computer assumes the role of simulation 'overseer'. It starts and stops the analog computer, provides it with variables through digital-to-analog converters, reads variables from the analog, performs the complex calculations and looks up non-linear data from data files or maps, and provides the communication path for the program user to interact with his simulation.

Figure 3.1 shows the main features of the interaction between the computers and the user. This simulation has been developed in the standard format described in Reference 3 and in the following paragraphs, a brief description is provided of the function of the standard subroutines used.

The actual running of the model is preceded by an initialization phase. A call to subroutine PARGET establishes the simulation parameters or model constants, all of them prefixed by the letters RC to identify them as Real Constants. Constants are generally grouped by the program subroutine in which they appear with the analog modules at the end. The

current version of PARGET should always be consulted for the values of the constants used in the simulation, rather than relying on program documentation which may quickly become out of date. Typical examples of model constants are RCML, the load mass, and RCG, the acceleration due to gravity.

Calling MISION establishes the simulation run conditions. The significant wave height chosen by the user is converted into first a series of sinusoidal waves of different amplitudes to define the sea state, then a series of sinusoidal ship motions as determined by the RAO's. The response amplitude operators (RAO) for the vessels selected by the user are retrieved from disc data files. Subroutine SCLGET establishes the model variable scale factors. All scale factors are preceded by the letters RS for Real Scale factor. These scale factors are used to scale digital variables prior to their being passed to the analog computer, and to descale variables read from the analog for use in the digital computer. For example, the variable for the inelastic boom tip position is defined as RVOT(3) in the digital program, the RV standing for Real Variable. Prior to being passed to the analog computer, RVOT(3) is "scaled" or divided by its scale factor, RSOT(3), which is the maximum value the variable is expected to reach. The new variable so created is always less than 1 and is denoted SVOT(3), meaning Scaled Variable.

The assignment of analog-to-digital (A/D) and digital-to-analog (D/A) channels through which the transfer of scaled variables between computers takes place is accomplished in subroutines ADCSET and DACSET prior to run time.

Certain constants, created from other constants may appear in the high speed loop. An example might be the computation of the area of a circle πr^2. Rather than repeat this calculation at each pass through the high speed loop, new constants are computed in subroutine CMPUTE during the initialization phase to replace groups of constants.

The last subroutine to be called before the high speed loop is POTSET. In this subroutine, pot settings are calculated and potentiometer and digitally controlled attenuator (DCA) assignments are made. At the end of this subroutine, the pots are set, clearing the way for operation of the model.

The three subroutines forming the highspeed loop, and their functions are:

INALG Scaled Variables are read from the analog computer through their assigned channels (ADCSET) and converted to real variables by multiplying by their scale factors.

MODEL Subroutines comprising the model are called sequentially within this subroutine.

OUTALG Real digital variables required by the analog computer are divided by their scale factor and output to the analog through their assigned D/A channels.

During each pass through the highspeed loop, the computer looks for user initiated requests for offline operations. The user may halt the program at any time to change model parameters such as boom stiffness, RCKSB. Both CMPUTE and POTSET are executed to update model constants and potsettings.

The user may also change simulation run conditions such as sea state, and such a request causes the model to execute the subroutines in MISION.

The crane dynamic simulation normally takes place in real time, but it is possible to operate either faster or slower than real time if required.

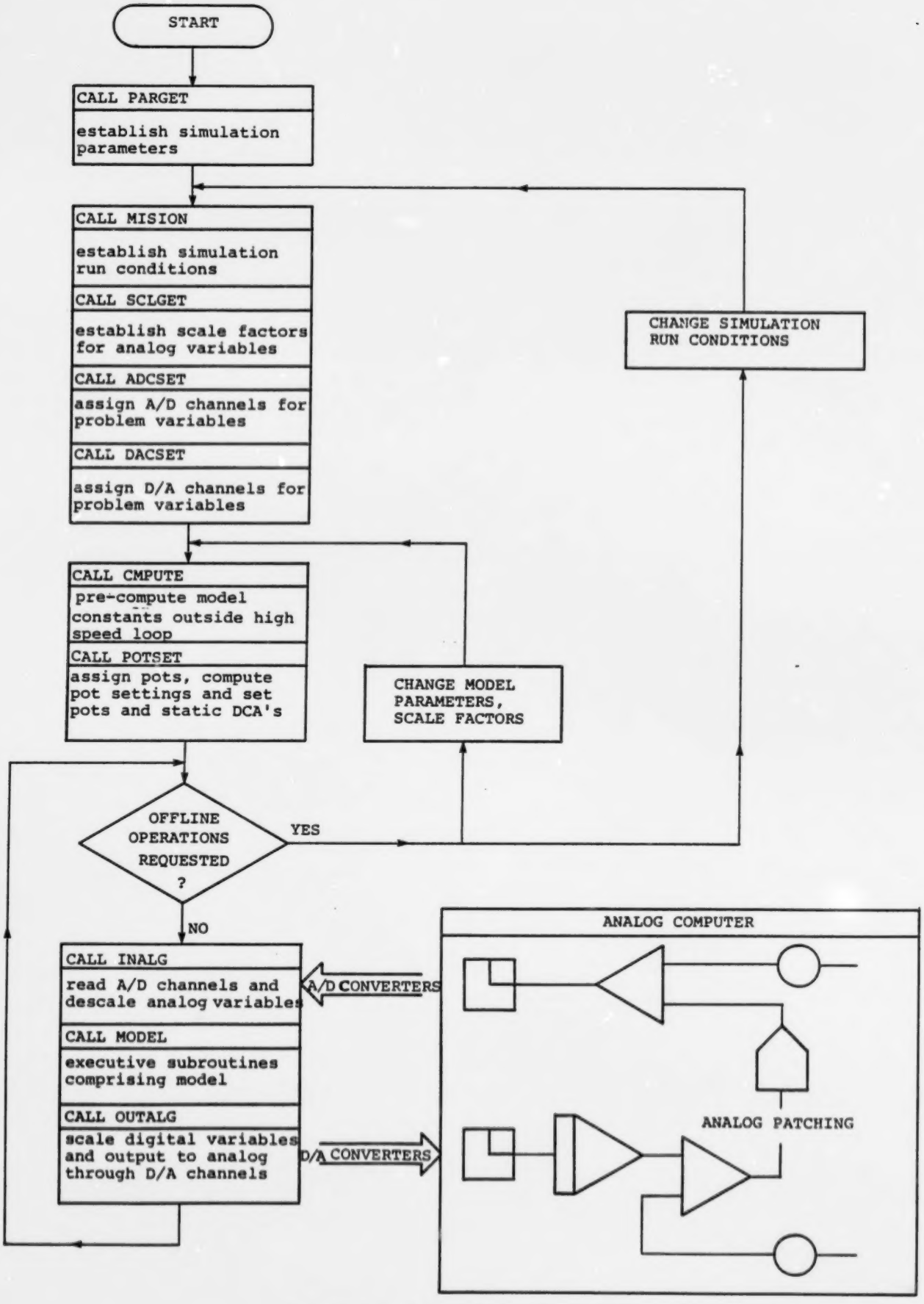

Figure 3.1 Program Organization

4. DIGITAL MODULES

In this section, the parts of the model which are implemented on the digital computer are described in terms of their theoretical derivation followed by a discussion of the programming used.

4.1 Sea Model

A most important objective of the simulation is to provide realistic modelling of the disturbances which adversely affect the operator's performance. These disturbances must cover the frequency range normally encountered in a given sea state, and include the random combination of waves that give rise to periods of wave action of substantially greater amplitude than the mean.

4.1.1 Background

In developing a model for the sea state, it is assumed that

- all wave components travel in the same direction;
- the straight crests extend to infinity in a direction normal to the direction of wave travel.

Such a system is called a long-crested irregular wave system and is considered as being one-dimensional in frequency only. A more general treatment of a sea state would combine individual wave components travelling in different directions; the resultant pattern would not exhibit long crests but rather a series of bumps and hollows, and would be considered two-dimensional with both frequency and direction defined. The assumption of uniform wave direction is a conservative one from the point of view of the simulation as the resultant wave energy will be greater than that of a two-dimensional sea. The one-dimensional assumption is also necessary for the use of the vessel response amplitude operators as described in section 4.4.

An irregular sea is considered to be the summation of an infinitely large number of regular sinusoidal waves of different, but small, amplitudes and random phase angles. The continuous distribution of amplitude as a function of frequency defines the sea spectrum, an example of which is shown in Figure 4.2. For such a spectrum, the area under the curve, termed m_o is equal to the mean square of the surface elevation.

For waves represented by a Rayleigh distribution, the following hold:

average wave amplitude = $1.25 \sqrt{m_o}$

average amplitude of 1/3 highest waves = $\zeta 1/3 = 2 \sqrt{m_o}$

average amplitude of 1/10 highest waves = $2.55 \sqrt{m_o}$

Because the simulation is to run in real time, execution speed is an important factor. This imposes a severe limitation on the number of sine waves that may be used to formulate the model. When a finite number of wave components is used to model the irregular wave, the plot of amplitude versus frequency is now termed a line spectrum as shown in Figure 4.1. When approximating a continuous spectrum by a discrete spectrum, the probability of a number of waves being nearly in phase at repetitive intervals increases, leading to irregular waves with abnormally high amplitudes.

To maintain realistic wave heights, the maximum wave amplitude is limited to $2.75 \sqrt{m_o}$.

This limitation was computed using the probability equation

$$P(Z) = 1\text{-erf} \left[Z / \sqrt{2m_o} \right]$$

where Z is the magnitude of the wave amplitude.

$$\text{For } Z = 2.75 \sqrt{m_o}, \text{ then } P(Z) = .006$$

In other words, the probability of encountering a wave of amplitude higher than $2.75 \sqrt{m_o}$ in a continuous spectrum is 0.006. A small error in replicating the continuous spectrum is introduced by this limitation but the unrealistically high amplitudes that the discrete spectrum can introduce are eliminated.

Various wave spectra have been developed to match the statis-

tics of seas measured in different parts of the world, and the spectrum chosen for this simulation is that adopted for general purposes by the International Towing Tank Conference (ITTC) and also accepted by the International Ship Structures Congress. The wave spectrum S (illustrated in Figure 4.4 as a function of wave height) is defined as

$$S_\zeta(\omega) = \frac{a}{\omega^5} \exp(-b/\omega^4)$$

Where ω is the circular frequency of the waves (rad/s), and a and b are dimensional constants.

For a given significant wave height, the amplitude as a function of frequency is given by :

$$A_\zeta(\omega) = \sqrt{2S_\zeta(\omega)}$$

For a model based only on the significant wave height,

$$a = 8.10 \times 10^{-3} \times g^2$$

$$b = 3.11/\zeta^2$$

Significant wave height is a good indication of sea state as shown in Table 4.1. The sea model was derived on the basis of a specified significant wave height but where conditions require a certain sea state to be modelled, this table may be used to determine the equivalent significant wave height.

The discrete spectrum, comprised of 9 components, is selected by determining the frequency at which $S(\omega)$ is a maximum. This frequency is termed the central frequency, ω_o. Four frequencies are selected on either side of the central frequency by specifying four ratios $K_i = S(\omega_i) / S(\omega_o)$, where ω_i is the discrete frequency.

A change in ship's velocity causes a change in the apparent sea spectrum or spectrum of encounter in accordance with the equations

$$\omega_E = \omega\left(1 - \frac{\omega v}{g} \cos\gamma\right)$$

$$S(\omega_E) = \frac{S(\omega)}{1 - (2\omega v/g)\cos\gamma}$$

where V = ship speed and γ = the angle between wave direction and ship's direction.

Figure 4.3 illustrates how increasing the ships forward speed flattens the sea spectrum and shifts the central frequency to the right. In spite of the distortion of the spectrum, the area under the curve remains constant as ship's speed increases. This assumes the ship's presence does not influence the waves.

4.1.2 Sea Model Digital Implementation

Figure 4.6 outlines the modular structure of the sea state model, and Figure 4.5 itemizes the steps a program user should follow when initiating a sea model to meet his requirements.

The following notes apply to Figure 4.5:

NOTE 1: The user has the flexibility of choosing the position of the discrete spectral frequencies other than the central frequency, up to a maximum of 8. The number of frequencies to the left of the central frequency is n_1 and to the right n_2. The user specifies the ratios K_i to ensure full coverage of the spectrum.

NOTE 2: If the ship's speed is zero, there will be no difference between the frequencies of encounter and the frequencies computed directly from the Absolute Energy Spectrum.

NOTE 3: It is assumed the vessel response amplitude operators are independent of ship speed.

As mentioned in Section 3, a standard subroutine called MISION is called prior to the high speed loop to establish the simulation run conditions. See Figure 4.8 for details.

Figure 4.1 Line Spectrum

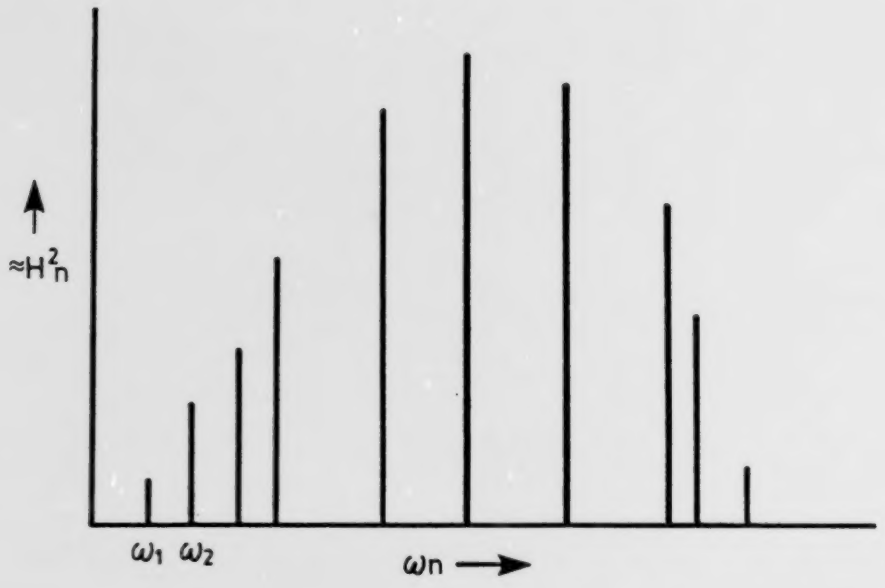

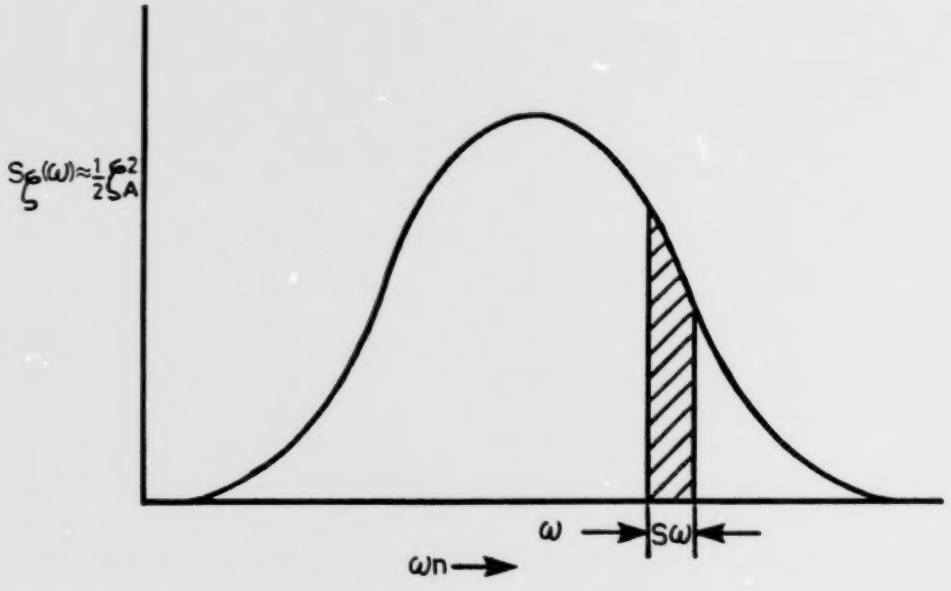

Figure 4.2 Continuous Spectrum

Figure 4.3 Energy Spectrum For Different Ship Speeds

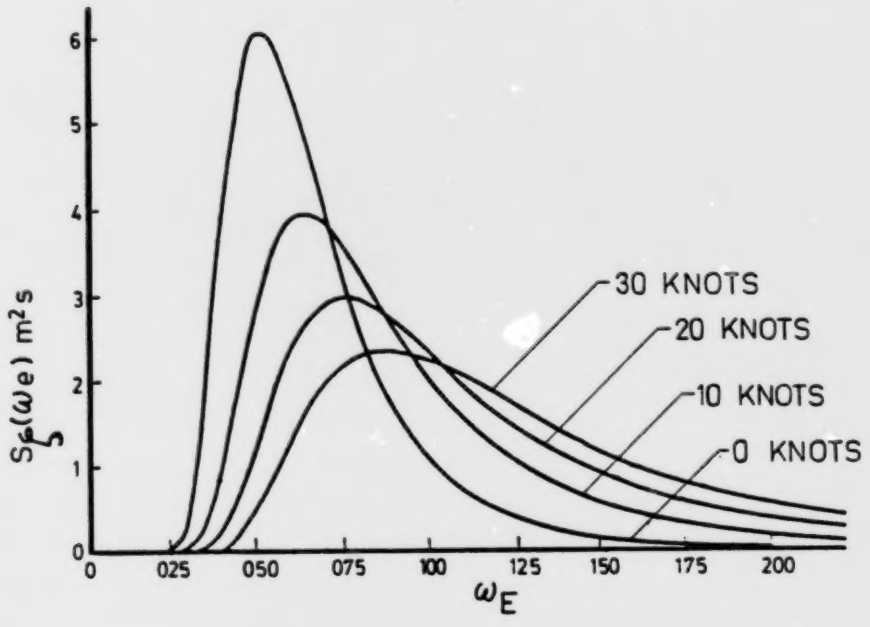

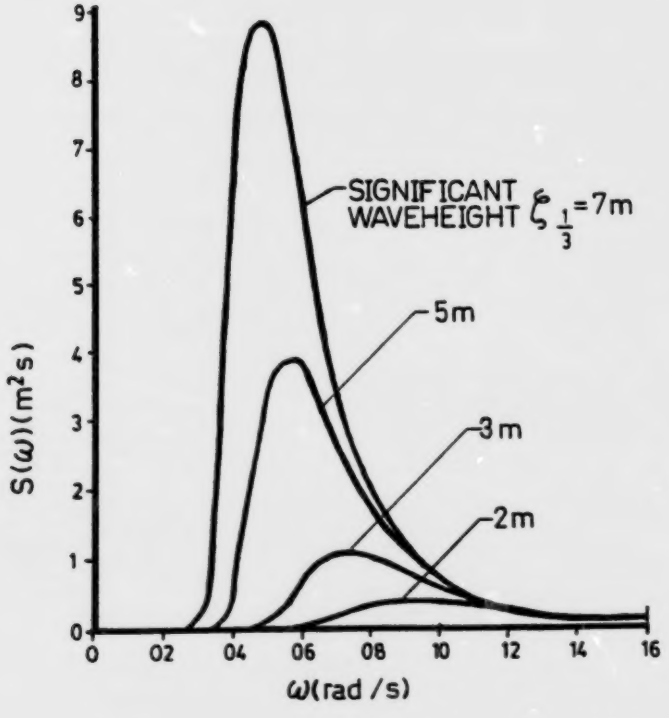

Figure 4.4 Energy Spectrum For Different Significant Wave Heights

Table 4.1 Sea State Codes

Code	Description of Sea	Significant Wave Height ζ (m)
0	Calm (glassy)	0
1	Calm (rippled)	0. - 0.1
2	Smooth (wavelets)	0.1 - 0.5
3	Slight	0.5 - 1.25
4	Moderate	1.25 - 2.50
5	Rough	2.50 - 4.00
6	Very rough	4.0 - 6.0
7	High	6.0 - 9.0
8	Very high	9.0 - 14.0
9	Phenomenal	Over 14.0

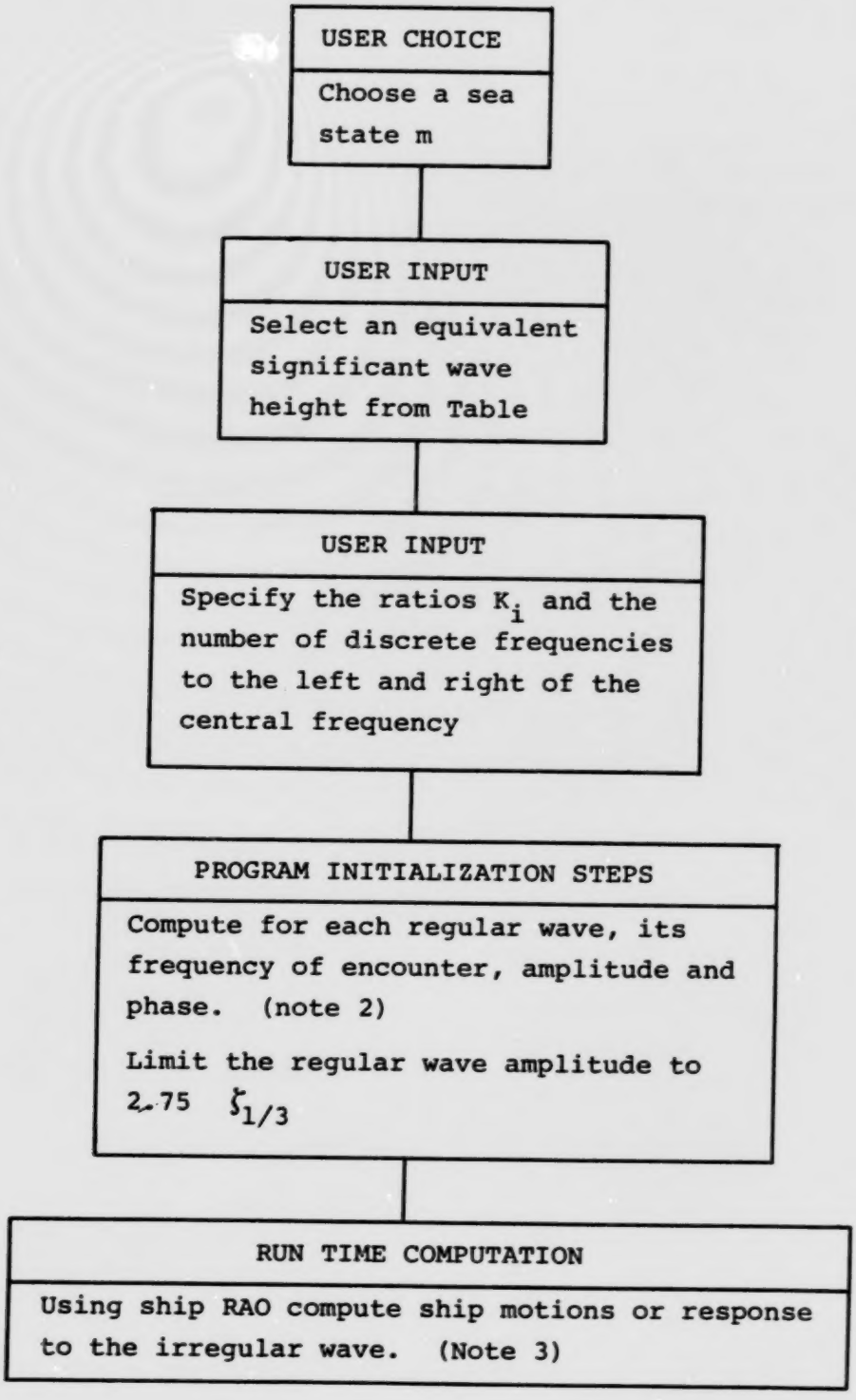
USER CHOICE
Choose a sea state m
USER INPUT
Select an equivalent significant wave height from Table
USER INPUT
Specify the ratios K_i and the number of discrete frequencies to the left and right of the central frequency
PROGRAM INITIALIZATION STEPS
Compute for each regular wave, its frequency of encounter, amplitude and phase. (note 2)
Limit the regular wave amplitude to 2.75 $\zeta_{1/3}$
RUN TIME COMPUTATION
Using ship RAO compute ship motions or response to the irregular wave. (Note 3)

Figure 4.5 User Interaction

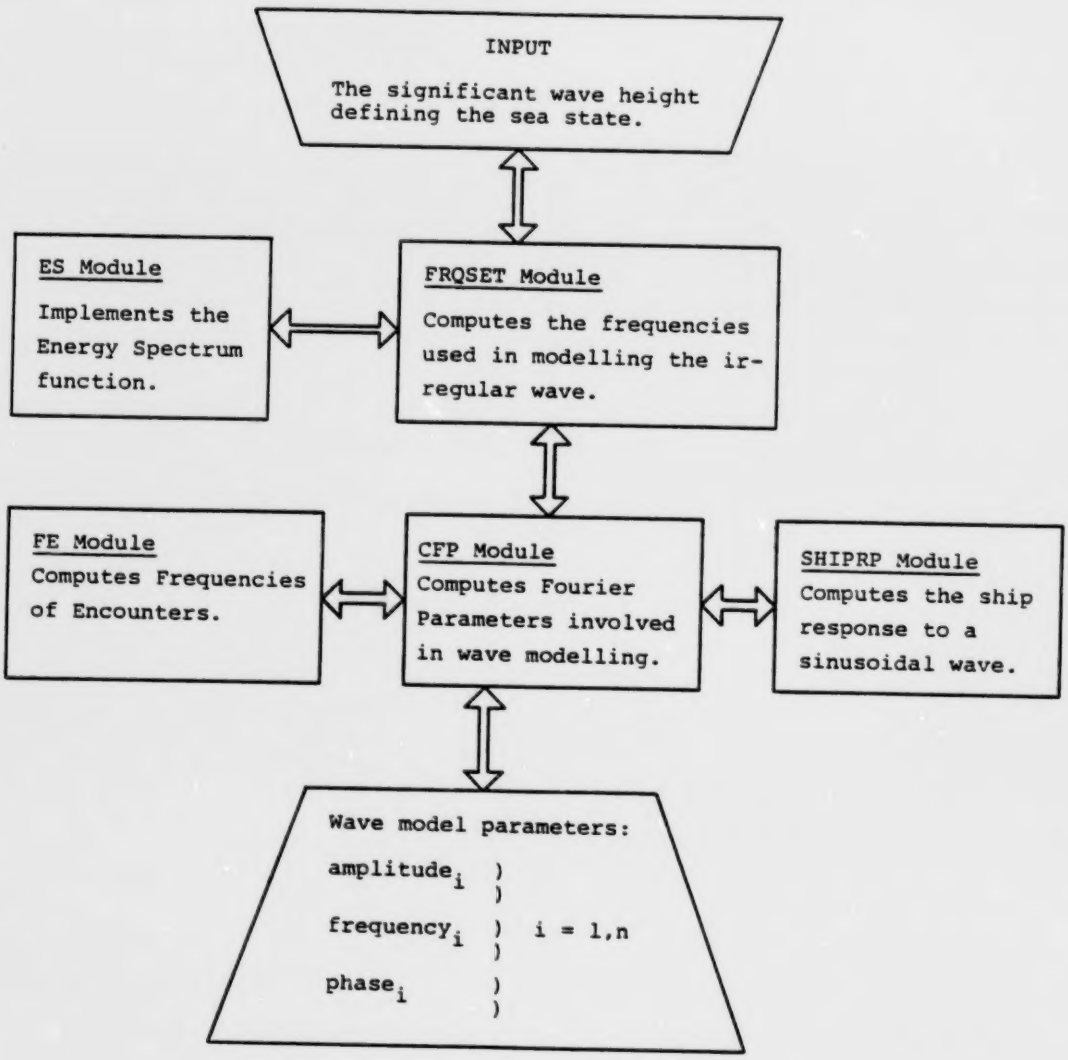

Figure 4.6 Sea State Model Modular Structure

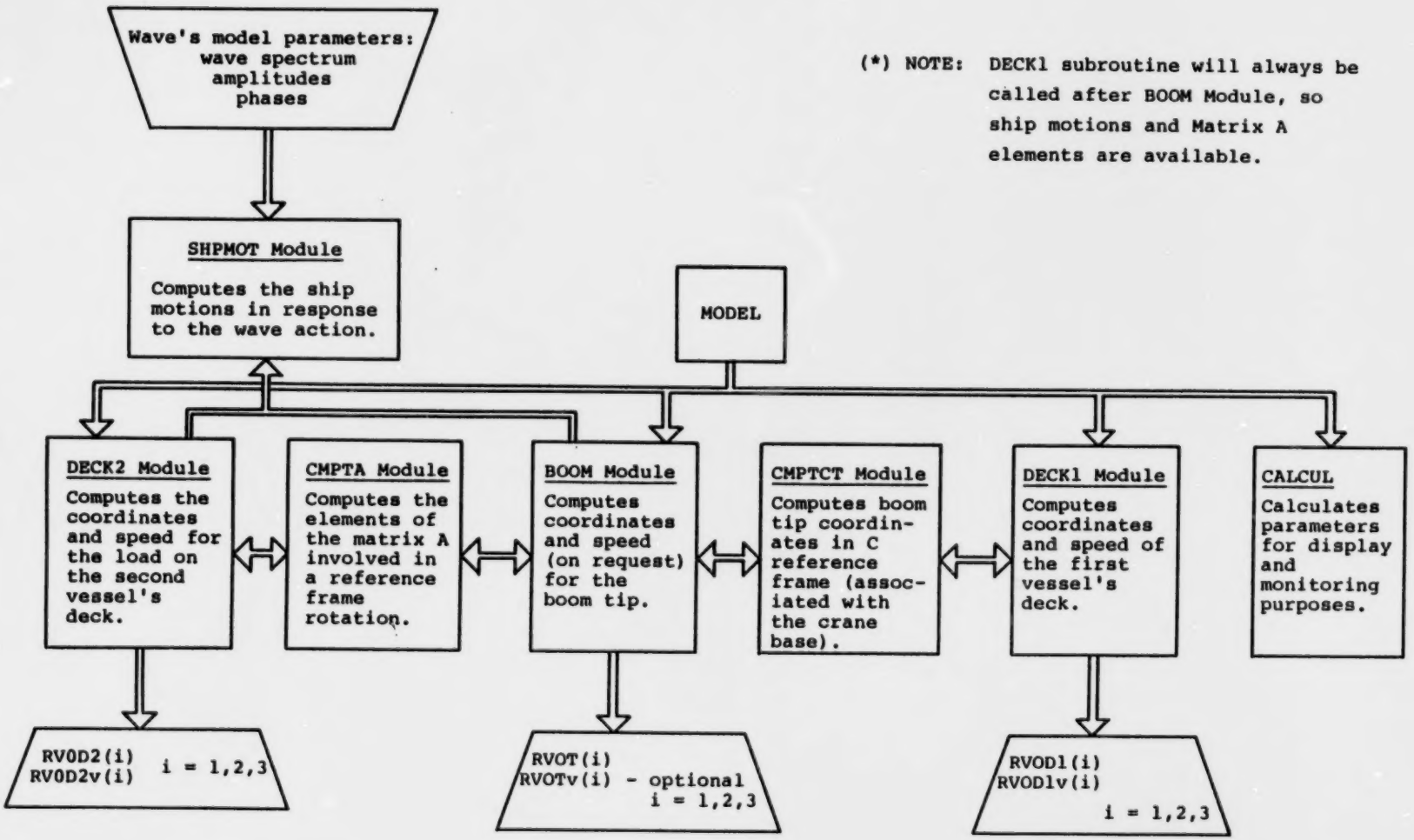
Wave's model parameters:
wave spectrum
amplitudes
phases
(*) NOTE: DECK1 subroutine will always be called after BOOM Module, so ship motions and Matrix A elements are available.
SHPMOT Module
Computes the ship motions in response to the wave action.
MODEL
DECK2 Module
Computes the coordinates and speed for the load on the second vessel's deck.
CMPTA Module
Computes the elements of the matrix A involved in a reference frame rotation.
BOOM Module
Computes coordinates and speed (on request) for the boom tip.
CMPTCT Module
Computes boom tip coordinates in C reference frame (associated with the crane base).
DECK1 Module
Computes coordinates and speed of the first vessel's deck.
CALCUL
Calculates parameters for display and monitoring purposes.
RVOD2(i)
RVOD2v(i) i = 1,2,3
RVOT(i)
RVOTv(i) - optional
i = 1,2,3
RVOD1(i)
RVOD1v(i)
i = 1,2,3

Figure 4.7 Crane And Deck Model Modular Structure

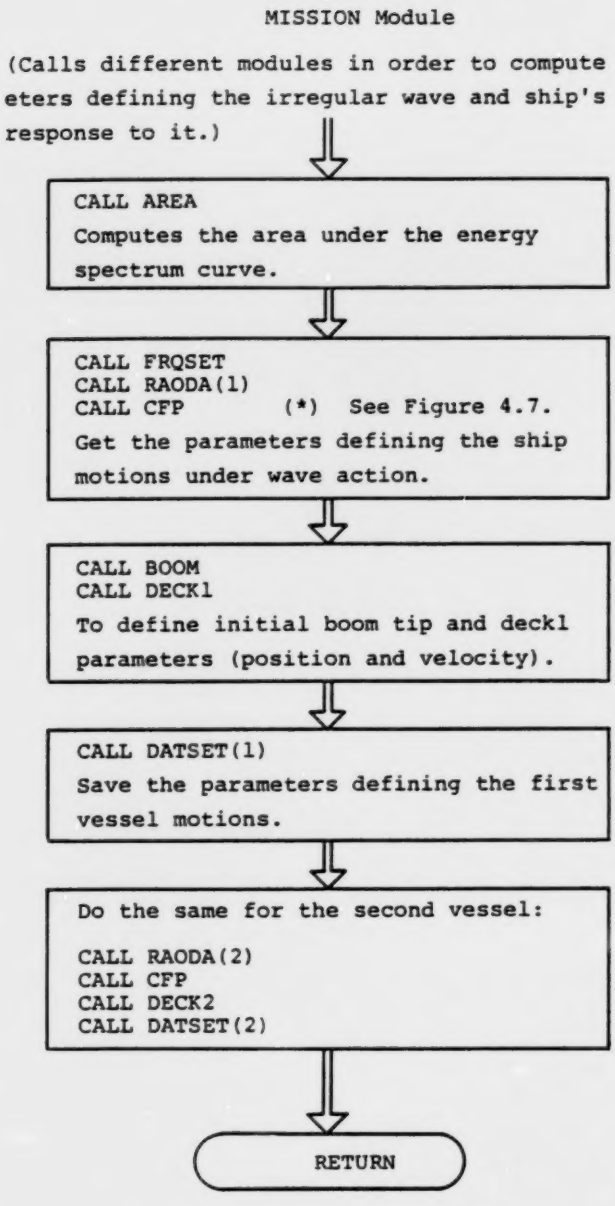
MISSION Module
(Calls different modules in order to compute parameters defining the irregular wave and ship's response to it.)
CALL AREA
Computes the area under the energy spectrum curve.
CALL FRQSET
CALL RAODA(1)
CALL CFP (*) See Figure 4.7.
Get the parameters defining the ship motions under wave action.
CALL BOOM
CALL DECK1
To define initial boom tip and deck1 parameters (position and velocity).
CALL DATSET(1)
Save the parameters defining the first vessel motions.
Do the same for the second vessel:
CALL RAODA(2)
CALL CFP
CALL DECK2
CALL DATSET(2)
RETURN

Figure 4.8 Mission Module Structure

4.2 The Axes System

The principle axes system is a right-handed, Cartesian co-ordinate reference frame, the origin of which is denoted "o". This axes system constitutes an inertial reference frame and is located at the mean position of the centre of gravity of vessel 1, the ship bearing the crane. See Figure 4.9. Vessel 1 is assumed to travel at an average uniform (or zero) velocity in the direction of its longitudinal axis. The 1- or X-axis of the o-frame is aligned with the mean longitudinal axis of the vessel; the 2- or Y-axis is aligned with the mean starboard athwartships direction, and the 3- or Z-axis is oriented downward in the gravitational vertical direction.

A second set of axes denoted the G-axes system is fixed to vessel 1 with its origin at the centre of gravity. These are termed body-fixed axes. The 1- or X-axis in G is parallel to the mean waterline of the vessel and aligned fore and aft. The Z- or Y-axis is also parallel to the mean waterline and aligned with the starboard athwartships. The 3- or Z-axis is perpendicular to the plane of the 1- and 2- axes and is positive in the downward direction.

The vessel translations surge, sway and heave take place in the 1-, 2-, and 3-axial directions, respectively. The rotations roll, pitch and yaw take place about the 1-, 2-, and 3-axes respectively, in the conventional right-hand sense.

At any given instant in time, the position of the centre of gravity of vessel 1 may be expressed in vector notation as

$$ {}_{o}\overline{G} = \begin{bmatrix} {}_{o}G(1) \\ {}_{o}G(2) \\ {}_{o}G(3) \end{bmatrix} $$

where the subscript o preceding the G, indicates that its position is being expressed in the o-reference frame.

By convention, roll, pitch and yaw have been defined as ϕ, θ, and ψ. In this program, for convenience, the rotations about the G-axes are given as

$$ {}_{G}\overline{I} = \begin{bmatrix} {}_{G}i(1) \\ {}_{G}i(2) \\ {}_{G}i(3) \end{bmatrix} $$

with the similarity to translations being evident. For computational convenience within the source program, the rotations are redefined as

$$ \begin{bmatrix} {}_{G}i(1) \\ {}_{G}i(2) \\ {}_{G}i(3) \end{bmatrix} = \begin{bmatrix} {}_{o}G(4) \\ {}_{o}G(5) \\ {}_{o}G(6) \end{bmatrix} $$

A third axes system, the C-frame, is located with its origin at a point C considered to be the intersection point for all of the crane rotations. The C-frame axes are parallel to their counterparts in the G-frame. The point C, when defined in the G-frame as

$$ {}_{G}\overline{C} = \begin{bmatrix} {}_{G}C(1) \\ {}_{G}C(2) \\ {}_{G}C(3) \end{bmatrix} $$

represents the coordinates of the location of the crane in terms of the vessel 1 coordinate system, and is shown in Figure 4.10.

The cartesian coordinate position of the tip of an inelastic boom is defined in the C-frame as

$$ {}_C\overline{T} = \begin{bmatrix} {}_CT(1) \\ {}_CT(2) \\ {}_CT(3) \end{bmatrix} $$

and is derived from the transformation of the crane actuator positions illustrated in the spherical axes system of Figure 4.11. Here, the crane azimuth (or slewing) angle β is the angle measured clockwise from the ${}_C1$-axis around the ${}_C3$-axis. The boom elevation angle α is the angle the boom makes with respect to the ${}_C12$-plane, while the boom extension r is the length of the boom from its pivot point to the load suspension point.

A second inertial reference frame Q, is located at the mean centre of gravity position of vessel 2, the ship onto which the load is to be placed. It is assumed for all the simulation studies that vessel 2 maintains a fixed position relative to vessel 1. The vector ${}_O\overline{Q}$ defines its coordinates in the o-reference frame, as seen in Figure 4.9.

The location of the centre of gravity of vessel 2 as a function of time is given by

$$ {}_Q\overline{H} = \begin{bmatrix} {}_QH(1) \\ {}_QH(2) \\ {}_QH(3) \end{bmatrix} $$

The rotations about the H axes (roll, pitch and yaw) are expressed as

$$ {}_{H}\bar{I} = \begin{bmatrix} {}_{H}i(1) \\ {}_{H}i(2) \\ {}_{H}i(3) \end{bmatrix} $$

but again for convenience, these angles are redefined as

$$ \begin{bmatrix} {}_{H}i(1) \\ {}_{H}i(2) \\ {}_{H}i(3) \end{bmatrix} == \begin{bmatrix} {}_{Q}H(4) \\ {}_{Q}H(5) \\ {}_{Q}H(6) \end{bmatrix} $$

Finally, the location of the deck on vessel 2 onto which the load is to be placed is defined as

$$ {}_{H}\bar{D}_2 = \begin{bmatrix} {}_{H}D_2(1) \\ {}_{H}D_2(2) \\ {}_{H}D_2(3) \end{bmatrix} $$

and its relationship to the H-frame is illustrated in Figure 4.10.

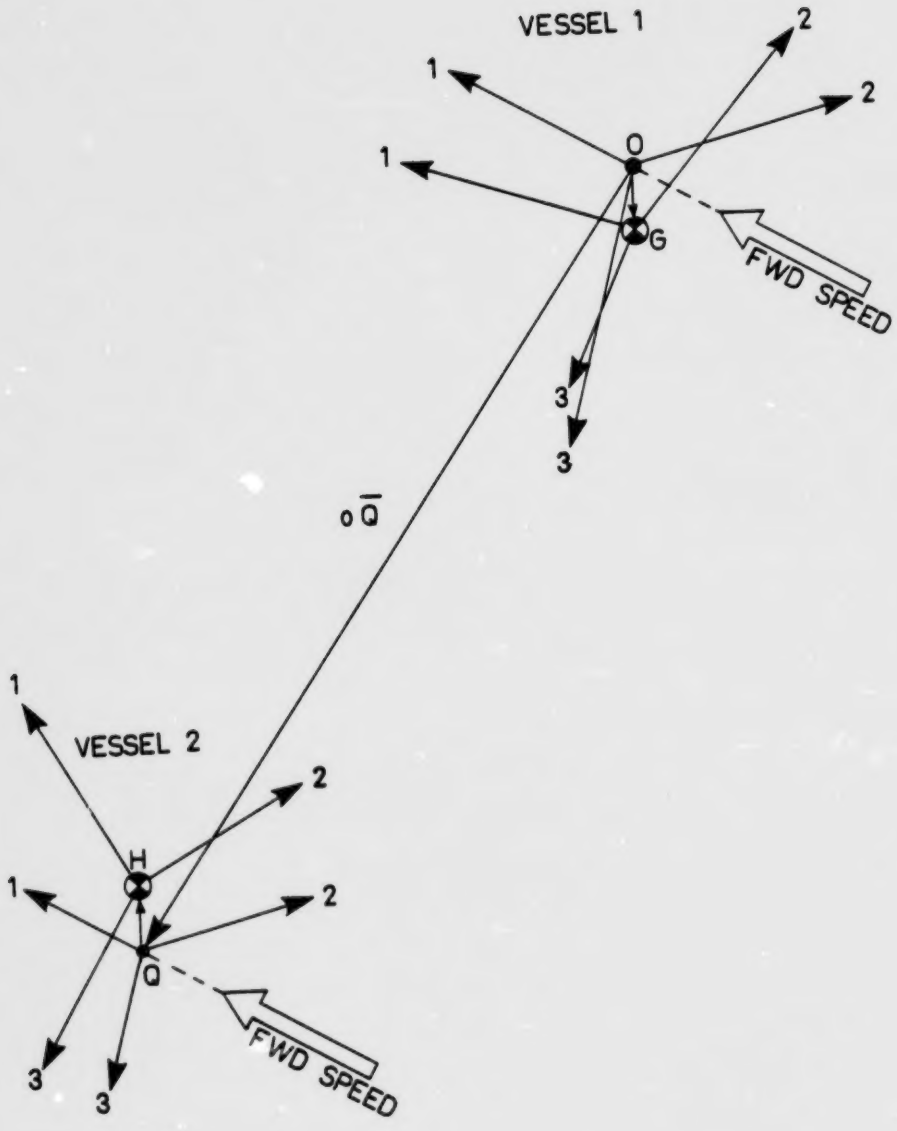

Figure 4.9 Coordinate References Frames

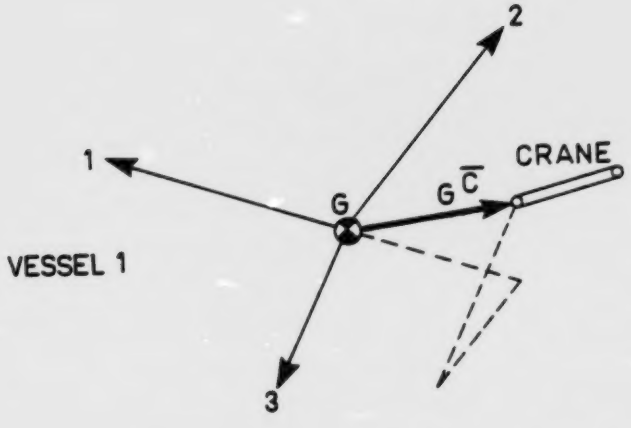

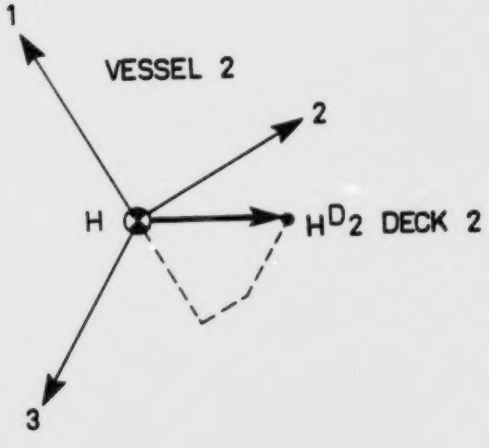

Figure 4.10 Body Fixed Axes

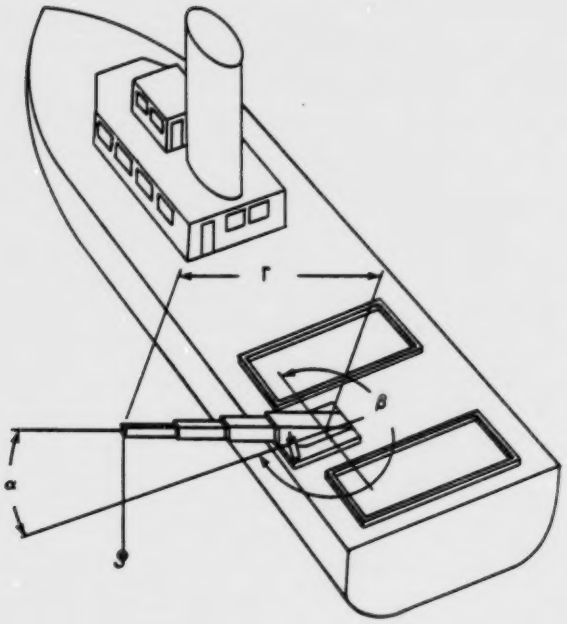

Figure 4.11 Crane Boom Coordinate System

4.3 Axes Transformations

The position of the rigid boom tip in the C-frame is a function of the actuator positions, expressed as

$$ {}_{c}\overline{T} = f(\alpha, \beta, r) $$

The spherical coordinate position of the crane boom tip is converted to the cartesian coordinate C-frame by the equations

$$ {}_{c}\overline{T} = \begin{bmatrix} r \cos\alpha \cos\beta \\ r \cos\alpha \sin\beta \\ r \sin\alpha \end{bmatrix} $$

where α , β , and r may vary with time.

In the G-frame or body fixed axes of vessel 1, the rigid boom tip position becomes

$$ {}_{G}\overline{T} = {}_{G}\overline{C} + {}_{c}\overline{T} $$

with the column vector ${}_{G}\overline{C}$ defining the location of the crane with respect to the centre of gravity of vessel 1.

The position of the origin of the G-frame is defined in the o-frame as

$$ {}_{o}\overline{G} = \begin{bmatrix} {}_{o}G(1) \\ {}_{o}G(2) \\ {}_{o}G(3) \end{bmatrix} $$

Now the position of the origin of the G-frame and its orientation changes continuously with time. When the co-ordinates of a point expressed in the G-frame are to be converted to the o-frame of reference, the transformed

coordinates are the vector sum of the displacement of the G-frame origin and the vector product of the inverse of the Eulerian angle transformation matrix **A** and the displacement vector in the G-frame to the point - in this case, the rigid boom tip.

$$ {}_{o}\overline{T} = {}_{o}\overline{G} + \mathbf{A}^{-1} \times {}_{G}\overline{T} $$

Because the transformation relates two orthogonal systems, the inverse transformation matrix is the transpose of **A**

$$ \text{i.e.} \quad \mathbf{A}^{-1} = \mathbf{A}^{T} $$

The elements of $\mathbf{A}^{-1}$ are defined as

$$ a^{1}_{11} = \sin\psi . \sin\phi . \sin\theta + \cos\psi . \cos\theta $$

$$ a^{1}_{12} = \cos\psi . \sin\phi . \sin\theta - \sin\psi . \cos\theta $$

$$ a^{1}_{13} = \cos\phi . \sin\theta $$

$$ a^{1}_{21} = \sin\psi . \cos\phi $$

$$ a^{1}_{22} = \cos\psi . \cos\phi $$

$$ a^{1}_{23} = -\sin\phi $$

$$ a^{1}_{31} = \sin\psi \sin\phi \cos\theta - \cos\psi . \sin\theta $$

$$a^{1}_{32} = \cos\psi \sin\phi \cos\theta + \sin\psi \cdot \sin\theta$$

$$a^{1}_{33} = \cos\phi \cos\theta$$

The angular rotations about the axes are not fixed, but are varying with time. A part of the problem solution requires the use of boom tip speed in each of the principle axes, and since the rotations of the axes are comprised of a number of sine waves, differentiation of the analytical expression for boom tip position is practical.

Boom tip speed may be expressed as

$$\dot{T}_{o} = \dot{G}_{o} + \Omega \, x_{G}\bar{T}$$

where Ω is the first derivative of A^{-1}

$$\Omega = \frac{d}{dt} A^{-1}$$

or: $$\omega_{i,j} = \frac{d}{dt} a^{1}_{i,j} \qquad \begin{matrix} i = 1, 2, 3 \\ j = 1, 2, 3 \end{matrix}$$

4.4 Moment Calculations

In analyzing load transfer operations at sea, an important aspect is the determination of the loading induced on the crane by vessel motions and operator input. The three principle loadings are cable tension, overturning moment and slewing moment.

Cable tension under dynamic conditions is crucial in establishing safety factors. When combined with cable rate, it also sets the minimum winching power requirements. The calculation of cable tension is described in Section 5. The overturning moment, which is the moment in the topping plane about the boom pivot point or footpin, is used to calculate bending moments in the boom, and overturning stresses in the slewing gear and pedestal. The moment about the crane vert-

ical or slewing axis ('kingpin') is termed the slewing moment. Power and strength requirements of the slewing gear and lateral stiffness of the boom depend largely on the externally applied slewing moment. A problem with ship-mounted cranes is the substantial slewing moments encountered when the slewing axis departs from the vertical due to ship rotations and when the load swings away from plumb in motion-induced pendulous action.

The cable tension components in the inertial reference frame are the components of the force applied at the load suspension point or boom tip and are given by

$$ {}_{o}\bar{F}_{SC} = \begin{bmatrix} {}_{o}F_{SC}(1) \\ {}_{o}F_{SC}(2) \\ {}_{o}F_{SC}(3) \end{bmatrix} $$

These must be mapped into the crane coordinate system or C-frame. This mapping is given by the expression

$$ {}_{c}\bar{F}_{SC} = \mathbf{A} \cdot {}_{o}\bar{F}_{SC} $$

where $\mathbf{A}$ is the Eulerian transformation matrix described in Section 4.3.

A final rotation through angle β about the slewing axis maps the cable tension into an intermediate axis system, the C^1-frame, the 13-plane of which coincides with the topping plane of the crane.

$$ {}_{c^1}\bar{F}_{SC} = \begin{bmatrix} \cos\beta & \sin\beta & 0 \\ -\sin\beta & \cos\beta & 0 \\ 0 & 0 & 1 \end{bmatrix} \cdot {}_{c}\bar{F}_{SC} $$

Now the vector product of the cable tension and the boom tip coordinates in the C^1-frame gives the moments generated by the load, i.e.

$$ {}_{c^1}\bar{M} = {}_{c^1}\bar{r} \times {}_{c^1}\bar{F}_{SC} $$

or

$$\begin{bmatrix} {}_{c}{}^{l}M(1) \\ {}_{c}{}^{l}M(2) \\ {}_{c}{}^{l}M(3) \end{bmatrix} = \begin{bmatrix} r\cos\alpha \\ 0 \\ r\sin\alpha \end{bmatrix} \times \begin{bmatrix} {}_{c}{}^{l}F_{SC}(1) \\ {}_{c}{}^{l}F_{SC}(2) \\ {}_{c}{}^{l}F_{SC}(3) \end{bmatrix}$$

where

$${}_{c}{}^{l}M(1) = M_{RO} = -r\sin\alpha\,(\cos\beta - {}_{c}F_{SC}(2) - \sin\beta \cdot {}_{c}F_{SC}(1))$$

$${}_{c}{}^{l}M(2) = M_{OT} = -r\cos\alpha \cdot {}_{c}F_{SC}(3) + r\sin\alpha\,(\cos\beta \cdot {}_{c}F_{SC}(1) + \sin\beta \cdot {}_{c}F_{SC}(2))$$

$${}_{c}{}^{l}M(3) = M_{SL} = +r\cos\alpha\,(\cos\beta \cdot {}_{c}F_{SC}(2) - \sin\beta \cdot {}_{c}F_{SC}(1))$$

where

M_{RO} is the rolling moment

M_{OT} is the overturning moment

and M_{SL} is the slewing moment.

These calculations are performed in subroutine CALCUL.

4.5 RAO Method

One method of describing the response of a vessel in a regular sea is by means of Response Amplitude Operator curves or RAO's. These continuous curves represent the ratio of the vessel's response amplitudes to the wave amplitude, as a function of frequency of encounter where frequency of encounter is the wave frequency modified by the ship's speed. For example, if it was determined that a frequency of encounter of 1 rad/s with waves of 2 m in amplitude generated a pitch response amplitude of 1.2 degrees, the response amplitude ratio for 1 rad/s would be computed as 0.6. From this value, the pitch response amplitude for seas of 0.5 m but of the same frequency, can be computed as 0.3 degrees.

It takes six curves to describe the response of the vessel - the units of the rotations, roll, pitch and yaw being degrees of rotation per metre of wave amplitude, and the displacement surge, sway and heave appearing in non-dimensional form (m/m). A particular set of RAO's is applicable only to a given direction of seas, such as head seas; other directions of encounter, for instance quartering and beam seas, require separate families of curves.

To compute the response of a vessel to a discrete wave spectrum, the amplitude of each discrete sine wave component is multiplied by the amplitude ratio at the same frequency of the RAO for the motion under consideration. The vessel response in that degree of freedom is the sum of the discrete sine waves so computed. This is illustrated in Figure 4.12.

Each of the remaining degrees of freedom is treated in exactly the same way.

The ship response is calculated in the digital part of the program by calling subroutine SHIPRP (W,M) where

ω - is the frequency of encounter being examined at the time of the call.

M - is one of the six degrees of freedom defining the vessel's motions.

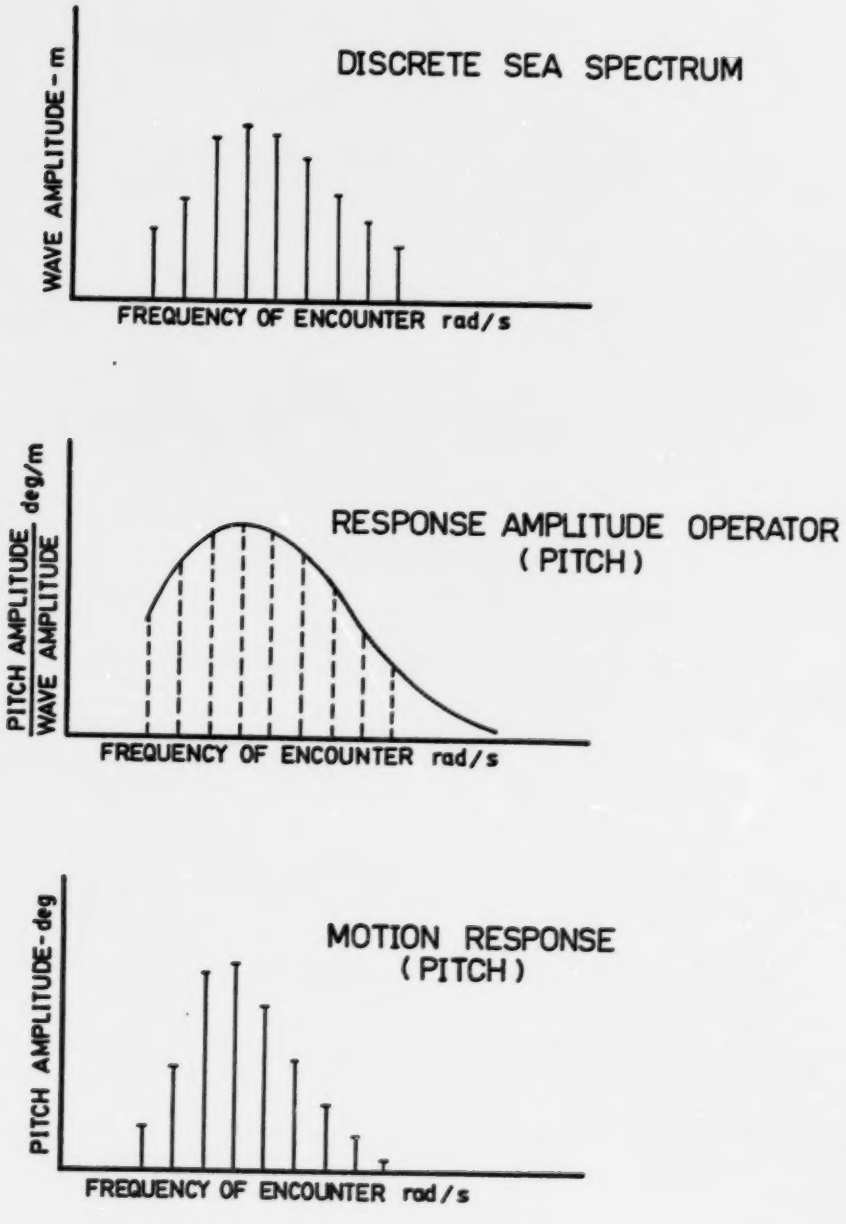

Figure 4.12 Determination of Ships' Motions

5.0 ANALOG MODULES

This section describes the modules implemented on the analog portion of the hybrid computer.

5.1 Crane Boom Model

The crane is modelled as a two degree of freedom system consisting of the boom, treated as a lightly damped spring-mass system, and the cable with suspended load, modelled as another lightly damped spring-mass system in series with the first.

To model the boom in this fashion, the following assumptions are made:

- significant elastic deformation takes place only in the topping plane - that is, no consideration is given to torsional loads or to lateral loads;
- ship rotations or angular displacements are small, such that motion in the topping plane can be considered to take place only in the vertical;
- the boom may be approximated by a massless section of stiffness K_{SB} and a mass m_B concentrated at the free end of the boom.
- motions of m_B are small and occur only in the vertical direction.
- damping of the boom motion is viscous in nature with damping coefficient K_{DB};
- changes in boom elevation with respect to the horizon are small during the simulation so that boom stiffness may be considered constant.

The position of the unloaded boom tip (see Fig. 5.1 in the inertial reference frame is defined as ${}_oT(3)$ and varies with time. This position includes the static deflection brought about by the weight of the boom itself, but does not include its dynamic deflections nor the deflections caused by cable tension. The dynamic position of the boom tip in the inertial space is given as ${}_oT_L(3)$, the result of three forces:

F_{SB} boom spring force

F_{DB} boom damping force

F_C cable tension

Boom tip acceleration in the vertical direction, a_{ZB} is computed from the equation:

$$a_{ZB} = \frac{1}{m_B}\left[-F_{SB}-F_{DB}+F_C\right]$$

Spring force is determined as

$$F_{SB} = K_{SB} \cdot dZ_B$$

where

$$dZ_B = {}_oT_L(3) - {}_oT(3)$$

and the viscous damping force is computed as

$$F_{DB} = K_{DB} \cdot V_{ZB}$$

or $$F_{DB} = K_{DB} \cdot \frac{d}{dt}\left[{}_oT_L(3) - {}_oT(3)\right]$$

It should be noted that V_{ZB} is the relative velocity between the dynamic boom tip position ${}_oT_L(3)$ and the rigid boom tip position ${}_oT(3)$, whereas the boom tip velocity in inertial space is defined as ${}_oT_{VA}(3)$.

The block diagram implementation of these equations is presented in Figure 5.2. At time $t = 0$ or at the beginning of the simulation, the initial boom tip velocity and boom tip position must be defined. The boom tip velocity ${}_oT_{VA}(3)$ is always taken as the first derivative of ${}_oT(3)$; in other words,

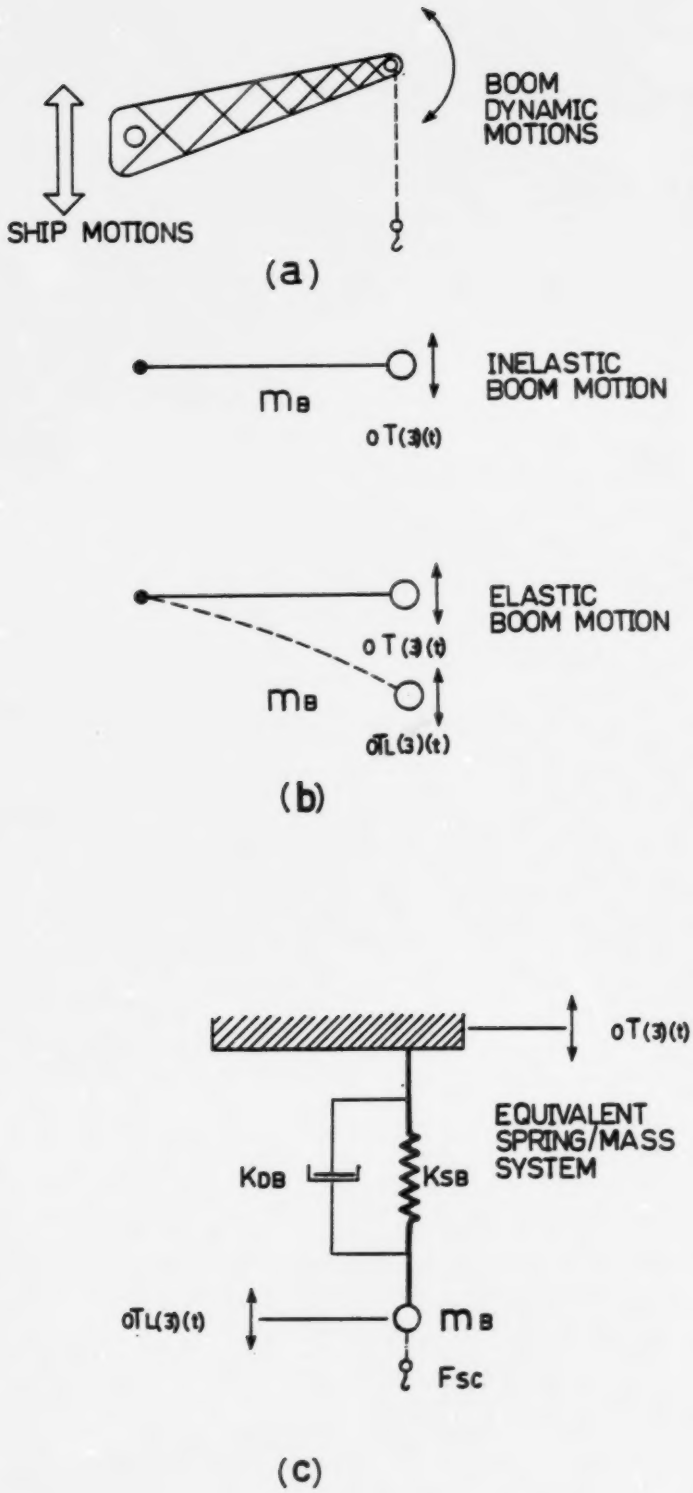

Figure 5.1 Crane Boom Model

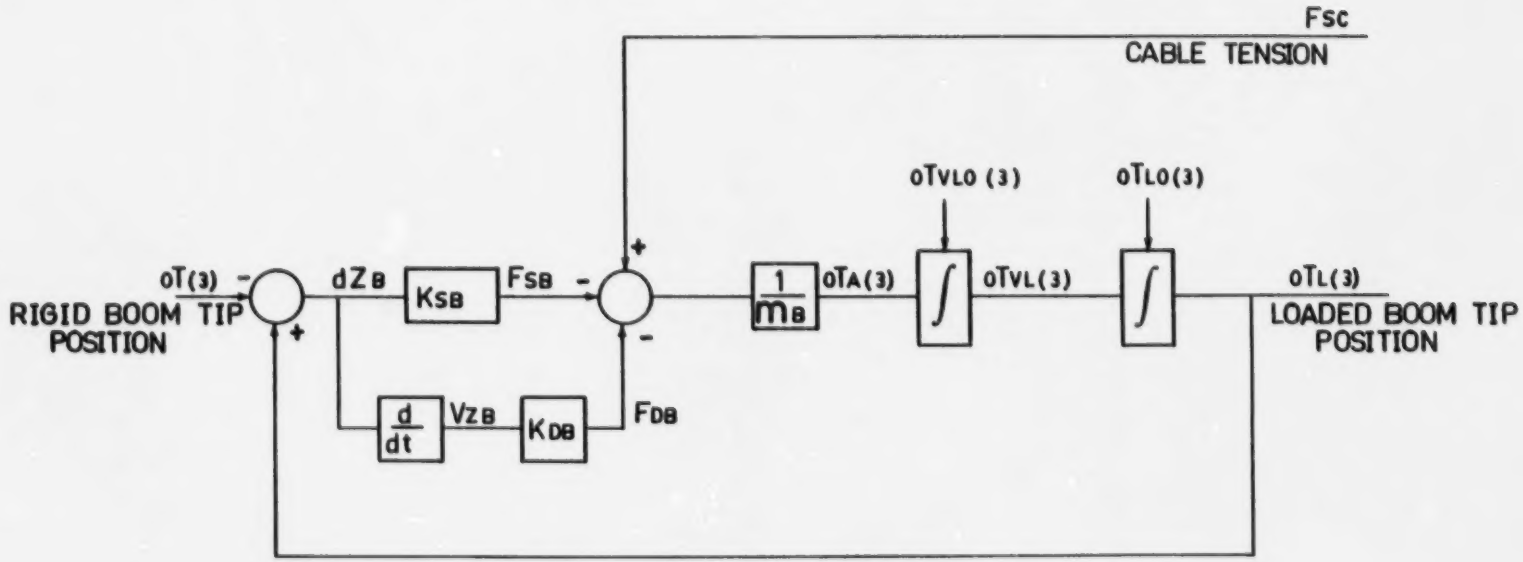

Figure 5.2 Crane Boom Model Block Diagram

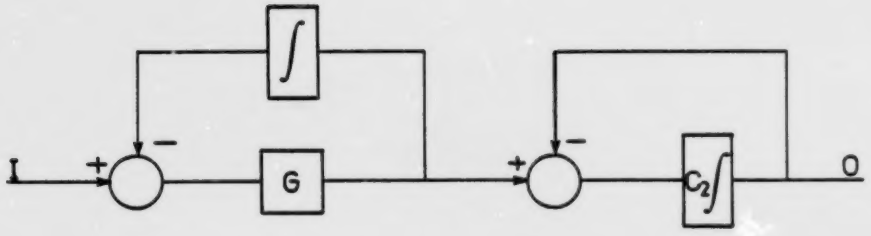

(a) DIFFERENTIATOR IMPLEMENTATION

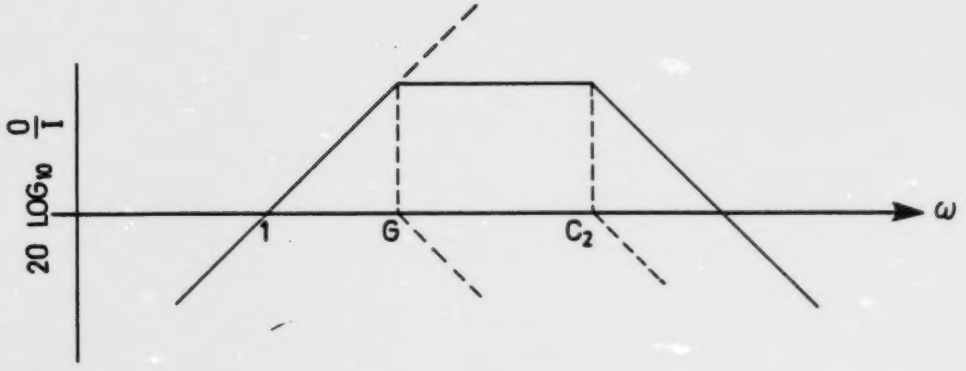

(b) DIFFERENTIATOR RESPONSE

Figure 5.3 Differentiator Performance

the elastic boom tip velocity initially equals the inelastic boom tip velocity. The elastic boom tip position at time $t = 0$ is defined as

$$ {}_{o}T_{L_o}(3) = {}_{o}T_{o}(3) + \frac{m_L \cdot g}{K_{SB}} $$

where m_L is the load mass and g is the acceleration due to gravity. This is the static deflection from the unaccelerated suspended load.

The analog patching for these equations is contained in the Appendix A as Figure 2-1.

Of further note in the analog implementation is the method of differentiating the boom deformation to obtain relative velocity. Pure differentiation amplifies noise, making it necessary to limit the bandwidth of the differentiator with at least a two pole filter. The block diagram of the implementation is given in Figure 5.3(a) and its equivalent transfer function is

$$ \frac{O}{I} = \frac{s}{\left(s\frac{1}{G_{diF}} + 1\right)\left(s\frac{1}{C_2} + 1\right)} $$

The values of G_{dif} and C_2 are the break frequencies of the poles of the filter. An asymptotic Bode plot of the transfer function is shown in Figure 5.3 (b).

5.2 Crane Cable and Load Model

5.2.1 Vertical Dynamics

The dynamic behaviour of the cable and load in the vertical direction is similar in many respects to the crane boom model. Taking the vertical response as being independent of the horizontal (or pendulous) motions, the following assumptions apply:

- the load is a point mass;

- pendulous accelerations do not affect cable tension;

- the cable has weak damping;

- the effective spring constant of the cable is independent of the cable length over the range of interest.

The position a load would take with an inelastic cable of length S_C is defined as ${}_oL(3)$. This position is dependent on the loaded boom tip position ${}_oT_L(3)$ and varies with time. When allowance is made for cable elasticity, the load position becomes ${}_oL_L(3)$ as shown in Figure 5.4(a). This position is dependent on the three forces:

F_{SC} cable spring force

F_{DC} cable damping force

$m_L g$ load weight

The acceleration of the load is computed from the force balance as

$$a_{ZC} = \frac{1}{m_L} (F_{SC} - F_{DC} + m_L g)$$

Similarly to the boom model, the cable tension or spring force and damping force are calculated as

$$F_{SC} = K_{SC} \cdot dZc$$

and

$$F_{DC} = K_{DC} \cdot \frac{d}{dt} \left[{}_oT_L(3) + S_C - {}_oL_L(3) \right]$$

Once again it is noted that damping forces are dependent on the relative velocity V_{ZC} between load and boom tip, while the vertical load velocity in inertial space is defined as ${}_oL_{LV}(3)$.

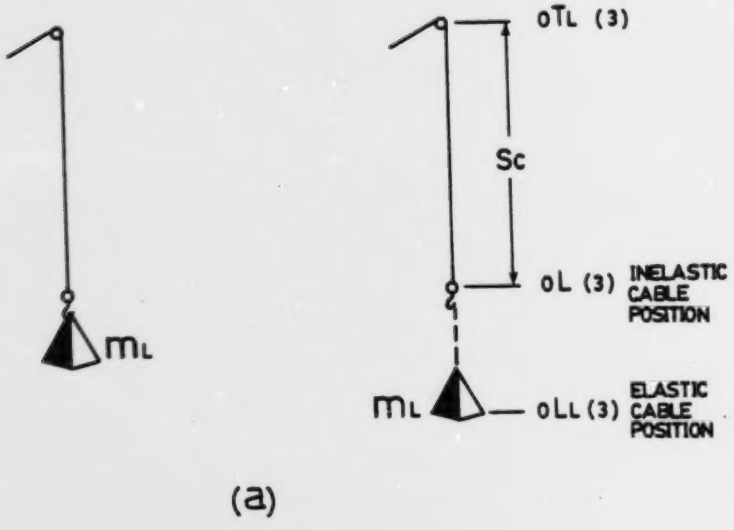

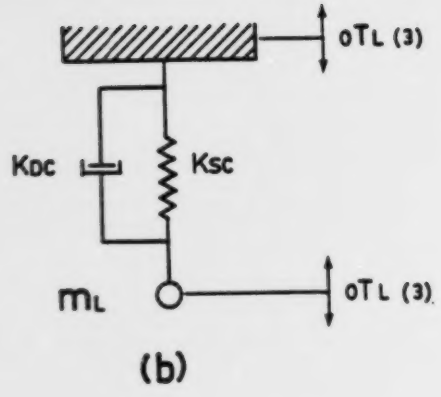

Figure 5.4 Crane Cable Model

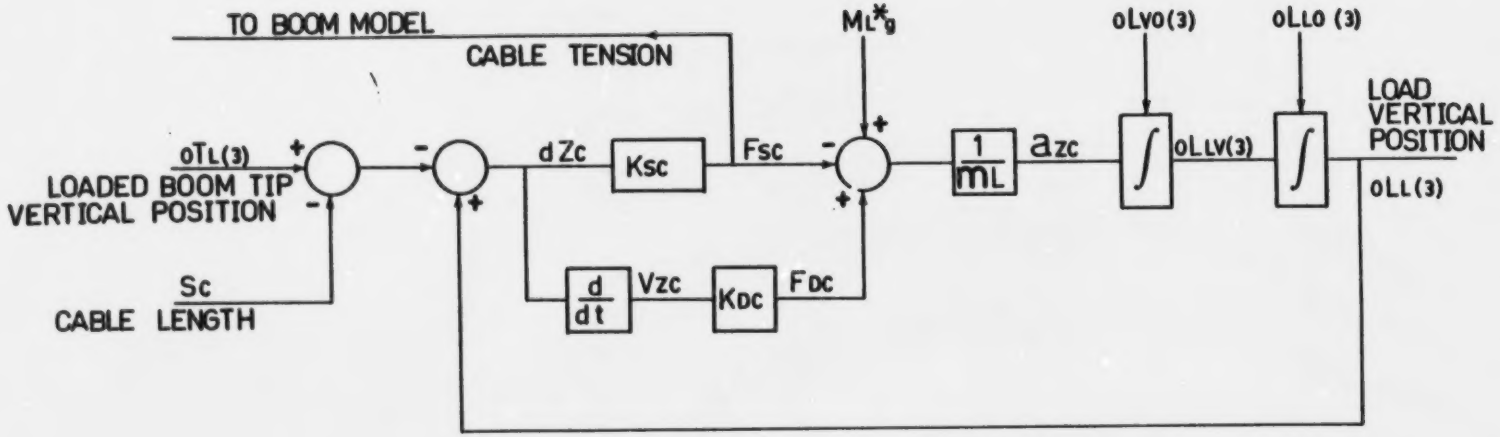

Figure 5.5 Crane Cable Model Block Diagram

The block diagram implementation of these equations is shown in Figure 5.5. At time $t = 0$, the initial load position is set to a position defined by the sum of the initial loaded boom position, plus the initial cable length S_{Co}, plus the elastic cable stretch established by the static cable deflection, or

$$ {}_{o}^{L}L_{o}(3) = {}_{o}^{T}L_{o}(3) + S_{C} + \frac{m_{L}g}{K_{SC}} $$

The initial load velocity in inertial space is the sum of the inelastic boom tip velocity plus the initial cable rate. As with the boom model, the velocity giving rise to viscous damping is taken as zero at time $t = 0$.

The analog patching for the cable model is contained in the Appendix as Figure 2-1. The analog implementation embodies the same differentiation technique with the same filter time constants as in the crane boom model.

5.2.2 Pendulous Motion

The following assumptions were made in developing a model of the pendulous action of the load:

- the range of the pendulous motion is small such that small angle assumptions pertain ($S_{c} >> \Delta x, \Delta y$);
- motions in the fore and aft direction are independent of motions in the athwartships direction;
- vertical accelerations due to pendulous motions are small relative to other vertical forces;
- cable mass is negligible and the cable remains straight with its line of action passing through the centre of the load;
- the unloaded and loaded cable lengths are approximately equal;
- the load is taken as a point mass with no angular acceleration;
- damping forces act on the load itself rather than on the cable.

With reference to Figure 5.6 , the cable tension ${}_o\overline{F}_{SC}$ can be resolved into its constituent components defined as

$$ {}_o\overline{F}_{SC} = \begin{bmatrix} {}_oF_{SC}(1) \\ {}_oF_{SC}(2) \\ {}_oF_{SC}(3) \end{bmatrix} = \begin{bmatrix} F_{SCX} \\ F_{SCY} \\ F_{SCZ} \end{bmatrix} $$

Using the small angle assumptions,

$$ F_{SCZ} \approx \left| F_{SC} \right| $$

and

$$ F_{SCX} = \frac{\Delta X}{S_C} \cdot \left| F_{SC} \right| $$

$$ F_{SCY} = \frac{\Delta Y}{S_C} \cdot \left| F_{SC} \right| $$

A force balance on the load in X direction gives

$$ \frac{F_{SCX} - F_{DX}}{m_L} = a_x $$

where F_{DX} is the damping force.

Damping, which would be a combination of aerodynamic drag and mechanical damping in the cable, is treated as a function of the square of the load velocity in the X-direction

$$ F_{DX} = K_{CD} V_X^2 $$

Now K_{CD} is defined as

$$ K_{CD} = \frac{1}{2} \rho A_E C_D $$

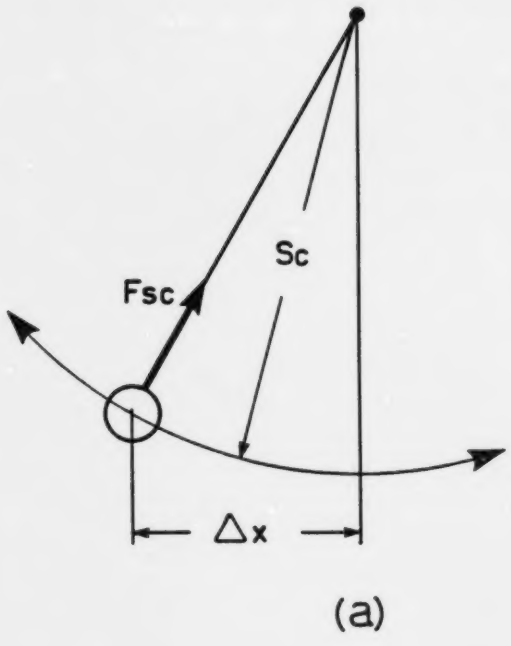

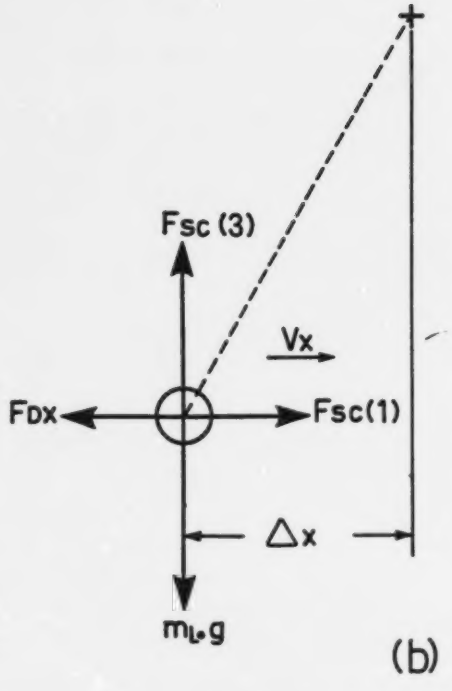

Figure 5.6 Pendulous Motion Model

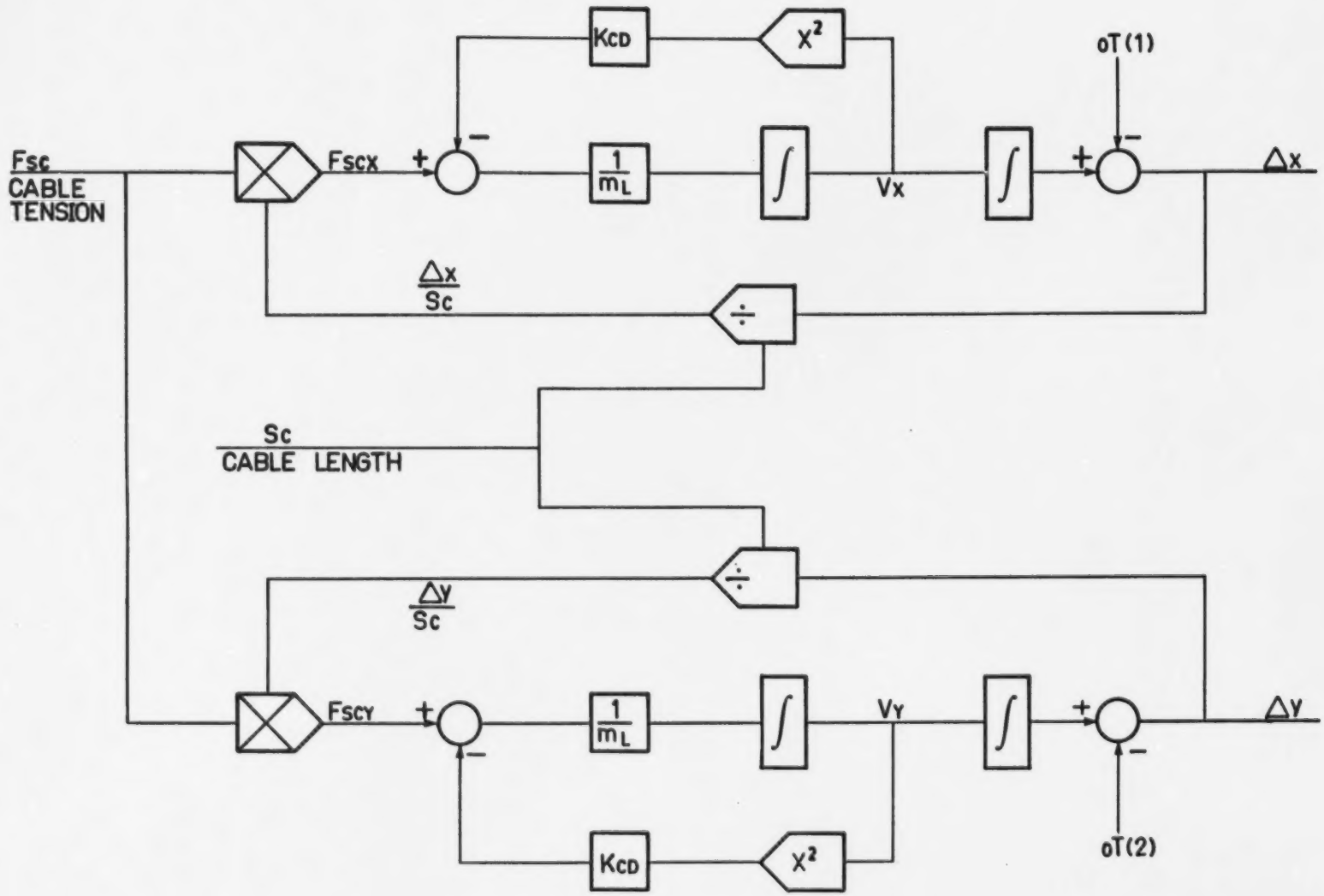

Figure 5.7 Pendulous Motion Block Diagram

where ρ = density of air Kg/m^3

A_E = effective area m^2

C_D = non-dimensional drag coefficient

The values of A_E and C_D are adjusted to make allowance for the mechanical damping in the cable. It is suggested that realistic values of this damping force be determined experimentally using equipment similar to that being studied.

Integration of the acceleration in the X-direction provides the load velocity, V_X and a second integration gives the X-coordinate of the load in the o-frame. From this is subtracted ${}_oT(1)$, the rigid crane boom tip X-coordinate, to arrive at the displacement ΔX of the load relative to the crane boom tip. Using ΔX and the current unloaded cable length S_C, the component of the tension in the X-direction is then computed as previously shown. The initial velocity of the load in the X-direction at time $t = 0$ is set equal to the X-direction velocity of the rigid boom tip ${}_oT_{Vo}(1)$ and the initial position of the load in the X-direction is defined by the initial position of the crane boom tip ${}_oT_o(1)$.

Formulation of the Y-direction equations is exactly analagous. Implementation of these equations is shown in block diagram form in Figure 5.7 and the analog patching diagrams are contained in the Appendix as Figure 2.2.

5.3 Human Operator

5.3.1 Background

The task of the human operator is to control the vertical motion of the load in response to visually perceived errors. His task is complicated by motions of the vessel upon which the crane is mounted, and motions of the vessel onto which the load is to be lowered. The sum of these external disturbances is referred to as the system forcing function, i(t), and is pseudo-random in nature, as developed in the sea state model.

The error $e(t)$ perceived by this operator may be the difference between the load closing speed with deck 2, and a desired load closing speed known to the operator to be safe. It could also be the difference between the height of the load above deck 2 and a height at which the operator would like to maintain the load. The first case is termed rate control and the second is an example of position control (see Figure 5.8). In either case, the operator attempts to minimize $e(t)$ by manipulating the winching rate in order to overcome the motions of the vessels. The operator's output or control demand is termed $c(t)$, the crane response is denoted by $m(t)$. Using these definitions, and denoting the human operator describing function as Y_p and the crane dynamics transfer function as Y_c, the block diagram shown as Figure 5.8 (c) supports the following discussion of the behaviour of the human operator.

An important characteristic of the human operator is his ability to adapt to the element he is controlling. The operator's ability to adapt is most influenced by the bandwidth of the input or forcing function, $i(t)$. In the crane dynamics model, the bandwidth of the input function, termed ω_i, is the highest circular frequency transmitted through the vessels from the sea spectrum. For a sea state of 2 and a forward speed of 2.5 m/s (4.9 knots), the vertical motion spectrum typically covers the range 1.5 to 3.9 rad/s so $\omega_i = 3.9$ rad/s. In sea state 5, vessel motions occur in a frequency band of about 0.4 to 1.1 rad/s. As the input bandwidth increases, the operator's capacity for suppressing the disturbance deteriorates. By measuring the product $Y_p Y_c$, called the open loop gain, and plotting this versus input bandwidth ω_i, a characteristic curve similar to Figure 5.9 results. An examination of the curve shows the following:

- at very low frequencies, the modulus is high, indicating the operator is capable of producing good suppression of the error signals.

- as the input bandwidth increases, the modulus decreases at a near constant rate of -20 dB/decade.

- the point at which the modulus becomes unity (0 dB) is called the crossover frequency, and is generally of the order of 3 to 4 rad/s, depending on the characteristics of Y_c.

- as ω_i continues to increase, the modulus also increases

while the angle by which the output lags the input increases. This phenomenon is attributed to the neuromuscular characteristics of the operator.

It should be noted that whenever the bandwidth of the disturbing function under which the human operator is performing approaches the crossover frequency, a loss of performance occurs. This regression phenomenon results in a decrease in crossover frequency.

5.3.2 Mathematical Model

The general precision model for a single loop system is given by:

$$Y_p = K_p e^{-j\omega\tau_d} \left(\frac{T_L j\omega+1}{T_I j\omega+1}\right)\left(\frac{T_k j\omega+1}{T'_k j\omega+1}\right) \frac{}{(T_{N_1} j\omega+1)\left[\left(\frac{j\omega}{\omega_N}\right)^2 + \frac{2\zeta_N}{\omega_N} j\omega+1\right]}$$

Where:

Kp - gain

$e^{-j\omega\tau_d}$ - pure time delay

$\frac{T_L j\omega+1}{T_1 j\omega+1}$ - adaptive equalization characteristics

$\frac{T_K j\omega+1}{T'_K j\omega+1}$ - very-low-frequency lag-lead

$\frac{1}{\left(T_{N1} j\omega+1\right)\left[\left(\frac{j\omega}{\omega_N}\right)^2 + \frac{2\zeta_N}{\omega_N} j\omega + 1\right]}$ - neuromuscular actuation system

The general describing function representing the human operator characteristics must be adjusted or modified with regard to

- stability criteria,

- input forcing function bandwidth,

- controlled element characteristics.

The source of the input forcing function for typical at-sea lifting operations is the motion of the vessels in response to the sea condition. This bandwidth varies from about 0.2 to 1.6 rad/s with the vessels at rest, up to about 5 rad/s at a 10 Kt forward speed. From an operator's point of view, this input spectrum does not encompass very low frequencies. With this in mind, the very low frequency compensation terms can be eliminated from the describing function, providing the gain K is modified by multiplying by the modulus of these terms taken at the frequency range of interest.

The general set of values of the parameters of the describing function given in Reference 4 for an input bandwidth of 1.5 rad/s are repeated here as Table 5.1.

Table 5.1 Constants For Human Operator Model

Name	Value	Unit
ω_i	1.5	rad/s
Kp	45.4	-
τ_d	0.128	s
T_L	1/0.59	s
T_i	1/0.92	s
T_K	1/0.30	s
T_K'	1/0.01	s
T_{N_1}	1/8.9	s
ζ_N	0.16	2
ω_N	16.6	rad/s

These values were used as the starting point in establishing final values for the human operator by tuning to meet the stability criteria. For the input spectrum under consideration here, and with the values of T_K and T_K' in Table 5.1, the modified initial operator gain K_p falls within a range of 1.5 to 2.7.

Reference 6 suggests the neuromuscular actuation term can be approximated by

$$\frac{1}{T_N j\omega + 1}$$

where

$$T_N = T_{N_1} + \frac{2\zeta_N}{\omega_N}$$

From the values of T_{N_1} and ζ_N in Table 5.1, the initial value of T_N becomes 0.132s.

The operator is faced with phase lags in the response of the system due to the response characteristics of the boom, cable and winch. His ability to anticipate and correct for these characteristics is provided by the lag/lead compensatory term. Reference 6 recommends that the value for T_L be chosen to partially compensate for the sum of $\tau_d + T_N$.

where

T_N is defined as above.

The value given in Table 5.1 already exceeds this sum and so was readjusted to 0.026s. The lag factor T_I was set to 1.0s to provide a good low frequency closed-loop response to the system forcing function.

The pure time delay $e^{-j\omega\tau_d}$ required in the describing function presented some technical difficulties in its implementation on the analog computer. It was modelled as a first order Pade approximation by the transfer function

$$e^{-j\omega\tau_d} = -\frac{\frac{\tau_d}{2}\cdot j\omega - 1}{\frac{\tau_d}{2}\cdot j\omega + 1}$$

The response of the Padè approximation to a spectrum of sine waves is quite accurate. Its response to step or pulse inputs is not, so any initial transients associated with such tests must be disregarded when this approximation is used.

With the foregoing simplifications included, the human operator describing function becomes

$$Y_p = K'_p \frac{\frac{\tau_d}{2} j\omega - 1}{\frac{\tau_d}{2} j\omega + 1} \cdot \frac{\tau_1 j\omega + 1}{\tau_1 j\omega + 1} \cdot \frac{1}{\tau_N j\omega + 1}$$

The analog implementation of this model is contained in the Appendix, and a block diagram (extended to include the controlled element proportionality constant K_C) is shown in Figure 5.10.

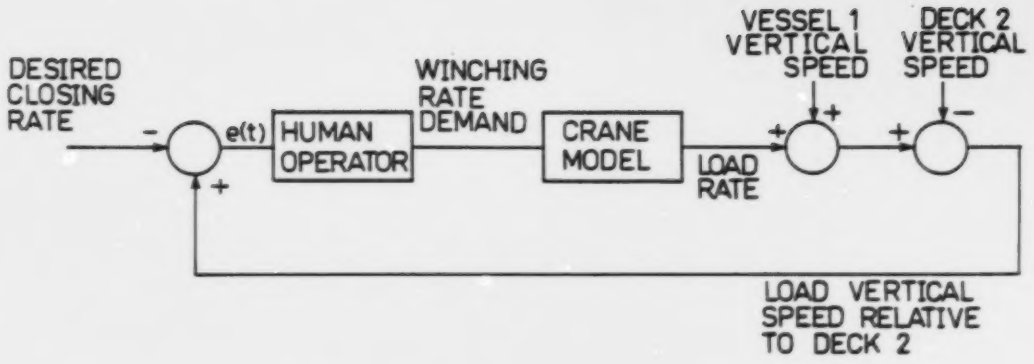

(a) RATE CONTROL DIAGRAM

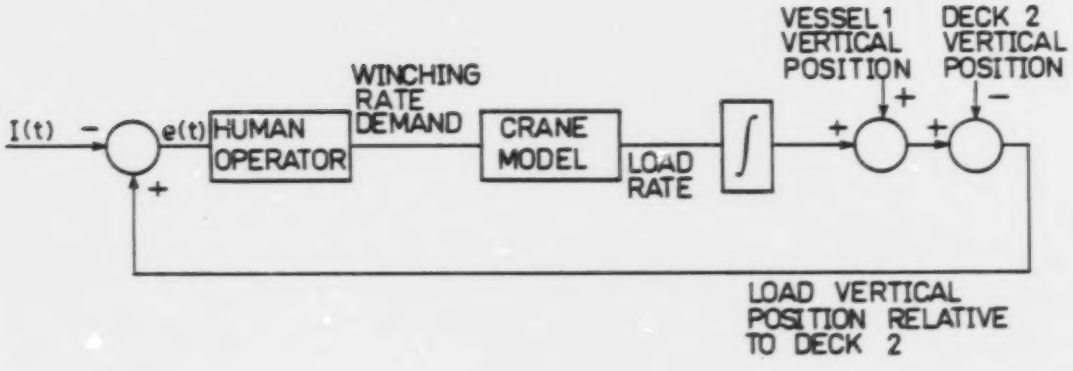

(b) POSITION CONTROL DIAGRAM

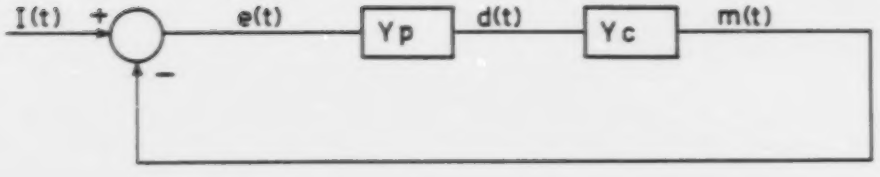

(c) OPERATOR - CONTROLLED ELEMENT MODEL

Figure 5.8 Human Operator Transfer Function

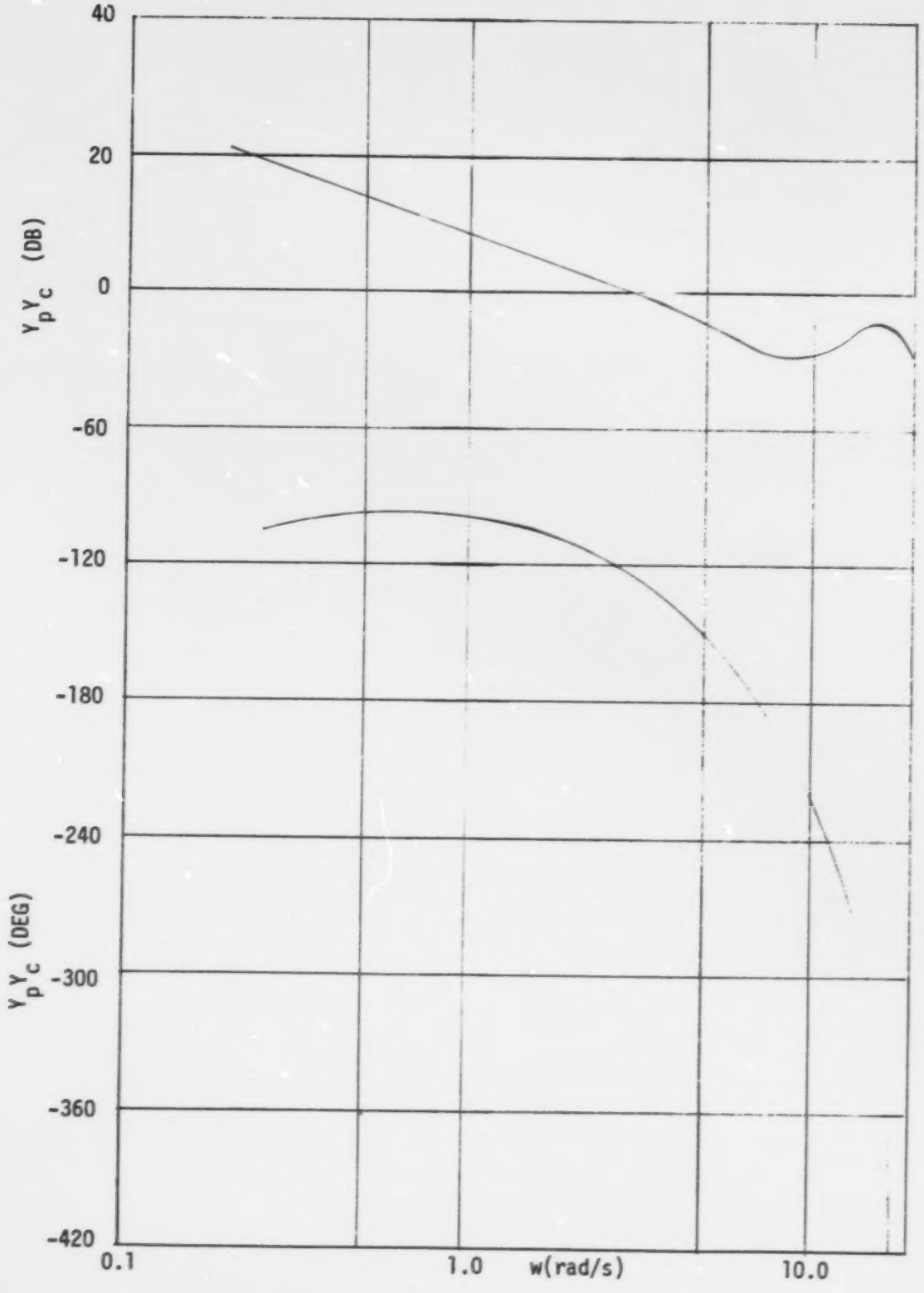

Figure 5.9 Operator-controlled Element Open Loop Response

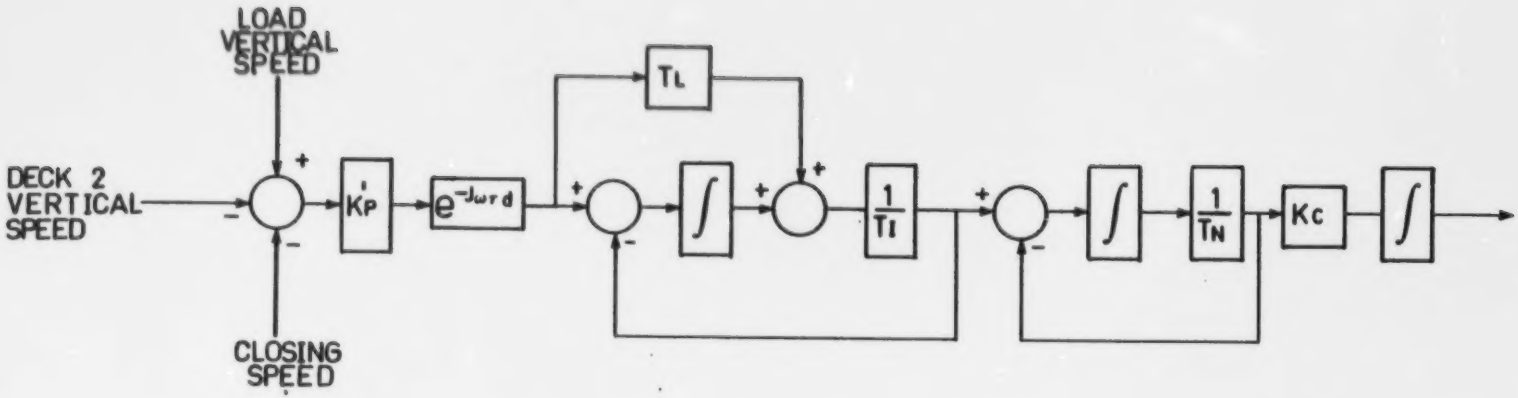

Figure 5.10 Human Operator Model Block Diagram

5.4 Winch Model

An important part of the operating loop is the winching system. Its characteristics, especially its limitations, have a pronounced effect on the performance of the operator at his task.

The model provided as part of the simulation is similar in characteristics to a hydraulic motor driven winch, supplied by a pressure compensated pump powered by an electric motor. The characteristics of this system include

- maximum winching rate limits set by maximum system flow capacity;
- maximum cable tension limit;
- maximum power limit established by the rating of the electric motor.

The block diagram for this system is shown as Figure 5.11. Here, the operator-commanded winching rate, S_{CV}, is limited to maximum positive and negative values L_{SCV} based on the limitations of the physical system being modelled. This rate limited command may be further modified to conform with tension and power limits. Cable tension F_{SC} is subtracted from the maximum tension allowed, $_{M}F_{SC}$, and the difference multiplied by the tension limiter gain G_{FMX}.

When this product is negative, meaning the tension limit has been exceeded, it is subtracted from the modified winching rate command, resulting in a reduced winching rate. In cases of extreme overtension, line will actually be payed out.

The power limit operates in a somewhat similar fashion. Cable power, P_C is computed as the product of winching rate and tension. When the power so computed exceeds the limit set by $_{M}P_C$, the product of the error and the power limit gain G_{PMX} reduces the command winching rate accordingly. The modified winching rate S_{CV} is then integrated to give the length of cable payed out.

At the beginning of the simulation the amount of cable initially payed out must be set as an initial condition, S_{CO}. This can be any positive value within the lifting range of the crane.

Although the model described above is of a specific system type, the flexibility of analog programming allows alternate systems to be easily modelled.

The analog programming for this model is shown as Figure 2-3 in Appendix.

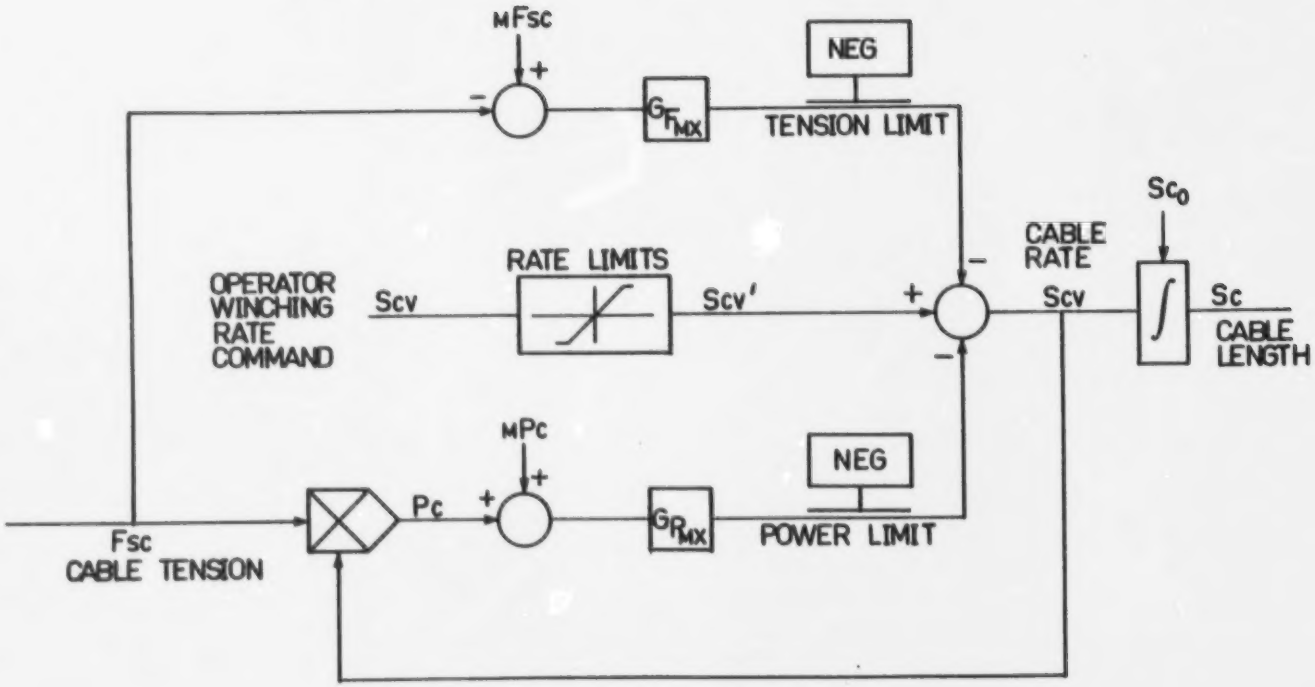

Figure 5.11 Winch Model Block Diagram

6.0 EVALUATION

In order to demonstrate the application of the program and to evaluate its usefulness, a load transfer situation was modelled and the performance of an operator was measured both with and without compensation. In the first phase of the project, only head seas were considered and observations were confined to motions in the vertical direction. During the second phase, operations in quartering seas were simulated and motions in all six degrees of freedom were modelled; however, the response of the operator was restricted to corrective action in the vertical direction only.

This section of the report describes the test program, and analyzes the results to provide an assessment of the usefulness of motion compensation in crane operations at sea.

6.1 Input Data

6.1.1 Sea State

In choosing sea states in which to model the lifting operations, it is desirable to span the range from a nearly-calm sea with only enough ripple to cause a slight load disturbance, to that sea state in which lifting operations are barely feasible. The sea states corresponding to these extremes are dependent on the sea keeping characteristics of the vessels involved, and to a lesser extent, on the geometry and positioning of the crane itself. An iterative procedure is necessary following the selection of vessels and crane parameters. Through experimentation, the sea states adopted for this study were sea states 2, 3, 4 and 5. Table 6.1 lists the characteristics of these sea states.

Table 6.1 Sea State Characteristics

Sea State Code	Description	Significant Wave Height Range (M)	Representative Significant Wave Height (M)
2	Smooth(wavelets)	0.1 - 0.5	0.3
3	Slight	0.5 - 1.25	1.0
4	Moderate	1.25 - 2.50	1.75
5	Rough	2.5 - 4.00	3.75

The energy ratios arbitrarily selected to define the discrete

spectral frequencies are listed in Table 6.2 where $K_5 = 1.0$ is the energy ratio of the central frequency. Four energy ratios were chosen to lie on either side of the central frequency energy ratio.

For the first phase of the project where only head seas were considered, an average vessel forward speed of zero was assumed so that the frequencies of encounter and the absolute frequency spectrum are the same. These spectral frequencies and their corresponding amplitudes based on the aforementioned energy ratios are given in Table 6.3 (a) for sea states 2, 4 and 5. The continuous traces of wave amplitude as a function of time shown in Figure 6.1 (a) are the summation of the spectral wave components with an initial phase angle established by a pseudo-random number generator. The absence of "stair-stepping" on these traces is an indication that the update rate of the digital computer is fast compared to the time frame of the wave generation process.

Table 6.2 Energy Ratios

K_1	K_2	K_3	K_4	K_5	K_6	K_7	K_8	K_9
0.10	0.31	0.54	0.71	1.00 (Default)	0.82	0.63	0.45	0.22

With the quartering seas modelled in the second phase of the project, an average forward speed of 2.5 m/s (4.9 kts) was assumed for each vessel. The sea spectrum parameters for this case are given in Table 6.3 (b) for sea states 2, 3, 4 and 5. Figure 6.1 (b) shows the resultant wave traces where, once again, the initial phase angles were defined in a random fashion. Also shown in this Figure are traces of the same sea states with a compressed time scale to illustrate the lack of periodicity of the seas used in the analyses. Figure 6.2 presents a line spectrum of the sea states in Figure 6.1 (b). The increased concentration of energy within a narrower frequency band as sea state increases is readily apparent.

Sea State	Freq. of encounter (rad/s)	1.592	1.735	1.853	1.945	2.293	2.679	2.946	3.246	3.864
2	Wave amplitude (m)	.010	.018	.023	.027	.032	.029	.025	.021	.015
Sea State	Freq. of encounter (rad/s)	.659	.718	.767	.805	.849	1.109	1.219	1.344	1.600
4	Wave amplitude (m)	.061	.107	.141	.161	.191	.173	.152	.128	.090
Sea State	Freq. of encounter (rad/s)	.450	.491	.524	.550	.649	.758	.833	.918	1.093
5	Wave amplitude (m)	.129	.228	.302	.346	.410	.372	.326	.275	.192

Table 6.3 (a) Frequency And Amplitude Spectrum - Ship Speed 0 Kts

Sea State 2	Freq. of encounter (rad/s)	2.238	2.502	2.728	2.908	3.633	4.507	5.159	5.930	7.669
	Wave amplitude (m)	0.014	0.025	0.032	0.037	0.042	0.036	0.031	0.025	0.017
Sea State 3	Freq. of encounter (rad/s)	1.066	1.180	1.277	1.354	1.658	2.016	2.277	2.583	3.258
	Wave amplitude (m)	0.046	0.080	0.105	0.119	0.137	0.120	0.103	0.085	0.057
Sea State 4	Freq. of encounter (rad/s)	0.770	0.850	0.917	0.970	1.179	1.422	1.599	1.804	2.252
	Wave amplitude (m)	0.081	0.140	0.183	0.209	0.242	0.213	0.183	0.152	0.102
Sea State 5	Freq. of encounter (rad/s)	0.502	0.552	0.594	0.627	0.756	0.904	1.010	1.133	1.397
	Wave amplitude (m)	0.170	0.297	0.389	0.444	0.517	0.459	0.397	0.330	0.224

Figure 6.3 (b) Frequency And Amplitude Spectrum - Ship Speed 4.9 Kts

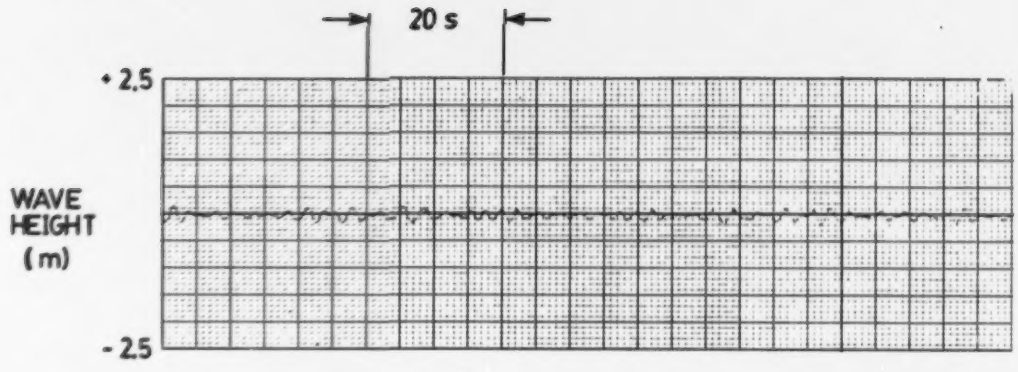

(a) SEA STATE 2, $\zeta_{1/3}$ =.3m

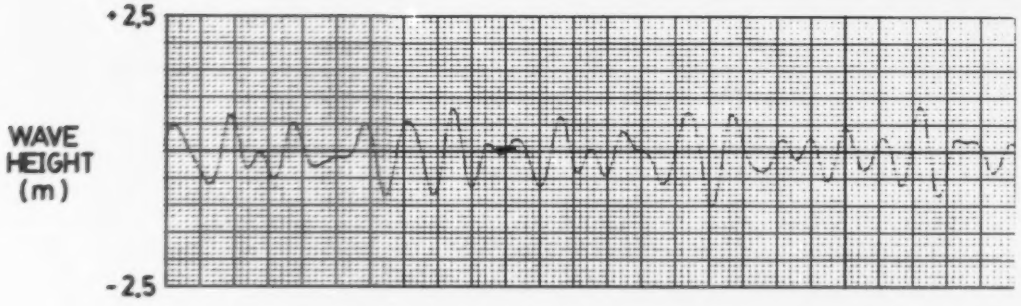

(b) SEA STATE 4, $\zeta_{1/3}$ = 1.75m

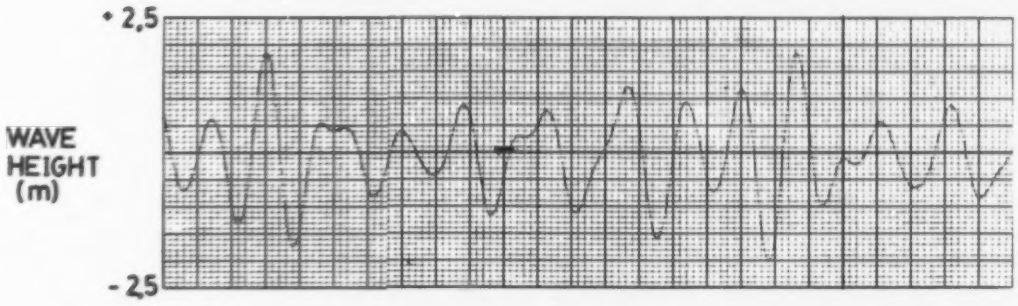

(c) SEA STATE 5, $\zeta_{1/3}$ = 3.75m

Figure 6.1 (a) Wave Height As A Function Of Time - Head Seas

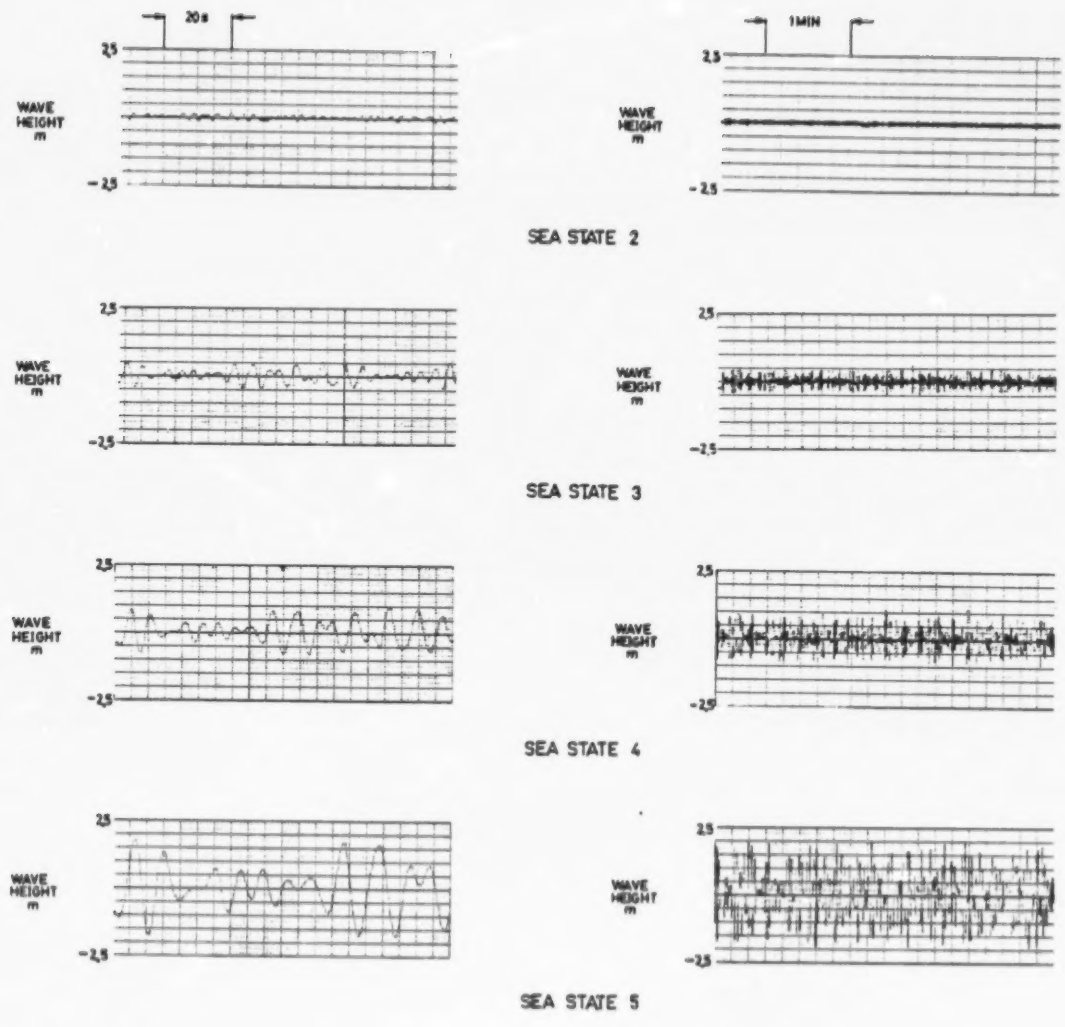

Figure 6.1 (b) Wave Height As A Function Of Time - Quartering Seas, 4.9 kts.

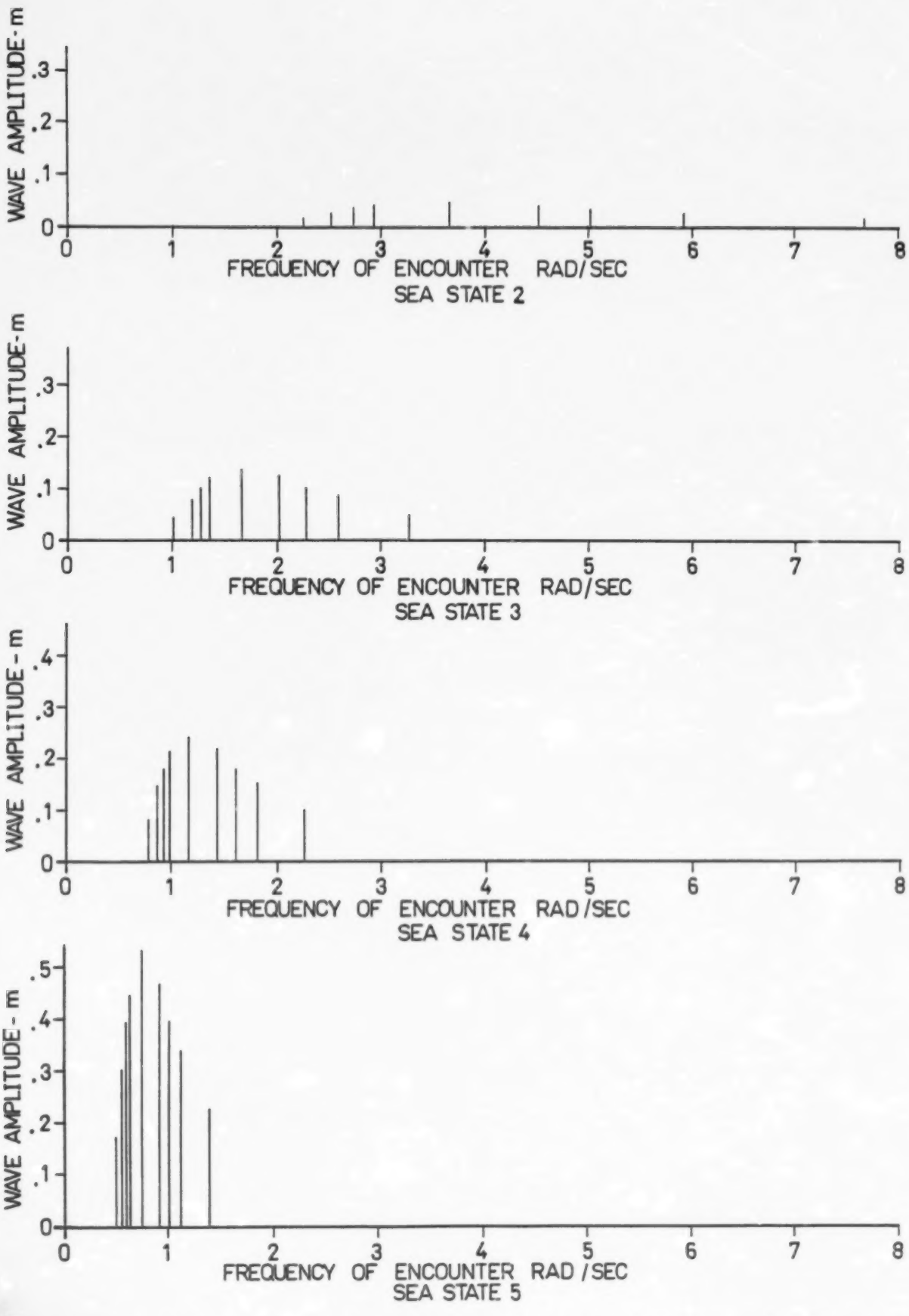

Figure 6.2 Discrete Sea Spectrum - Quartering Seas, 4.9 Kts.

6.1.2 Response Amplitude Operators

For the test program, two vessels were chosen for which response amplitude operator curves were already available. The first of these, upon which the crane would be mounted was a C4S1A cargo ship; the second was a barge designated an LCU-1610. Their relevant physical parameters are summarized in Table 6.4.

Table 6.4 Vessel Characteristics

Vessel	Length m (ft)	Beam m (ft)	Draft m (ft)	Displacement tonnes (L tons)
C4S1A	160.9 (528.0)	23.0 (75.7)	5.40 (17.96)	10160.5 (10000)
LCU-1610	36.1 (124.9	8.8 (29.0)	0.43 (1.40)	55.9 (55.0)

The RAO curves for these vessels were computed with program RELMO at the Naval and Civil Engineering Laboratory, USA, and reported by Summey and Watson in Reference 7. An advantage of this program is that the RAO curves it generates are independent of the forward velocity of the vessel.

The characteristic curves for the head seas condition are shown in Figure 6.3 (a) for both vessels. Because the head seas study was limited to one dimension, only the vessels' response in the pitching and heaving degrees of freedom need be considered.

For the three dimensional study with quartering seas, all six RAO curves are required for each vessel. These are shown in Figure 6.3 (b) and (c). The RAO curves used from Reference 7 were digitized and stored as data files in the computer. The curves reproduced in Figure 6.3 are computer-drawn using linear interpolation between points.

When the Crane Dynamics program is run with both the sea state model and the ship response model activated, the angular rotations of each vessel and the positions of their centres of gravity with respect to the mean centre of gravity position, are continuously calculated.

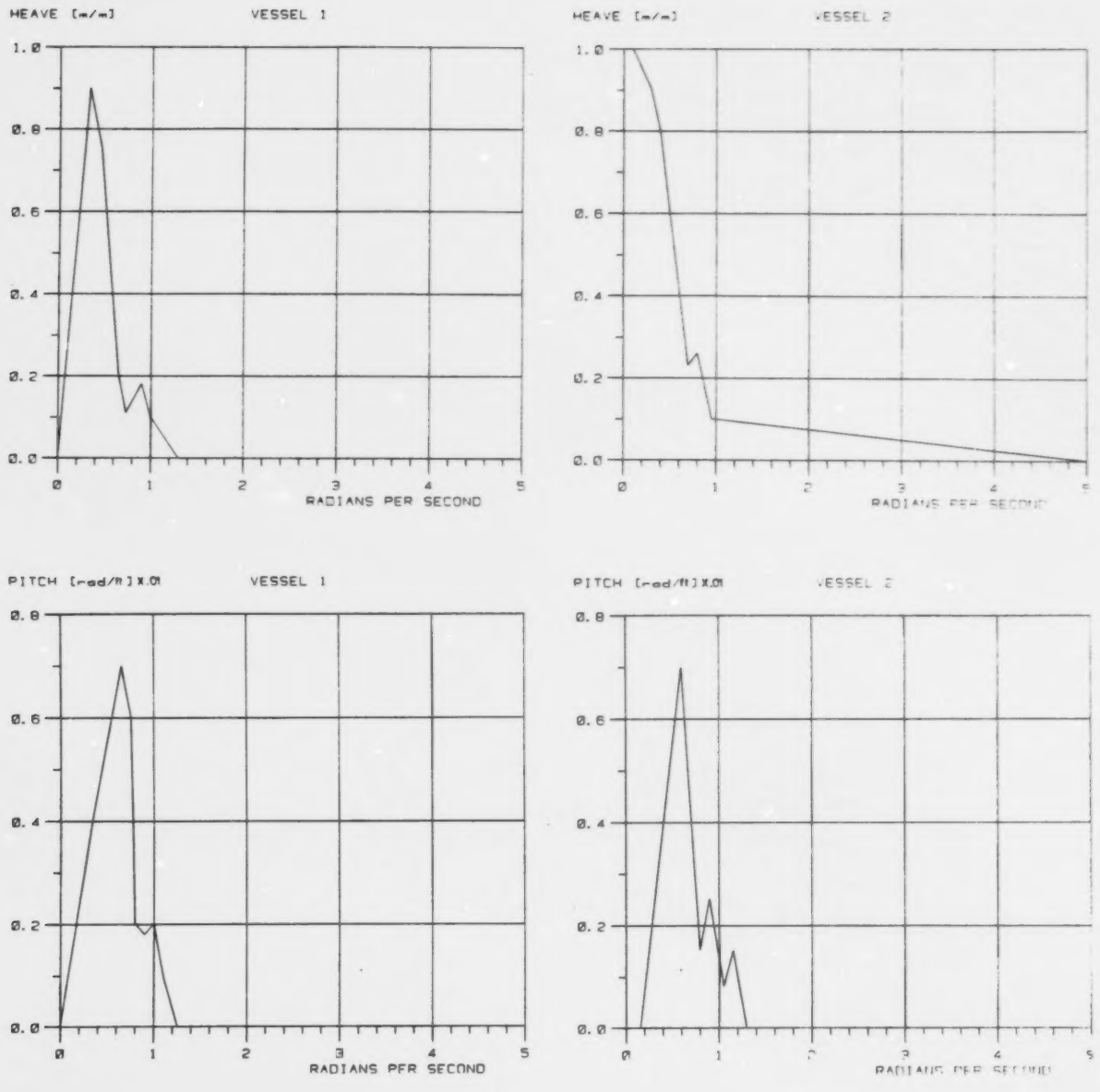

Figure 6.3 (a) Response Amplitude Operators - Head Seas

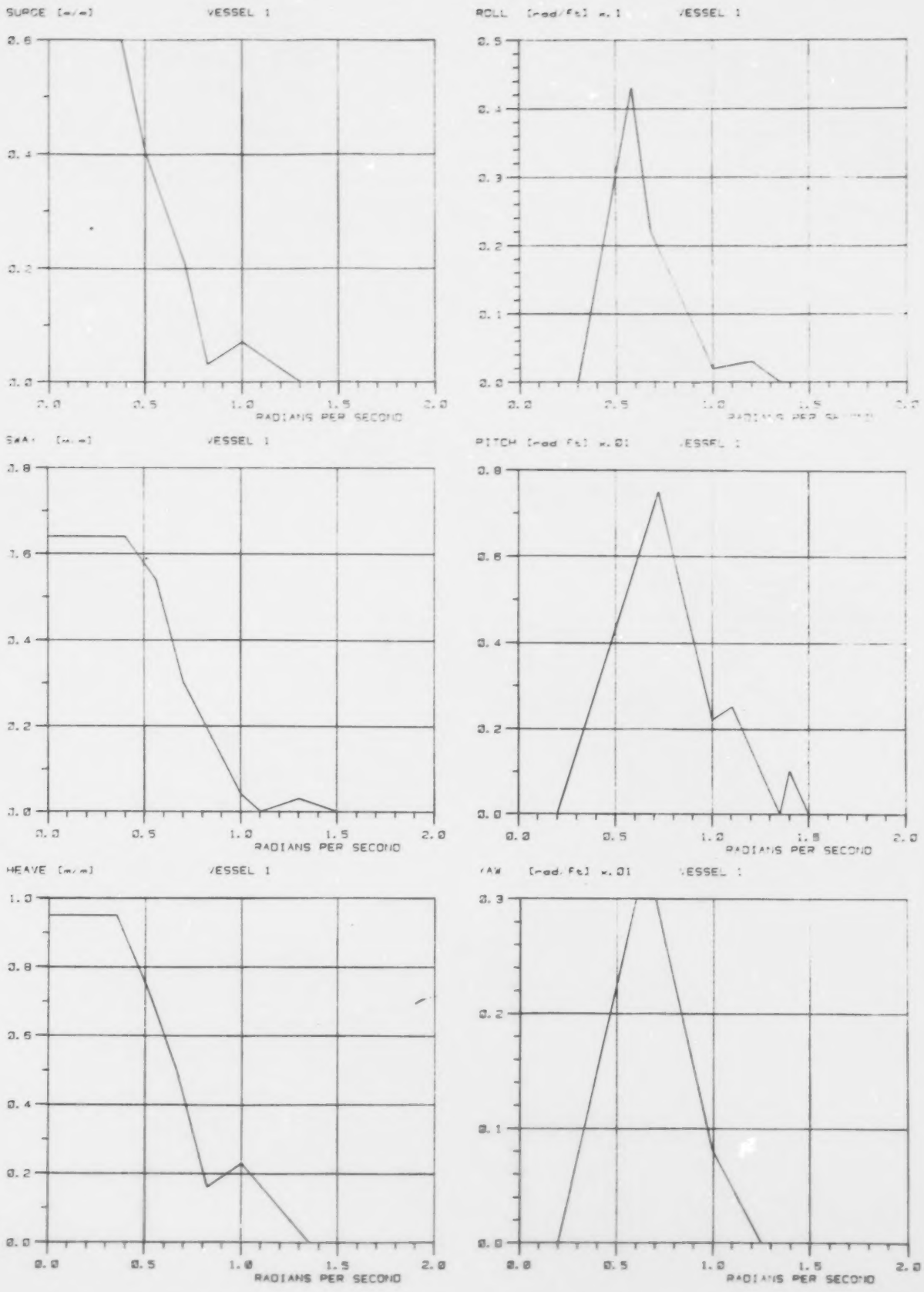

Figure 6.3(b) Response Amplitude Operator -Quartering Seas, Vessel 1

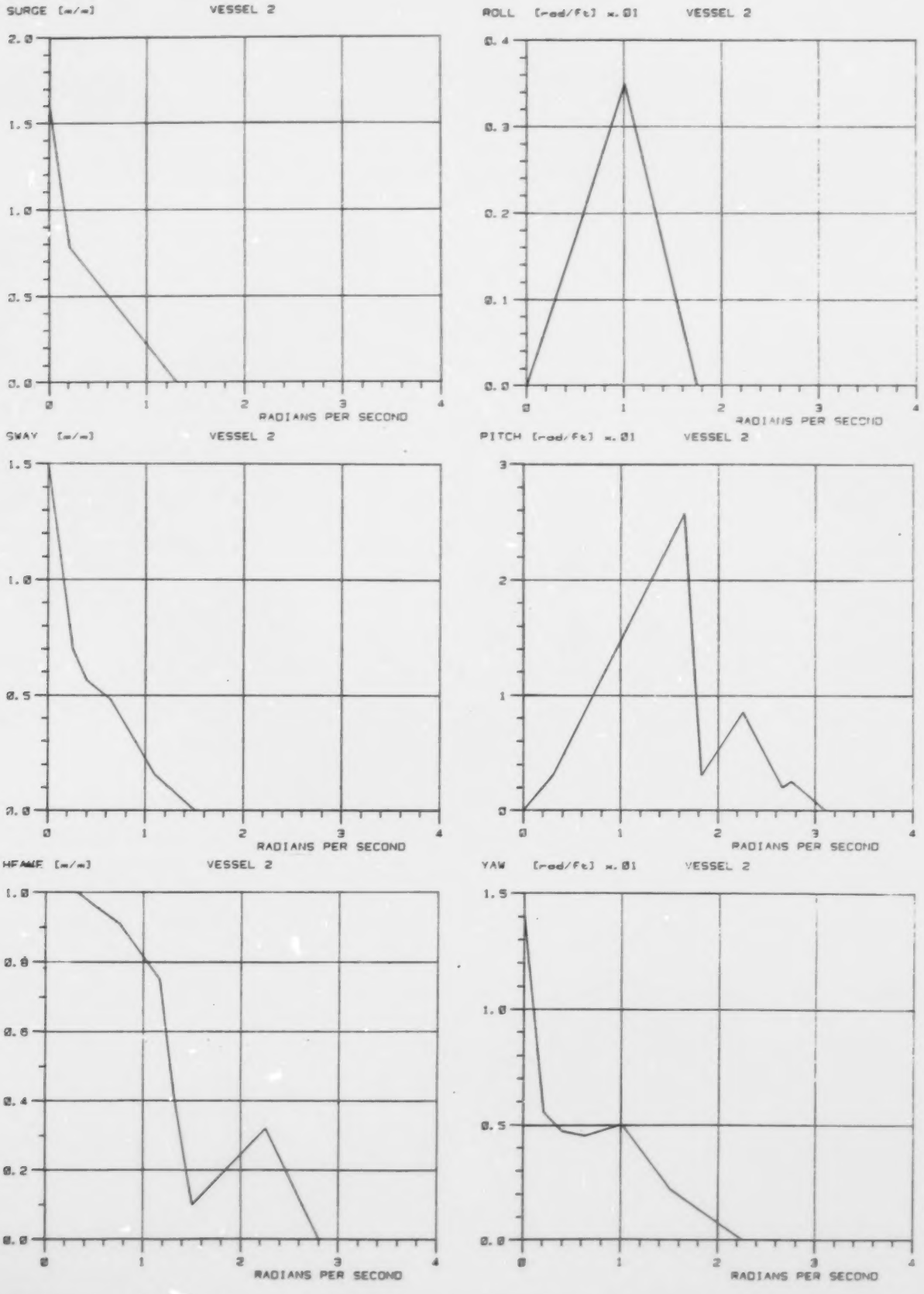

Figure 6.3(c) Response Amplitude Operator -Quartering Seas, Vessel 2

Records of the pitch and heave response of the vessels for sea states 2, 4 and 5 with head seas are shown in Figure 6.4 (a). For quartering seas, the vessels' response in all six degrees of freedom is shown in Figures 6.4 (b), (c) and (d), for sea states 3, 4 and 5 respectively.

An inspection of these traces reveals the following:

For head seas and 0 Kts forward speed:

- the pitch response of both vessels is zero in sea state 2, and heave is barely discernible.

- as sea state increases, vessel 2 follows the long period waves very closely in its pitch and heave response; the response of the first vessel also increases in amplitude and period but not to the same extent as vessel 2.

For quartering seas and 4.9 Kts forward speed:

- in addition to the foregoing comments which still pertain, vessel 1 shows a greater susceptibility to rolling motion as sea state increases than does vessel 2; this is attributable to the concentration of wave energy in a narrower frequency band close to the vessel's rolling natural frequency.

- vessel 2 shows a greater increase in pitching motion with increased sea state.

- the yawing response of vessel 1 remains well damped at higher sea states, in contrast to that of vessel 2.

6.1.3 Crane Data

The motion traces of Figures 6.4 (a) through 6.4 (d) were of the vessels' centres of gravity. For any other location, the effect of the angular rotations ϕ , θ , and ψ is to amplify the excursions about its mean position. When the coordinate positions of the crane boom tip on vessel 1 and the load deck on vessel 2 are specified, the centre of gravity motions can be transformed into boom tip and load deck motions. The crane base location coordinates in the G-frame, or vessel 1 coordinate axes, are given in Table 6.5. To these must be added the boom tip polar coordinates in the C frame or crane coordinate axes system. For the fixed boom portion of the simulation, the crane coordinates were adjusted manually using potentiometers on the analog console, to the values shown in Table 6.6. These polar coordinates show the boom to be extended to a length of 8 m; to be at a zero elevation angle or parallel with the horizon; and to be positioned

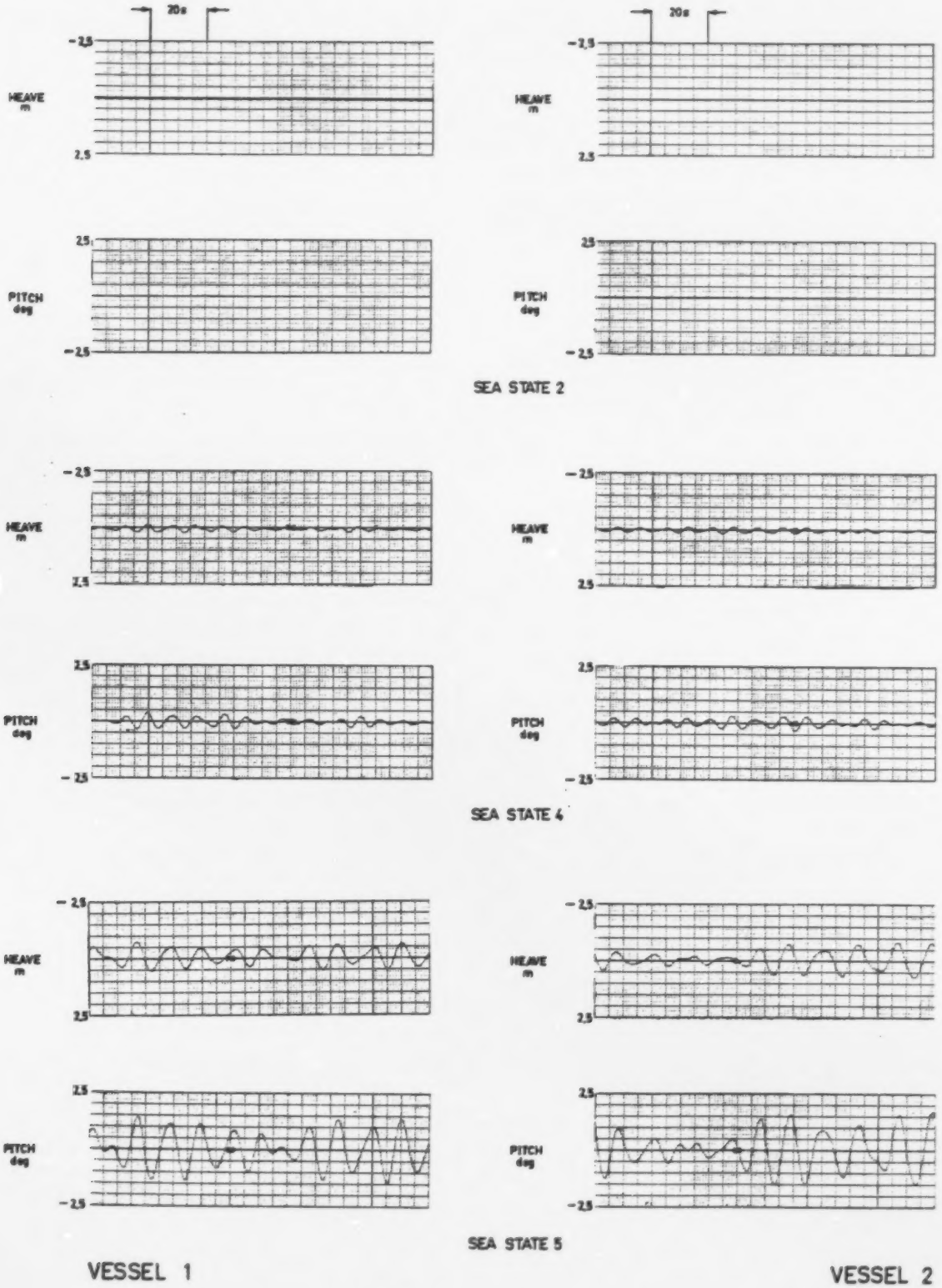

Figure 6.4 (a) Vessel Response - Head Seas, 0 kts

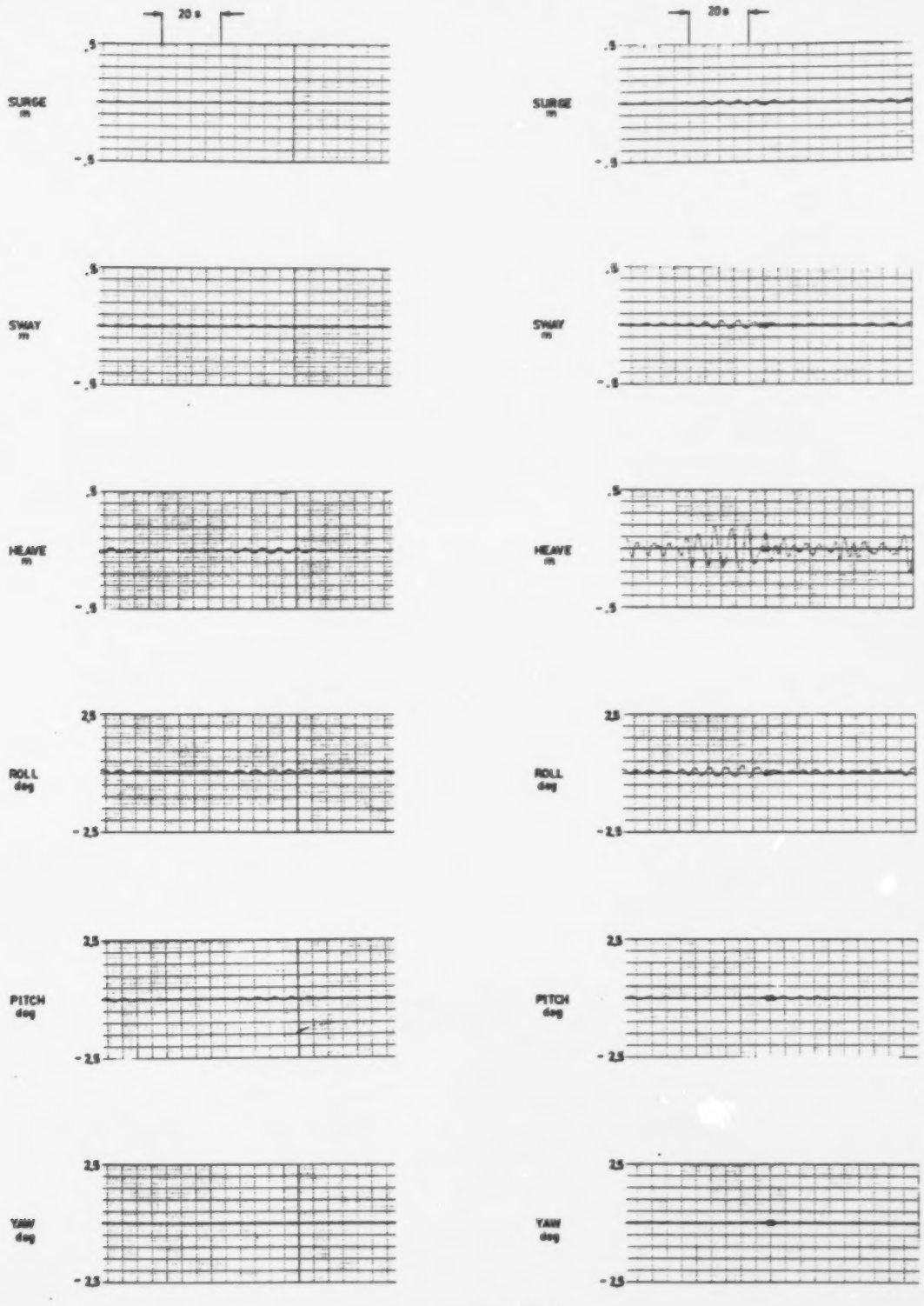

Figure 6.4 (b) Vessel Response - Quartering Seas, 4.9 kts

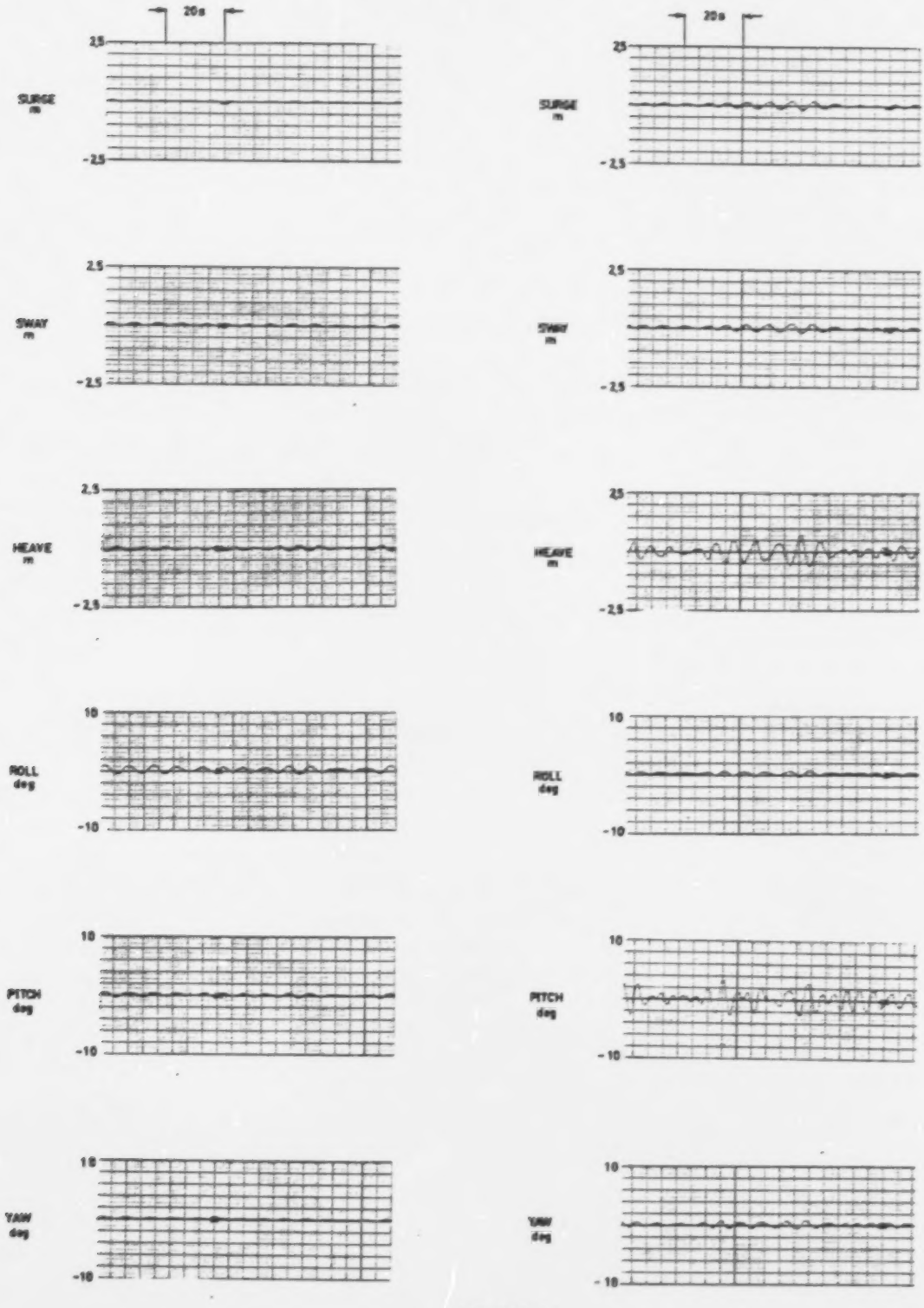

Figure 6.4 (c) Vessel Response - Quartering Seas, 4.9 kts

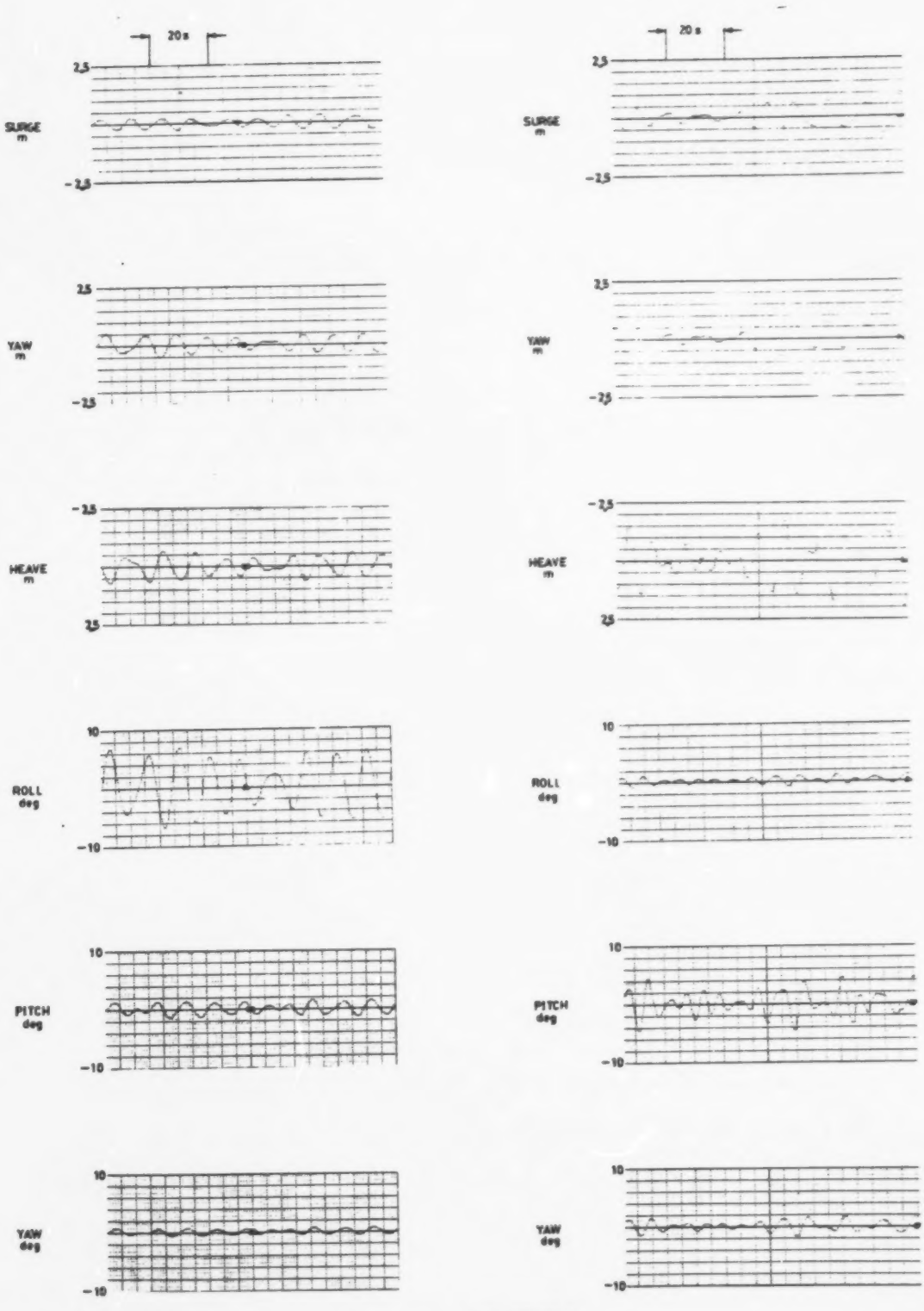

Figure 6.4 (d) Vessel Response - Quartering Seas, 4.9 kts.

perpendicular to the port side of the vessel (an azimuth or slewing angle of 3 $\pi/2$ radians).

For roll compensation studies, manual control of the boom elevating actuator was replaced by a model of an automatically controlled actuator with a representative time delay.

Table 6.5 Crane Base Location

${}_{G}C(1)$	-70.0 m
${}_{G}C(2)$	-3.0 m
${}_{G}C(3)$	-12.8 m

Table 6.6 Boom Tip Polar Coordinates

${}_{C}T(1)$	8.0 m
${}_{C}T(2)$	.0 rad
${}_{C}T(3)$	1.5 π rad

Traces of the rigid boom tip vertical position and vertical speed, head seas condition, are given in Figure 6.5.

Other parameters specified for the crane boom and cable were:

- boom stiffness 150,000 N/m
- boom damping 5636 N/m/s
- effective boom mass 680 kg

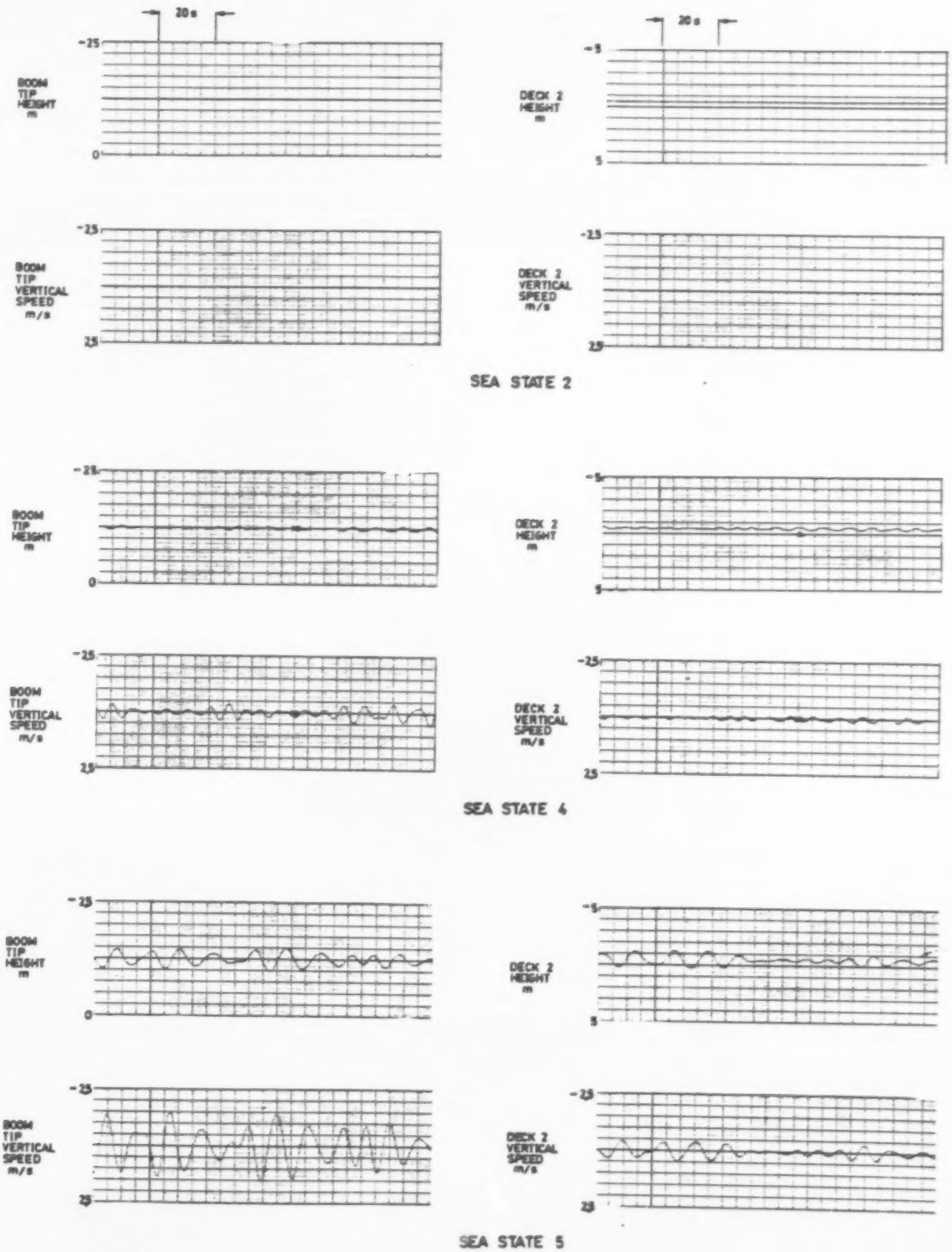

Figure 6.5 Boom Tip And Deck 2 Motion - Head Seas, 0 kts

- effective cable stiffness — 225,000 N/m
- cable damping — 14,000 N/m/s
- load mass
  - (a) 800 kg
  - (b) 1600 kg
  - (c) 2500 kg

From these parameters, the undamped natural frequency of the boom is calculated as 5.16 rad/s and its damping ratio is .3. For the load and cable combination, the undamped natural frequency varies from 16.8 rad/s at 800 kg to 9.49 rad/s at 2500 kg, while the damping ratio varies from 0.5 to 0.3 over the same load range. As is discussed later, these rather low natural frequencies significantly affected system stability and performance.

The pendular natural frequency of the load extended from approximately 0.9 rad/s to 2.2 rad/s, depending on the amount of line payed out.

Pendulous motion was not being controlled in this study, so control stability was not affected; however, under circumstances where the vessel response period approached the pendular period, large load oscillations resulted, as might be expected.

A cable tension limiter and a power limiter were modelled and tested during the development of the program. During the evaluation phase, these were removed and only a winching rate limiter was applied. This set limits of $\pm$ 1 m/s as the maximum rate at which cable could be payed out or retrieved.

6.1.4 Vessel 2

The physical parameters and sea-keeping characteristics of the second vessel onto which the load is to be placed were described in Section 6.1.2. However, to transform the motions of its centre of gravity into motions of its load deck requires a definition of the load deck coordinates in the H-frame of reference. These are given in Table 6.7.

Table 6.7 Vessel 2 Load Deck Coordinates

${}_{H}D_2(1)$	0. m
${}_{H}D_2(2)$	0. m
${}_{H}D_2(3)$	-0.16 m

The mean position of vessel 2 with respect to vessel 1 must also be specified in the 0-frame. These coordinates are given in Table 6.8.

Table 6.8 Mean Position of Vessel 2

${}_{O}Q(1)$	-70.0 m
${}_{O}Q(2)$	-11.0 m
${}_{O}Q(3)$	-0.34 m

These coordinates place vessel 2 under the tip of the crane boom on the port side of vessel 1. Traces of load deck speed and position are also found in Figure 6.5, and Figure 6.6 illustrates the relative positions of the vessels.

With quartering seas and the 3-D model, the loci shown in Figure 6.7 were obtained by plotting the vertical speed of the rigid boom tip against the vertical speed of the load deck on vessel 2 for each sea state. Some very useful information is contained in these plots. For example, with reference to Figure 6.7 (d) the maximum vertical closing speed between boom tip and deck is seen at point (1) where the perpendicular to the fourth quadrant bisector is tangent to the outer bound of the locus. The cable retrieval rate so established is the minimum rate that will ensure the second vessel cannot be driven up into the load after load pickup. When multiplied

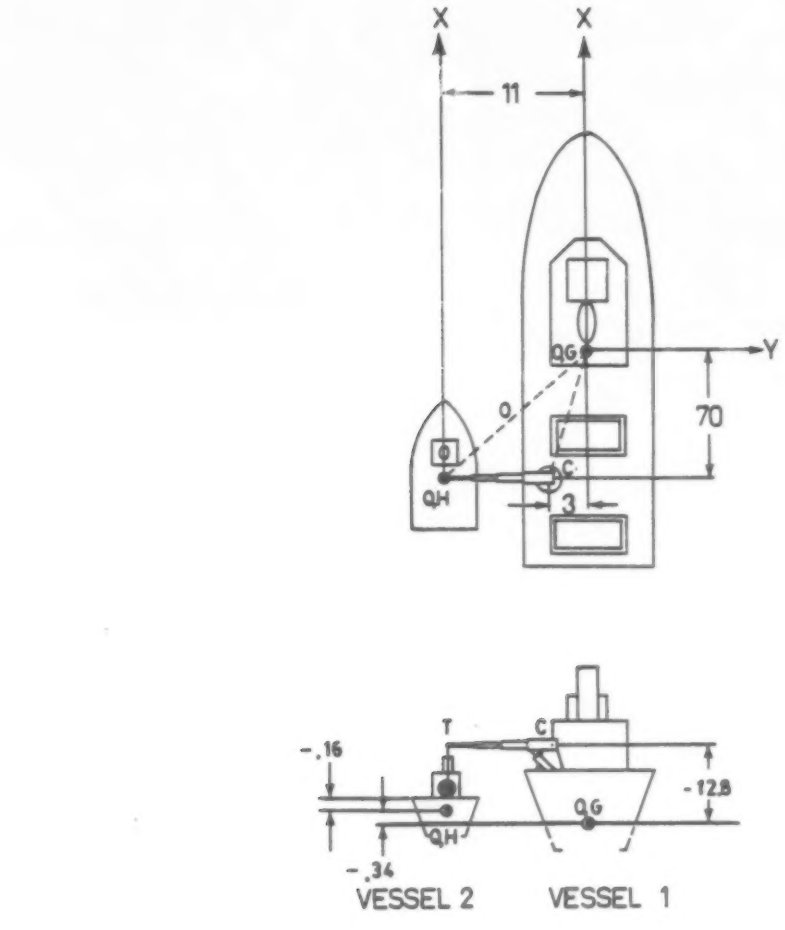

Figure 6.6 Relative Position of Vessels

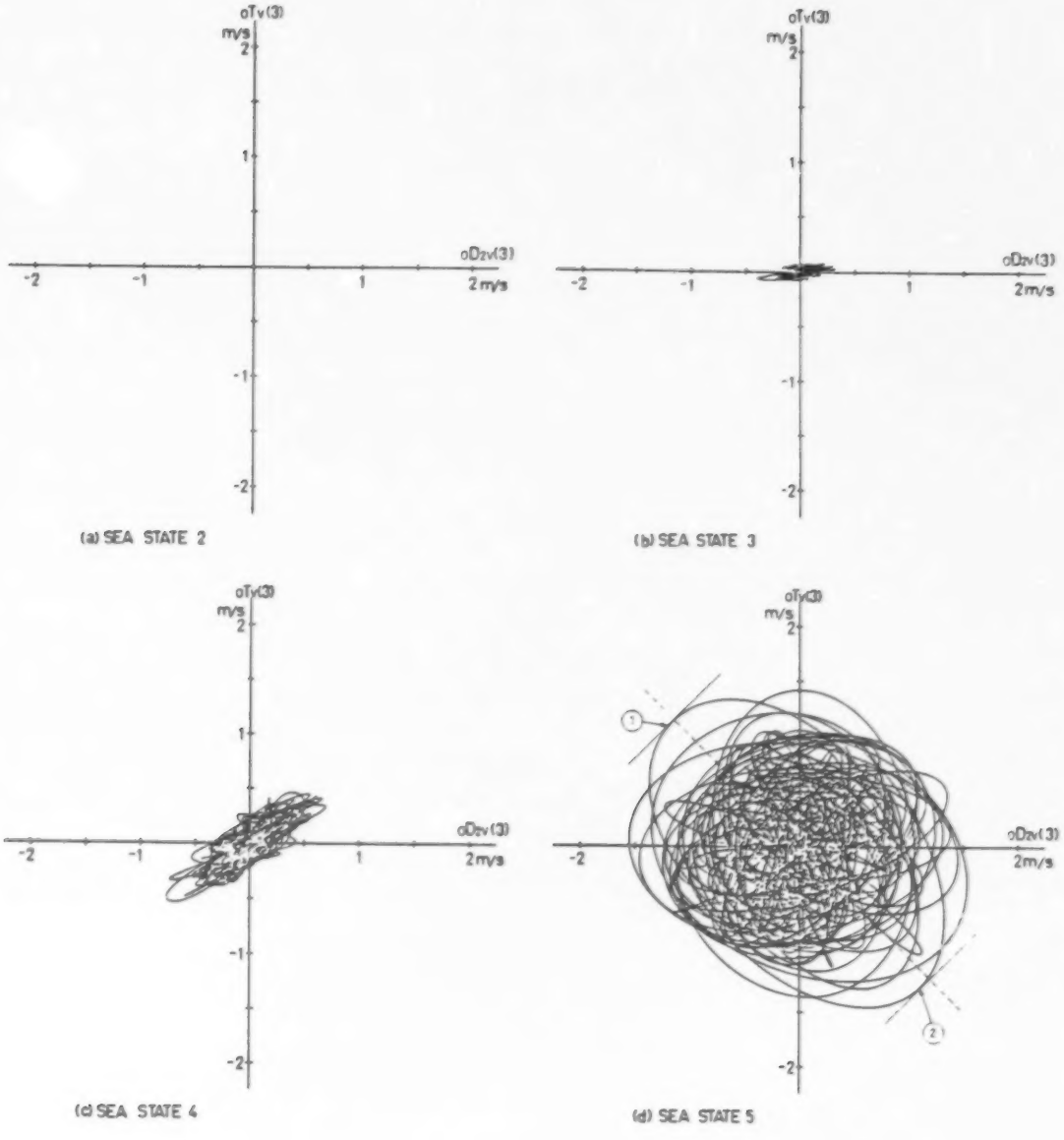

Figure 6.7 Vertical Speed Loci - Quartering Seas, 4.9 kts

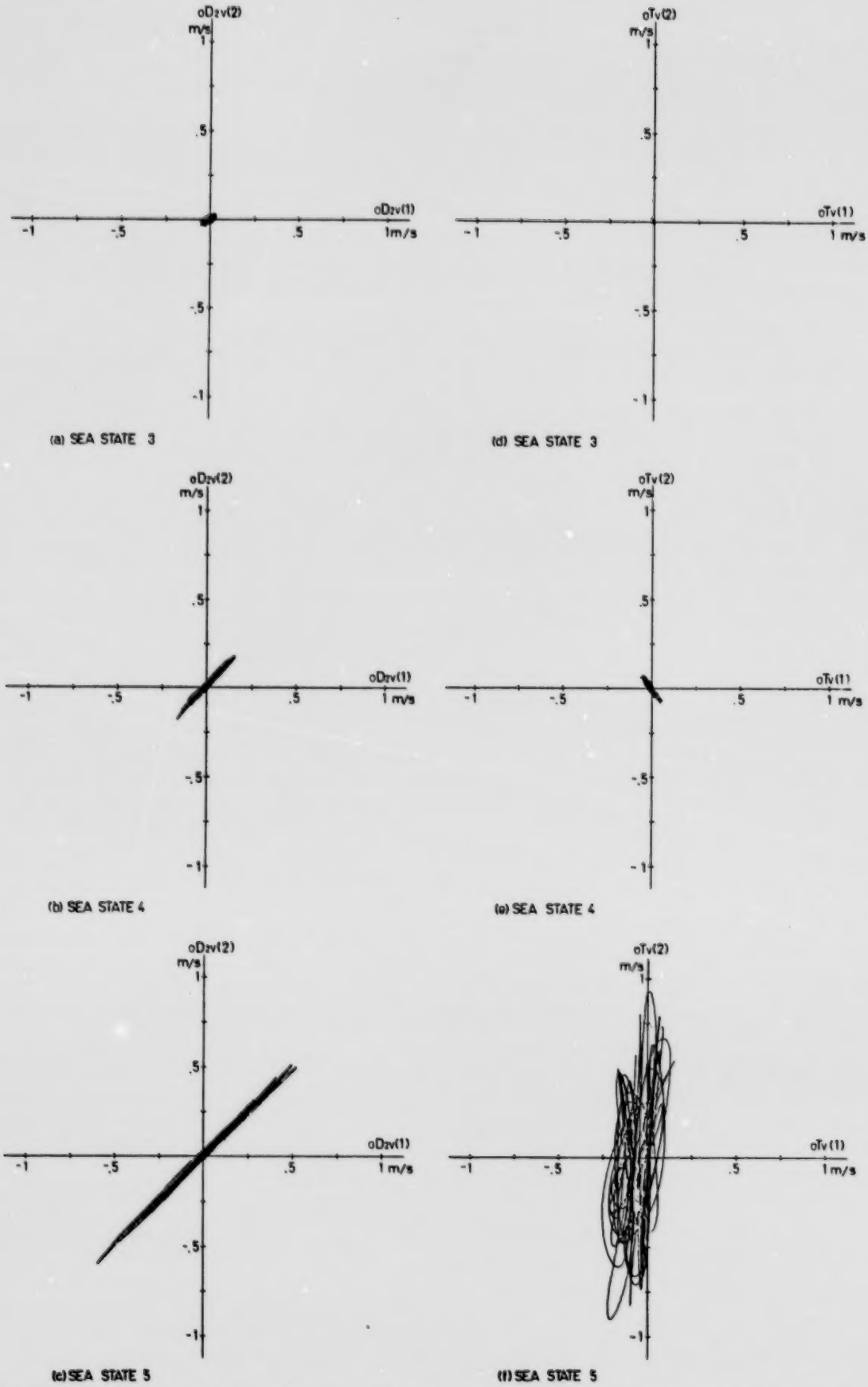

Figure 6.8 Horizontal Velocity Components - Quartering Seas, 4.9 kts

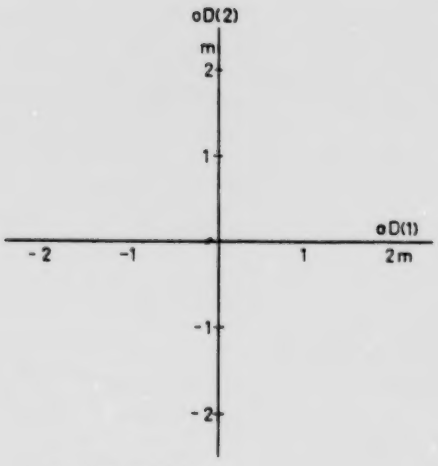

(a) SEA STATE 3

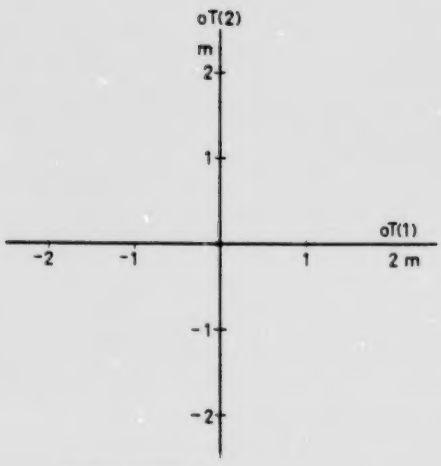

(d) SEA STATE 3

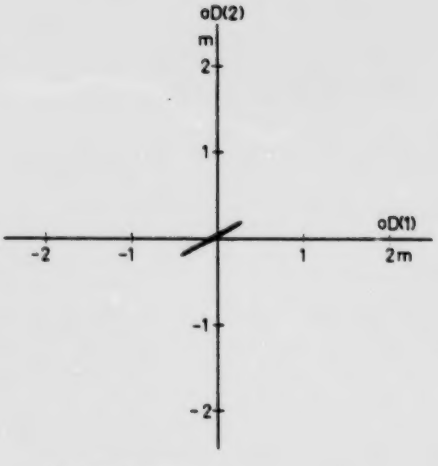

(b) SEA STATE 4

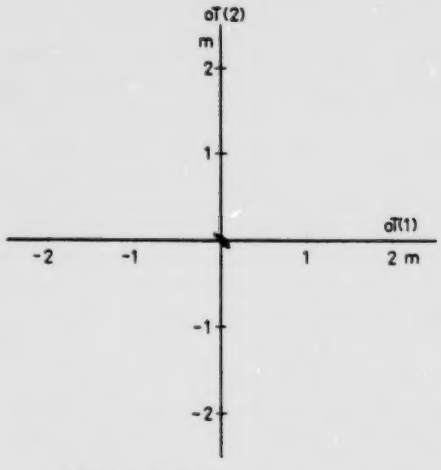

(e) SEA STATE 4

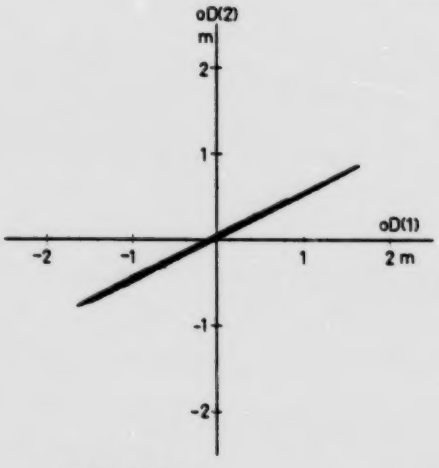

(c) SEA STATE 5

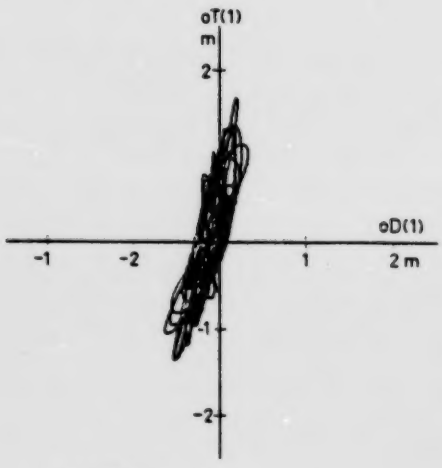

(d) SEA STATE 5

Figure 6.9 Horizontal Displacement Components-Quartering Seas, 4.9 kt

by the load weight, this rate also defines the minimum power requirements.

At the instant a load is placed on a deck, but before the cable is released, operators pay out cable to ensure a falling vessel or rising crane will not result in the load being lifted from the deck again. The minimum payout rate is determined as the point where the perpendicular to the quadrantal bisector is tangential to the envelope of the locus in the fourth quadrant, point (2).

This same maximum relative opening speed can also be used to calculate the worst case dynamic load by assuming the cable goes taught under these circumstances.

The shape of these loci depend of course, on sea state, vessel sea-keeping characteristics, crane and load deck positions, and crane geometry.

Figure 6.8 shows the loci of the horizontal velocity components for the load deck and for the crane boom tip. The loci of the corresponding horizontal displacements are given in Figure 6.9. These loci show a constant phase angle between the X and Y motions for each vessel, but it should be noted that this phenomenon is the result of the response amplitude operator method of modelling vessel motions, rather than being an indicator of the actual X-Y motion relationship.

The loci of Figures 6.8 and 6.9 can be used to obtain a quick comparison of the relative motion of various potential crane locations on board a ship. They can also be used in the design of equipment to provide horizontal load stabilization. For example, in the design of a tag line system, design winching rates can be set based on the worst case relative velocities in the fore-and-aft and athwartships directions.

6.1.5 Human Operator

In deciding how the human operator functioned at his control task, two possible modes of interaction were considered. It was hypothesized that the operator might try to maintain a constant closing rate between the load and the deck of the second vessel, or alternatively, he might maintain a constant load height above the second deck until he felt safely in control, then progressively reduce this height until deck contact was made. The first mode would require the operator to estimate, from a moving vantage point, the load closing rate to a second moving deck. Such estimating would be, at best, rather crude and choosing a safe closure rate would suffer from inaccuracy. The operator's output command (winching rate) being proportional to the perceived error (vertical speed), makes this a proportional control loop.

The second mode, that of stairstepping the load down to the deck is probably closer to what happens in fact. With this approach the operator would use constant position control. His winching rate output command is integrated to become load position, the source of the perceived error, creating an integral control loop.

Discussions with persons experienced in crane lifting operations indicated that the operator is very selective in choosing the moment to lift or lower, depending on vessel positions and the seas being experienced or anticipated. It could therefore be concluded that both modes of interaction are involved in each lift; however, to permit a clearer analysis and presentation of data, both modes were examined separately in this study.

The human operator model was initially tested with the values tabled in Section 5.3. Through a series of runs and repeated tunings, the values given in Table 6.9 were found to give good results. Additional experimentation with the tuning parameters showed further performance improvements were attainable but the extra effort for the amount of improvement was not justified.

Table 6.9 Human Operator Constants For Rate And Position Control

Constant	Load	Rate Control	Position Control
K_p	800	5.0	5.0
	1600	3.5	3.5
	2500	2.0	2.0
T_L(s)	All loads	0.028	0.128
T_I(s)	All loads	1.5	1.0
T_N(s)	All loads	0.132	0.132
τ_d(s)	All loads	0.128	0.128

Shown in Figure 6.10 (a) and (b) is a plot of the open loop transfer function $y_p y_c$ for the operator model controlling the deck closing speed of a 1600 kg load.

From the Figure 6.10 (a), it can be seen that the crossover frequency is 1.7 rad/s.

The human operator model turned out to be surprisingly intolerant to gain, not because of the ship response spectrum bandwidth which originally was believed to be the forcing function, but because of the low natural frequency of the load/boom combination. This unforeseen component of the forcing function lead to the regression phenomenom discussed in Section 5.3 as evidenced by the low crossover frequency.

6.1.6 Compensation

In addition to measuring operator performance, establishing power requirements and determining dynamic loads, one of the potential uses of the simulation is to ascertain if motion compensation would benefit at-sea lifting operations. To this end, three forms of motion compensation were modelled and evaluated.

The first of these, termed level 1 compensation in this study, represents an attempt to compensate for the motion of vessel 1, the ship carrying the crane. Perfect level 1 compensation would present the operator with a task comparable to loading and off-loading a moving vessel from a fixed platform or dock. Of course, the physiological influence his own motion would exert over the operator's performance could be expected to cause some degradation compared to his performance in lifting operations from a platform mounted crane. It was felt, nonetheless, that the potential benefits of reduced workload and decreased dynamic loading would still be there.

The second level of compensation involves removing the apparent motion of vessel 2 with respect to vessel 1. In other words, from the vantage point of the second vessel the load should appear suspended at a fixed height above the deck with no operator input. Because of the motions of vessel 2, winching rate and power requirements increase. The viability of level 2 compensation depends on having a reserve margin of performance in the lifting system.

Eliminating the effects of the motions of vessel 1 on the vertical position of the load is a problem of determining that component of load motion attributable to vessel motion, and modifying the winching rate to suppress it. If compensation is restricted to the vertical direction only, and if height is controlled solely by means of cable length, leaving boom

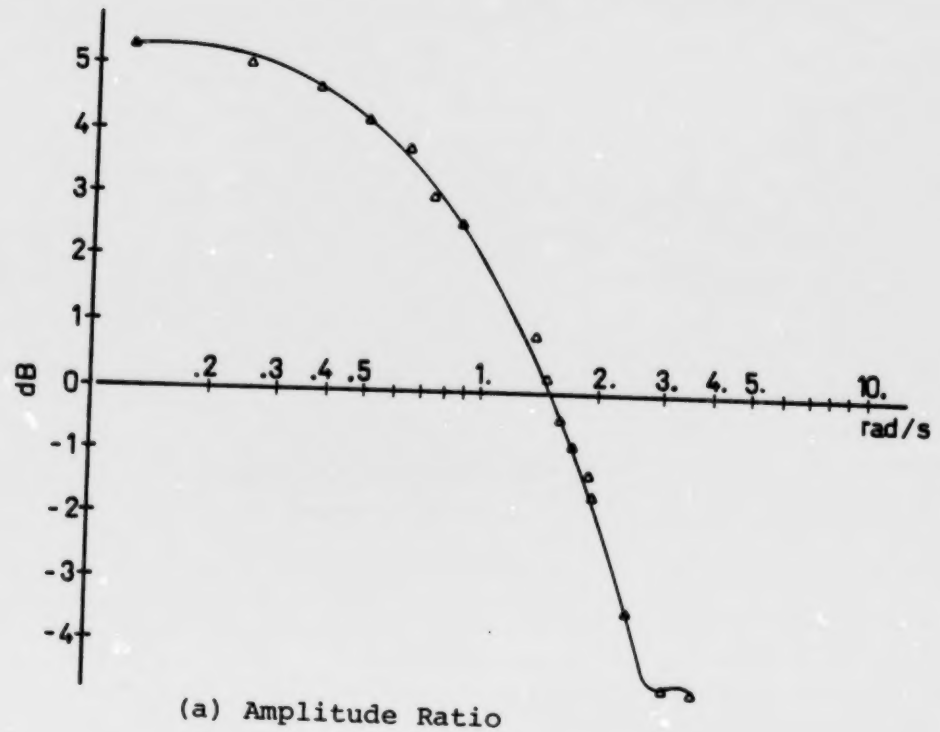

(a) Amplitude Ratio

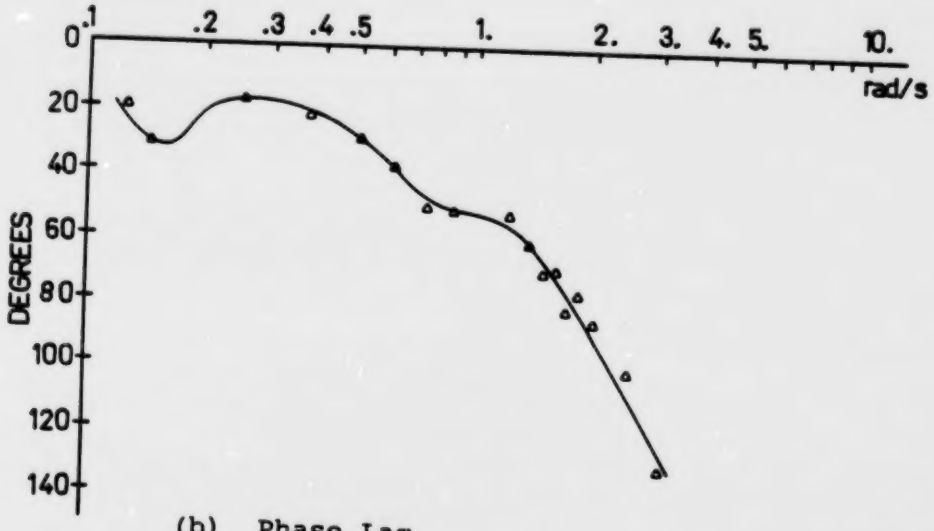

(b) Phase Lag

Figure 6.10 Operator-controlled Element Open Loop Response

elevation as a means of positioning the load, then the vertical component of the motion seen at the boom tip is the unwanted motion that must be eliminated. By taking the instantaneous speed in the vertical direction at the boom tip, and correcting the winching rate by an equal and opposite amount, the load should ideally appear fixed in space.

One possible method of achieving this is to place an accelerometer on the boom tip, and with the integral of this signal, compute a winching rate modifier as shown in the upper portion of Figure 6.11. Here, a weak feedback signal through gain a_1 is used to control integrator drift. The constant K_{C1} converts the computed vertical speed into a winch speed that will produce a cable rate equal and opposite to the input signal. Unfortunately, the boom tip is not an ideal location for such a sensor. Careful filtering of any signals from this location would be necessary to eliminate the cable, load, and boom natural frequencies, and special lag/lead circuits would be required to account for the winch operating lags.

Instead, a sensor package could be located in a more stable environment by mounting it on the ship's deck or crane base. To obtain a true measurement of the boom tip vertical speed, however, would require measurement of roll, pitch, yaw, and heave rates, and a mathematical determination of the corresponding boom tip vertical rate based on the crane boom azimuth, elevation, and extension. This may seem ponderously complex at first until it is noted that safe-load alerting systems (Ref. 8) are commonly installed in cranes nowadays, and such systems include many of these sensors already. Today's microprocessor technology can perform the safe-load computations as well as the motion compensating functions reliably and at reasonable cost.

To eliminate the apparent motion between the load lifting point on vessel 1 and the load deck on vessel 2 requires first a determination of the motion of the load deck on vessel 2, then the subsequent calculation of the relative motions between load deck and lifting point. If one were to assume an accelerometer were used, only vertical acceleration would have to be measured because the sensor could be placed close enough to the load deck that rotations of vessel 2 would have no appreciable affect on the vertical acceleration. By converting this acceleration signal to a vertical speed, and calculating an equivalent winching rate, the winching rate commanded by the operator may be modified to give level 2 compensation as shown in Figure 6.11. As with the level 1 compensating circuit previously described, a weak feedback signal of gain a_2 is used to overcome integrator drift, and

K_{CZ} is the proportionately constant between vertical speed and winch speed. Normally, the gains K_{C1} and K_{C2} would be set to ensure a one-to-one correspondence between vertical speed and corrective winching rate, but different gains might be selected based on power limitations or load natural frequencies to ensure the compensating controls do not introduce oscillation.

The use of an acceleration sensor on deck 2 suggests a sensor package must be permanently mounted on the second vessel, or transferred to it prior to lifting operations. In addition, the measured acceleration signal would have to be transmitted to the first vessel, perhaps as a radio frequency or infrared signal. This is quite feasible with current technology but where the crane-carrying vessel is serving many secondary vessels, measuring systems contained entirely on the vessel with the crane may have more appeal. One of several concepts is the use of laser-based triangulation. Motions of the load and the load deck are measured from the first vessel with a laser and compensating action initiated accordingly. Reference examines various alternatives.

Figure 6.12 shows one method of adding level 1 or level 2 compensation to an existing hydraulically operated winch. Here, the compensating controller modulates a servovalve which is "piggy-backed" onto the original system. The operator retains full manual authority to override the compensating system in the event of a failure.

More complicated algorithms may be derived to address special requirements. For example, if distance or height measurement were available (or calculated by triangulation) compensating lead could be applied to reduce closing speed just before load/deck contact. A load/cable/boom system with a soft spring constant and low natural frequency might benefit from compensation that would reduce load bounce and lessen the delay in load response to operator command. Measurement acceleration of the load itself would be required in such an algorithm. Such controls are beyond the scope of the current study.

A disadvantage of the implementation of level 1 and level 2 compensation as shown in Figure 6.12 is the high power consumption brought about by the compensating action. The energy dissipated as line is payed out is lost to the system, and line retrieval consumes energy while making the load appear stationary. References 9 and 10 describe systems using a bobbing-boom form of compensating system in which energy is stored and recovered during the compensating cycles. The

third method of compensation considered here is based on this principle. A crane mounted midships, extended over the port side, is modelled in which boom elevation is controlled by the roll angle of the vessel. This somewhat simpler algorithm, shown in Figure 6.13, provides a form of level 1 compensation in the most sensitive degree of freedom of the vessel. A detailed model of a hydraulic/pneumatic energy storage system was not attempted for this model, but could be added if establishing power requirements were an objective.

6.2 Performance Evaluation Results

6.2.1 Position Control Performance

For the position control performance evaluation, the human operator model was required to maintain the load at a height of 5 metres over the load deck of the second vessel. This task was repeated for a number of sea conditions, with three different load cases, without compensation, and with each of the two levels of winching rate compensation.

Strip chart records were made of various parameters including the height or position error seen by the operator, the forcing function position error (difference in relative height between boom tip and deck 2 from its at-rest nominal value), and the cable rate demanded by the operator. In addition, the position error and forcing function were each squared and integrated with respect to time to be used in comparing relative performance.

Tables 6.10 (a) through (c) summarize the performance for sea states 3, 4 and 5 respectively.

A performance number is calculated in power decibels as the ratio of the root-mean-square (RMS) position error and the RMS forcing function for each set of conditions. These values were obtained from runs of up to 4 minutes in length to ensure a representative wave sample and consistent average results.

From Table 6.10 (a), it can be seen that working without compensation, a human operator is able to suppress unwanted motions by -5.0 dB with an 800 Kg load, but with a 2500 Kg load, his achievement deteriorates to a suppression ratio of -1.8 dB. This degradation is attributable to lower natural frequency of the load and cable, causing regression in the operator's performance. The operator's activity also increases with increasing load as he 'chases' it.

As sea state increases, the operator's ability to suppress unwanted motion decreases with a very pronounced difference between sea state 4 and 5. In fact, without compensation, the

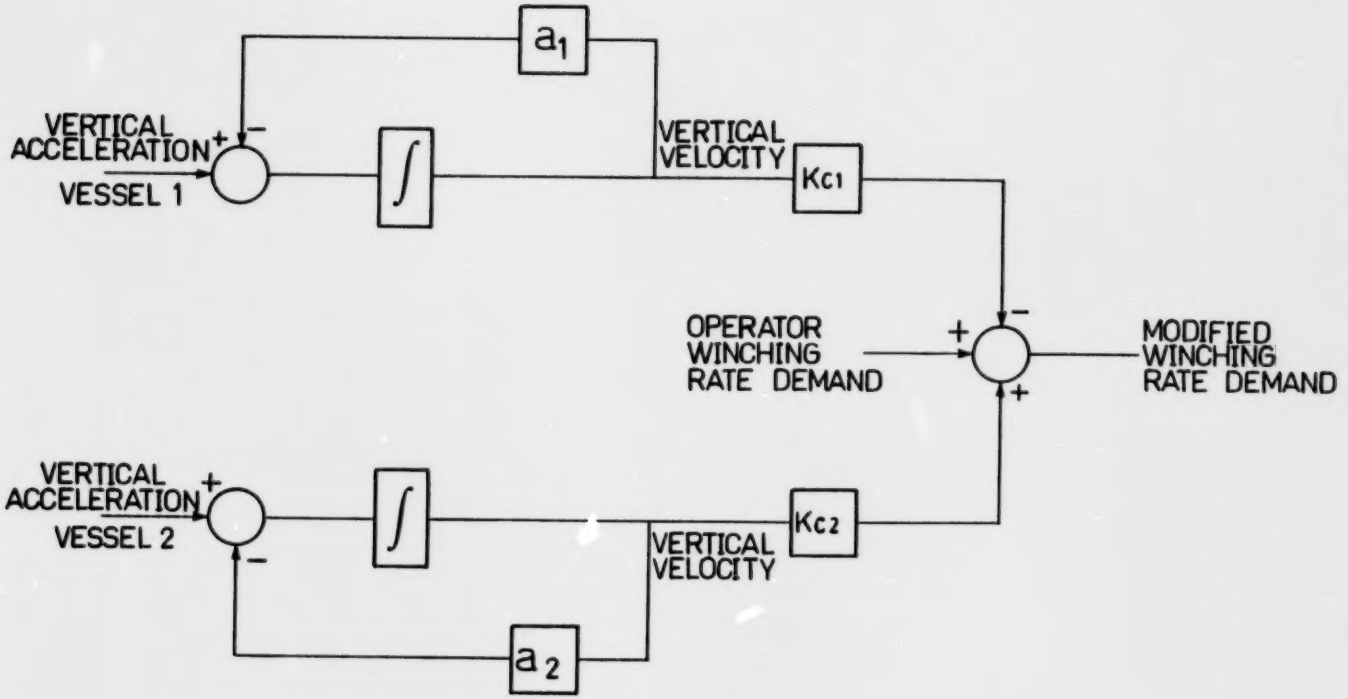

Figure 6.11 Level 2 Compensating Algorithm

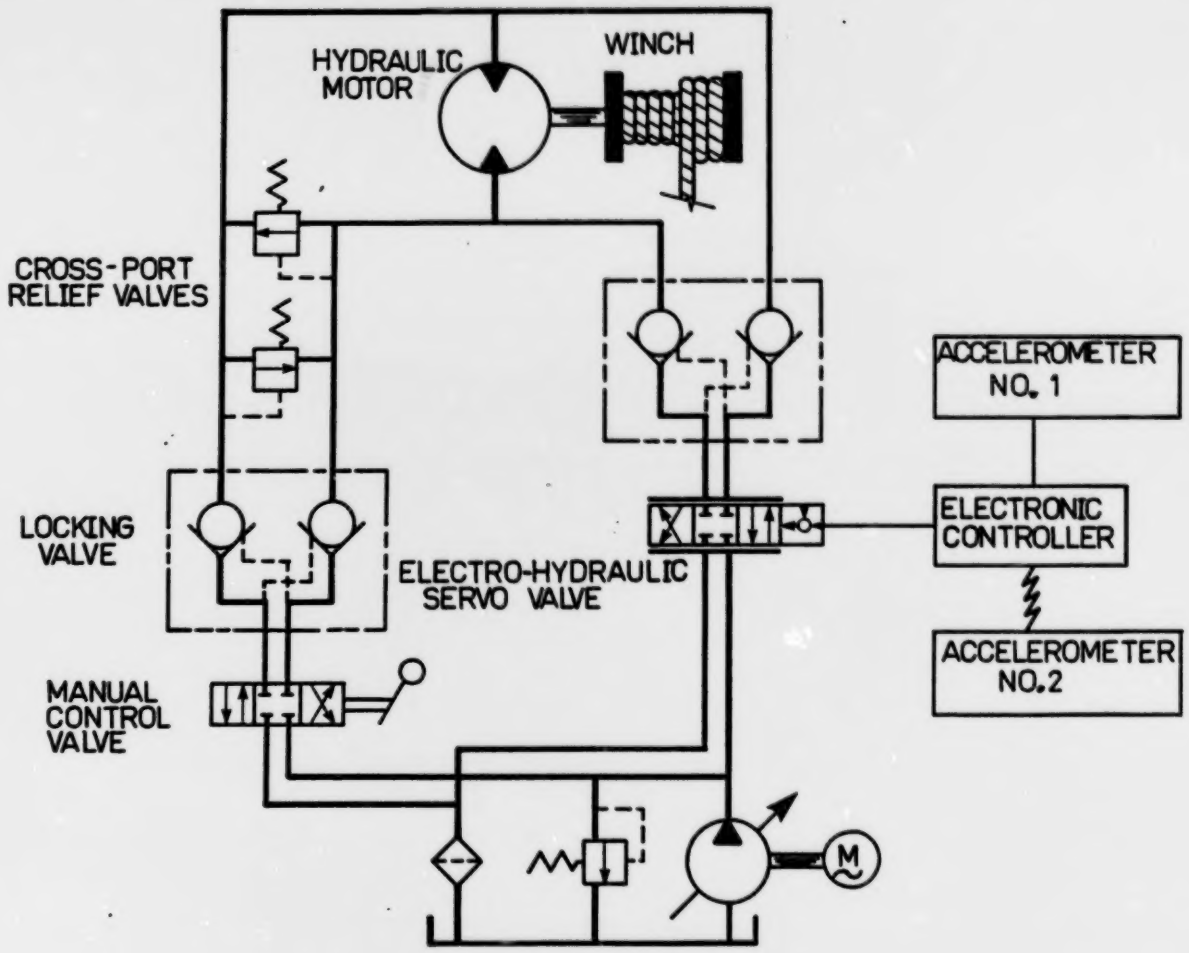

Figure 6.12 Typical Compensated Winching System

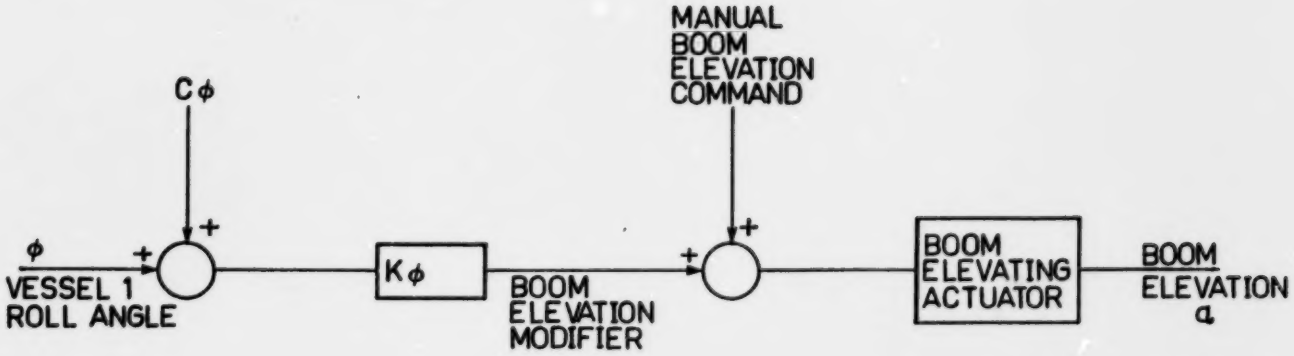

Figure 6.13 Roll Compensating Algorithm

operator actually makes matters worse in sea state 5 with a 2500 Kg load. An examination of Figure 6.14 (a) reveals that the cable rate demanded by the operator is not being satisfied- the maximum winching rate is being limited by system capability to $\pm$ 1 m/s, causing a gross deterioration in closed loop performance. The overcontrolling by the operator also produces dynamic factors of almost two, affecting cable tension, overturning moment and winching power.

The application of level 1 compensation results in an improvement in operator performance in all cases. The improvement is most pronounced in sea state 4 where operator performance without compensation is deteriorating, but unlike sea state 5, the physical limitations of the system have not yet begun to dominate the performance. Figure 6.14 (b) shows a slight reduction in the operator's cable rate demand, signifying that the compensating system is improving the overall position control performance by overcoming some of the operator's inherent lag. Reducing the delay before corrective action is applied reduces the amount of correction required.

Finally, full level 2 compensation appears to offer a most dramatic improvement, particularly in sea state 5 and with the heaviest load. Once again, by eliminating the operator's response lag, the amount of the corrective winching action is reduced. Figure 6.11 (c) shows that cable tension excursions have been reduced to less than 1.4 times their static value with equivalent reductions in winching power and overturning moment.

At the same time as the foregoing data was recorded, traces were made of the locus of the XY-position of the load in the inertial reference frame, and of the XY-components of its velocity. Compensation in the horizontal plane was not attempted in the current study but the loci provide some useful information. Figure 6.15 (a) shows the increasing amplitude of load oscillation with sea state, primarily in the Y-direction due to the sensitivity of vessel 1 to roll in higher sea states. The XY-velocity components corresponding to these excursions are contained in the same Figure. If the maximum velocities of these figures are added algebraically to the maximum velocities of deck 2 given in Figure 6.8, the maximum sideways deck contact speed can be computed. The displacement components for the load can be compared to the displacement components of deck 2 given in Figure 6.9 to arrive at a possible position error. Caution should be used in making these estimate for two reasons: first, the damping parameter for the pendulous motion has not been verified; and, second, the operator's tendency to be selective in choosing the moment to lower the load can reduce sliding contact velocities and load horizontal position errors.

SEA STATE 3 POSITION CONTROL

MASS (Kg)	COMPENSATION	E (m^2s)	E* (m^2s)	t (s)	$20 \log_{10} \frac{\sqrt{E(SS)}}{\sqrt{E^*(SS)}}$
800	NONE	.45	1.435	240	-5.0
	LVL 1	.35	1.435	240	-6.1
	LVL 2	.175	1.435	240	-9.1
1600	NONE	.44	1.435	240	-5.1
	LVL 1	.35	1.435	240	-6.1
	LVL 2	.17	1.435	240	-9.3
2500	NONE	.955	1.435	240	-1.8
	LVL 1	.59	1.435	240	-3.9
	LVL 2	.33	1.435	240	-6.4

Table 6.10 (a) Position Control Performance - Quartering Seas - Sea State 3

SEA STATE 4 POSITION CONTROL

MASS (Kg)	COMPENSATION	E (m^2s)	E* (m^2s)	t (s)	$20 \log_{10} \frac{\sqrt{E(SS)}}{\sqrt{E^*(SS)}}$
800	NONE	.355	15.91	108.0	-16.5
	LVL 1	.095	14.5	96.0	-21.8
	LVL 2	.005	16.25	108.0	-25.1
1600	NONE	.81	16.725	115.2	-13.1
	LVL 1	.22	15.26	108.0	-18.4
	LVL 2	.13	12.31	84.0	-19.8
2500	NONE	1.695	12.87	88.8	-8.8
	LVL 1	.4	12.0	84.0	-14.8
	LVL 2	.285	15.45	108.0	-17.3

Table 6.10 (b) Position Control Performance - Head Seas - Sea State 4

SEA STATE 5 POSITION CONTROL

MASS (Kg)	COMPENSATION	E (m^2s)	E* (m^2s)	t (s)	$20 \log \frac{\sqrt{E(SS)}}{\sqrt{E^*(SS)}}$
800	NONE	96.72	147.6	240	-1.8
	LVL 1	64.6	147.6	240	-3.6
	LVL 2	15.36	147.6	240	-9.8
1600	NONE	129.48	147.6	240	-0.669
	LVL 1	74.8	147.6	240	-3.0
	LVL 2	8.96	147.6	240	-12.2
2500	NONE	182.0	147.6	240	+0.9
	LVL 1	110.48	147.6	240	-1.3
	LVL 2	5.8	147.6	240	-14.1

Table 6.10 (c) Position Control Performance -Quartering Seas - Sea State 5

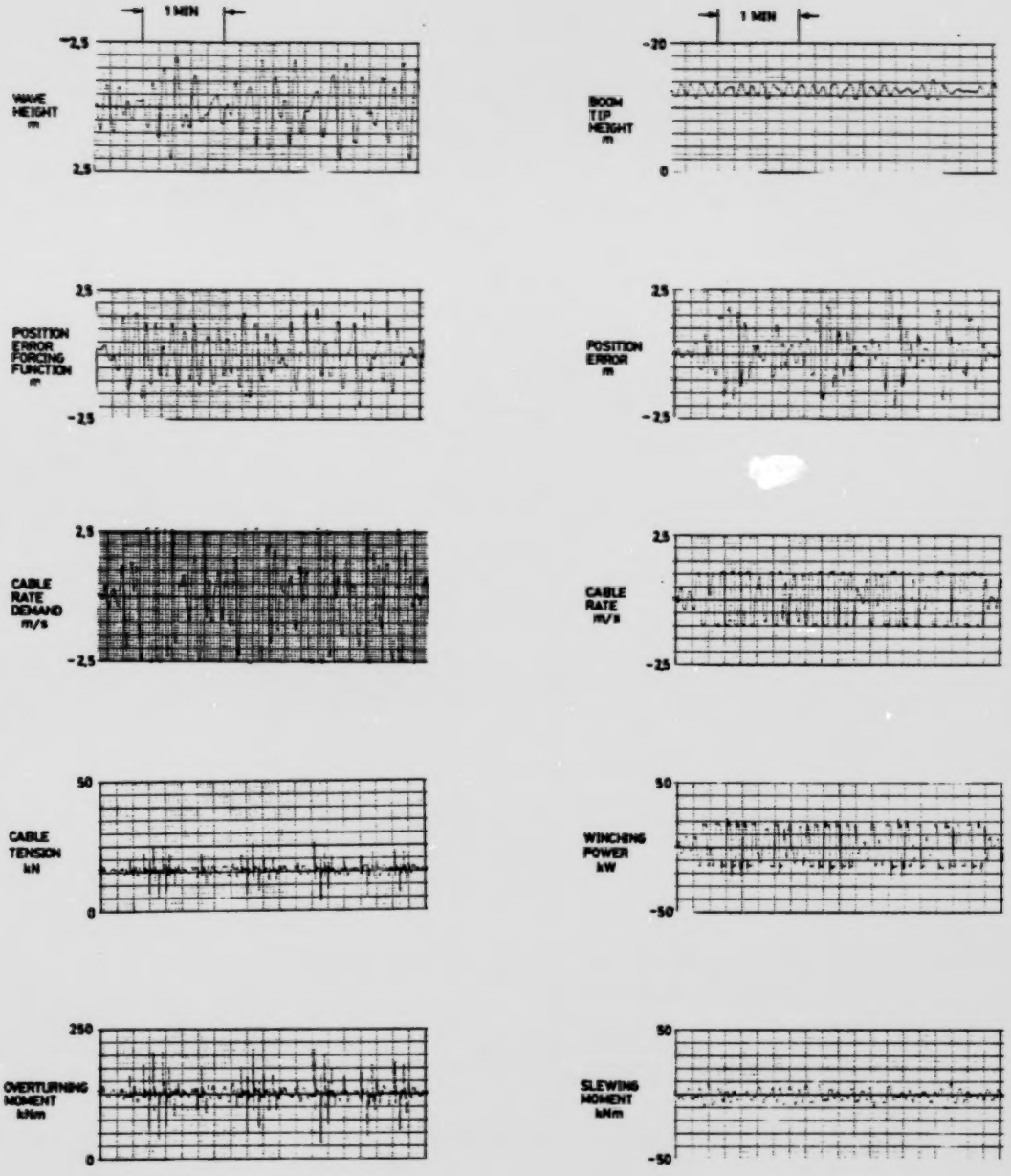

Figure 6.14 (a) Position Control Performance - Sea State 5 - No Compensation

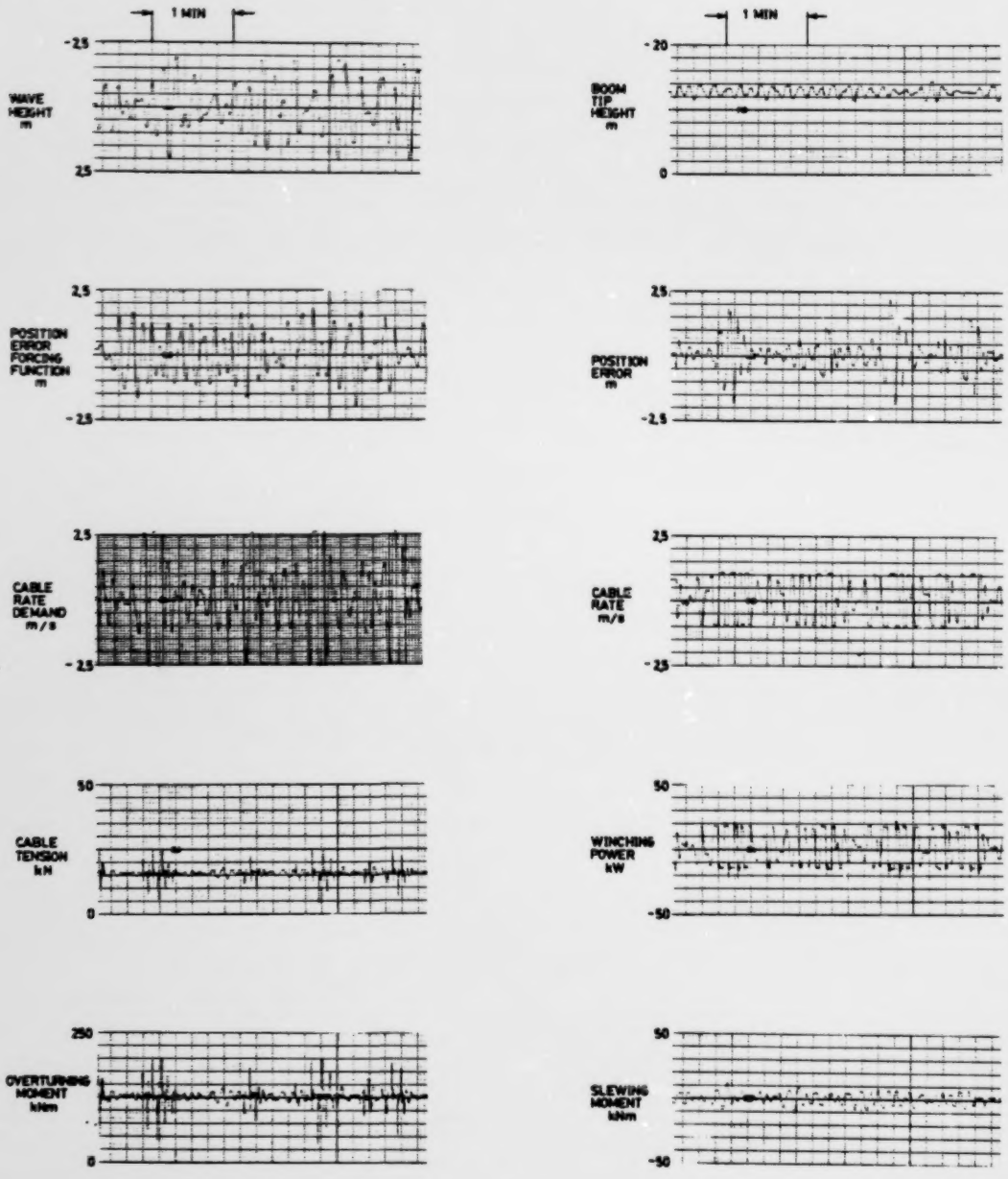

Figure 6.14 (b) Position Control Performance - Sea State 5 - Level 1 Compensation

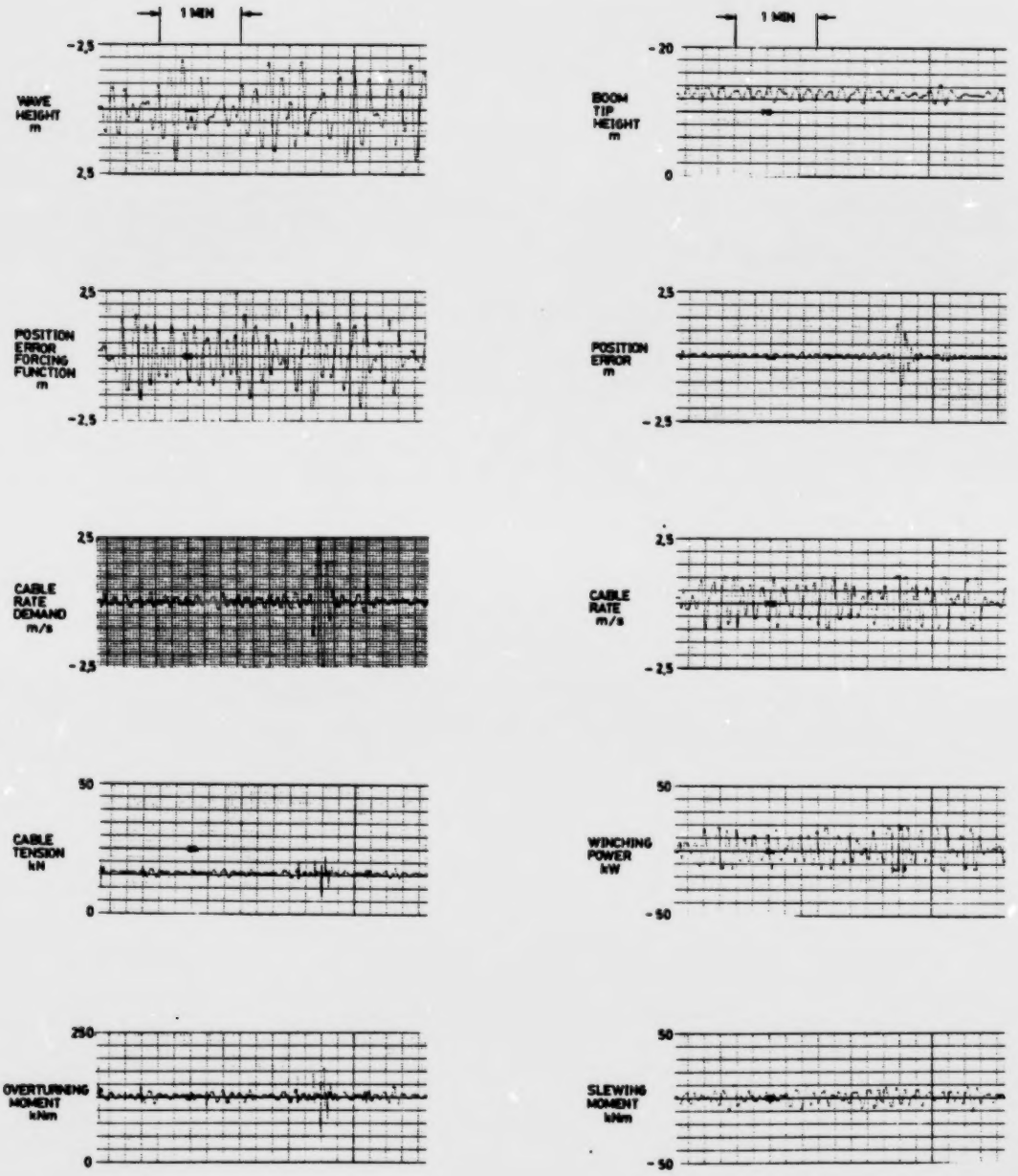

Figure 6.14 (c) Position Control Performance - Sea State 5 - Level 2 Compensation

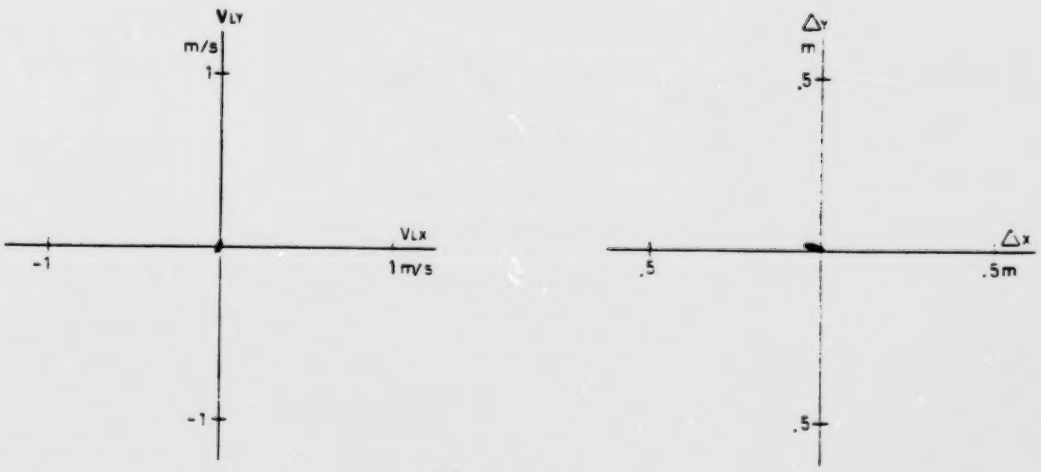

SEA STATE 3

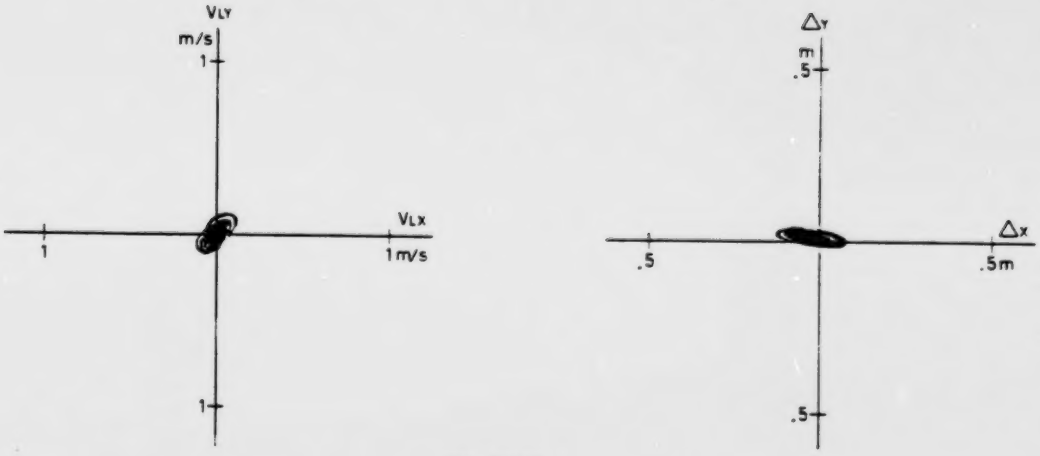

SEA STATE 4

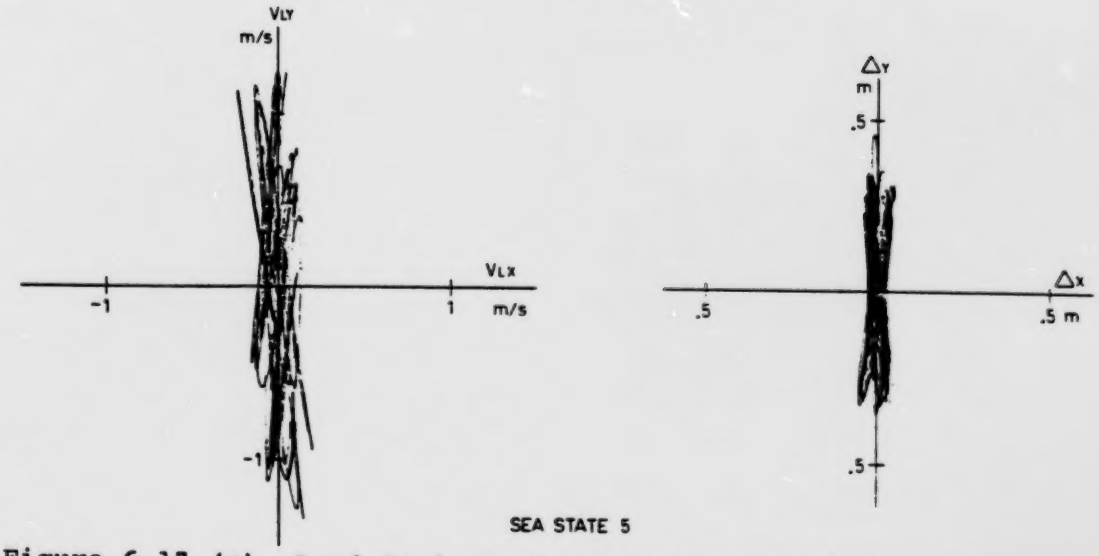

SEA STATE 5

Figure 6.15 (a) Load Horizontal, Velocity & Position -No Compensation

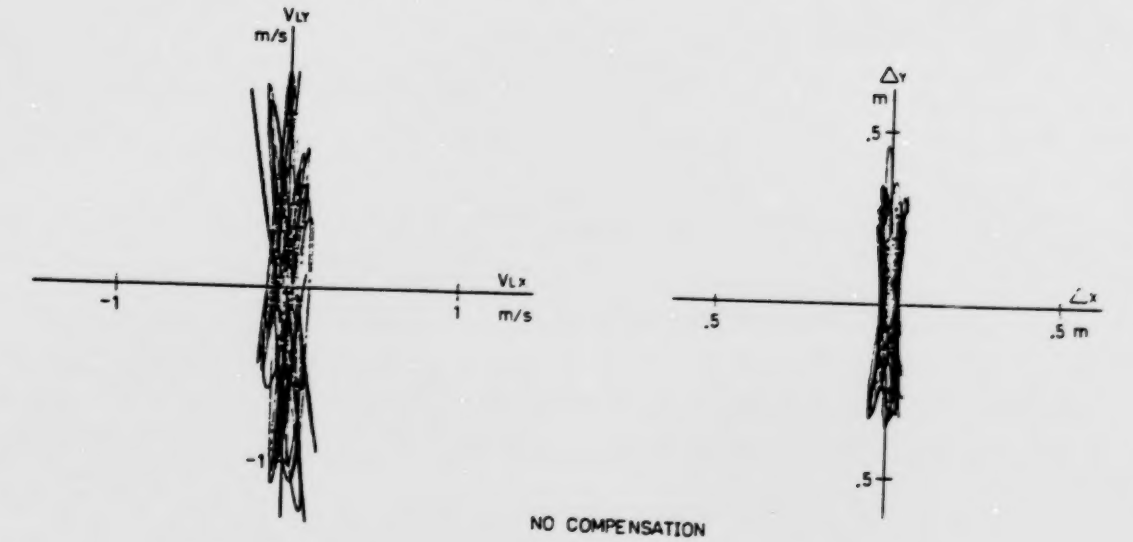

NO COMPENSATION

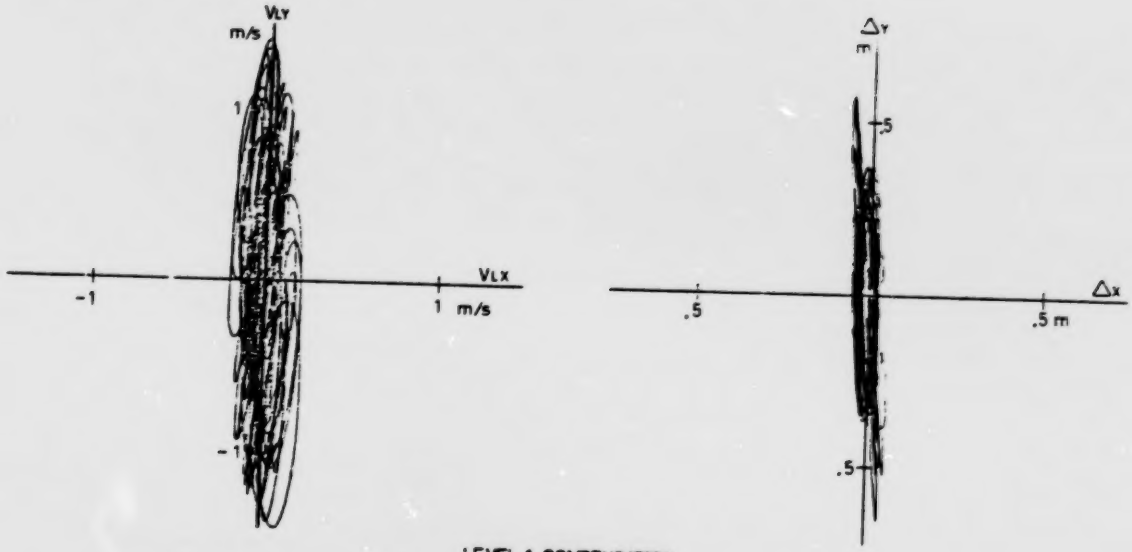

LEVEL 1 COMPENSATION

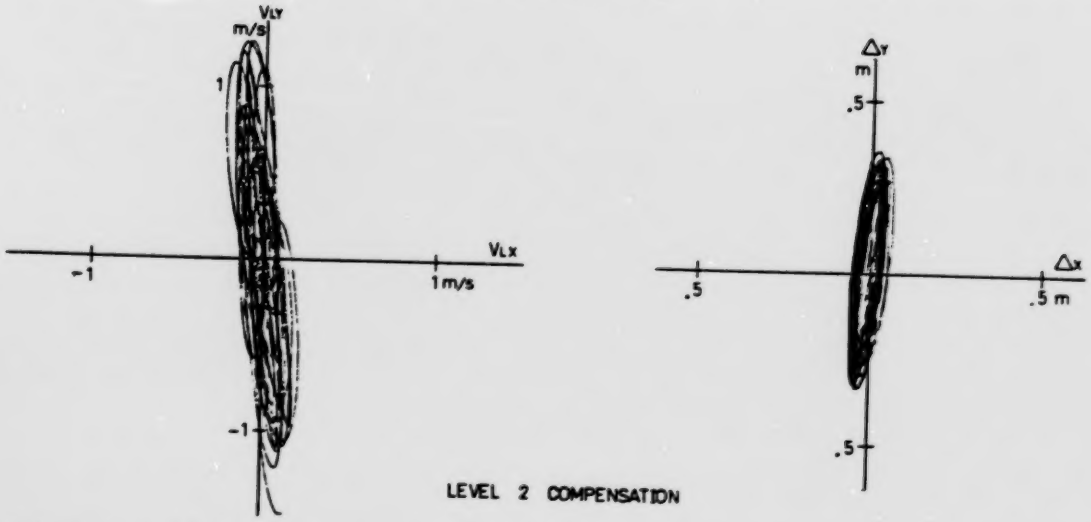

LEVEL 2 COMPENSATION

Figure 6.15 (b) Load Horizontal, Velocity & Position, Sea State 5

Figure 6.15 (b) is intended to illustrate the effect compensation in the vertical direction has on pendulous motion of the load. Though all loci appear dissimilar, no conclusions were drawn from these figures.

6.2.2 Rate Control Performance

A second series of runs was undertaken with the same sea states and loads as before, but employing the rate control strategy. The operator was required to lower the load from a nominal starting height of 10 m above the second vessel, while striving to maintain a constant closing rate of 0.4 m/s. This task was performed with no compensation, and repeated with each of level 1 and level 2 compensation.

This time, the error forcing function was the closing rate between the load and load deck of vessel 2, or the difference in their vertical speeds. The error signal perceived by the operator was the departure of the closing rate error from the nominal closing rate setpoint.

To arrive at a comparative performance number, the RMS value of the error signal for a given level of compensation, is divided by the RMS error under the same sea state and load condition, but without compensation. This number is then converted to power decibels. The results are shown in Tables 6.11 (a) through (c).

An examination of these tables discloses a number of instances where the measured performance figures depart from trends which might have been anticipated. This anomalous behaviour is attributable to the short period of observation - nominally 25 s - in which only some 2 to 4 wave crests were encountered. Because the control demand is proportional to the error signal, a winching rate command is produced only when a closing speed error exists. Whether this error is positive or negative depends on the relative phase of the vessels' vertical speeds. When both these factors are considered, it can be seen that substantial variation in lowering time can occur, depending on the ship motion and sea state at the start of the trace. The lowering time can also be altered by the relative vertical positions between vessels. If the second vessel is at a high point in its vertical excursions, and the crane-carrying vessel at a low point, the height between load and deck can be reduced from 10 to about 7 m, substantially shortening the cycle time. The converse is also true.

To improve the quality of the results would require repetition of the lowering cycles a number of times under the same conditions but with randomly selected starting times. When averaged, the results should overcome the aforementioned discrepancies.

SEA STATE 2 RATE CONTROL

MASS (Kg)	COMPENSATION	E (m^2/s)	E* (m^2/s)	t (s)	$20 \log_{10} \frac{\sqrt{\frac{E(CL)}{t}}}{\sqrt{\frac{E(NONE)}{t}}}$
800	NONE	.34	0	24.0	0.0
	LVL 1	.33	0	24.0	-.130
	LVL 2	.335	0	24.0	-.064
1600	NONE	.33	0	27.0	0.0
	LVL 1	.325	0	27.0	-.066
	LVL 2	.325	0	27.0	-.066
2500	NONE	.295	0	32.0	0.0
	LVL 1	.285	0	32.0	-.150
	LVL 2	.285	0	32.0	-.150

Table 6.11 (a) Rate Control Performance - Quartering Seas - Sea State 2

SEA STATE 3 RATE CONTROL

MASS (Kg)	COMPENSATION	E (m^2/s)	E* (m^2/s)	t (s)	$20 \log_{10} \frac{\sqrt{\frac{E(CL)}{t}}}{\sqrt{\frac{E(NONE)}{t}}}$
800	NONE	.350	.0325	25.5	0.0
	LVL 1	.330	.0325	23.5	+.1
	LVL 2	.335	.0325	25.0	-.04
1600	NONE	.335	.0325	26.0	0.0
	LVL 1	.330	.0325	26.0	-.065
	LVL 2	.325	.0325	26.0	-.199
2500	NONE	.310	.04	32.0	0.0
	LVL 1	.300	.04	32.0	-.142
	LVL 2	.295	.04	33.0	-.349

Table 6.11 (b) Rate Control Performance - Quartering Seas - Sea State 3

SEA STATE 4 RATE CONTROL

MASS (Kg)	COMPENSATION	E (m^2/s)	E* (m^2/s)	t (s)	$20 \log_{10} \frac{\sqrt{\frac{E(CL)}{t}}}{\sqrt{\frac{E(NONE)}{t}}}$
800	NONE	3.00	1.88	25.0	0.0
	LVL 1	2.68	1.88	25.0	-.490
	LVL 2	2.64	1.88	25.0	-.555
1600	NONE	3.08	1.96	26.0	0.0
	LVL 1	2.88	1.96	26.0	-.292
	LVL 2	2.72	1.96	26.0	-.540
2500	NONE	3.04	2.16	32.0	0.0
	LVL 1	2.88	2.16	32.0	-.235
	LVL 2	2.56	2.16	32.0	-.746

Table 6.11 (c) Rate Control Performance - Quartering Seas - Sea State 4

SEA STATE 5 RATE CONTROL

MASS (Kg)	COMPENSATION	E (m^2/s)	E* (m^2/s)	t (s)	$20 \log_{10} \frac{\sqrt{\frac{E(CL)}{t}}}{\sqrt{\frac{E(NONE)}{t}}}$
800	NONE	3.68	10.92	26.5	0.0
	LVL 1	3.40	10.92	27.0	-.425
	LVL 2	3.76	12.6	28.5	-.223
1600	NONE	4.04	11.32	27.5	0.0
	LVL 1	3.84	14.0	29.0	-.451
	LVL 2	3.6	15.8	32.0	-1.159
2500	NONE	5.96	16.72	33.5	0.0
	LVL 1	5.04	16.88	34.0	-.793
	LVL 2	4.08	21.08	39.0	-2.306

Table 6.11 (d) Rate Control Performance - Quartering Seas - Sea State 5

Notwithstanding the foregoing, the trends apparent in Table 6.11 lead to several observations. Operator activity is seen to increase with increasing load. Once more this can be related to the decreasing natural frequency of the load and the accompanying performance regression. Operator activity also increases with increasing sea state, and compensation appears to provide a performance improvement in higher sea states but the scatter of the results makes the difference between level 1 and level 2 compensation indiscernible.

Figures 6.17 (a) through (c) are strip chart records of the performance of the rate control strategy for sea state 5 and a 1600 kg load. Level 2 compensation offers a significant reduction in closing rate error with an accompanying reduction in operator activity. Actual winching rates appear slightly higher with little change in cable tension transients and overturning moment. These observations are due to the tighter control exercised by the compensating systems over the closing rate error. Such control requires increased winching rates while relieving the operator of some of the burden of applying corrective action.

The slewing moment is generated by the cable tension acting outside of the topping plane. Pendulous motion of the load, and ship's rotations which bring the topping plane out of plumb, produce the unwanted side loads on the boom which give rise to this moment.

6.2.3 Roll Compensation Performance

The traces of Figure 6.18 are records of system performance as the operator strives to maintain constant load position above deck 2 with assistance in the form of roll compensation. For these runs, the crane base was moved ahead to the vessel's centre of gravity.

Under sea state 5 conditions, and with an 800 kg load, the position error is markedly reduced even though boom elevation is responding only to the roll angle of vessel 1. This is just another form of level 1 compensation using a different degree of freedom of the crane (boom elevation) to provide the compensating motion.

The dominant reason for the observed improvement must be credited to the reduced winching rate requirements. By compensating for vessel 1 motion through the boom elevation angle, the full rate capability of the winch is available to the operator to correct for the unwanted motions of vessel 2. The less often the winch is limited by its own rate limits, the more accurately the load height may be controlled by the operator.

This approach to compensation concentrates the corrective action in the ship's degree of freedom most sensitive to sea conditions. The advantages include simplified sensors and controls. By applying the "bobbing-boom" type of compensation, an energy conserving system could be used, reducing the power requirements of compensation.

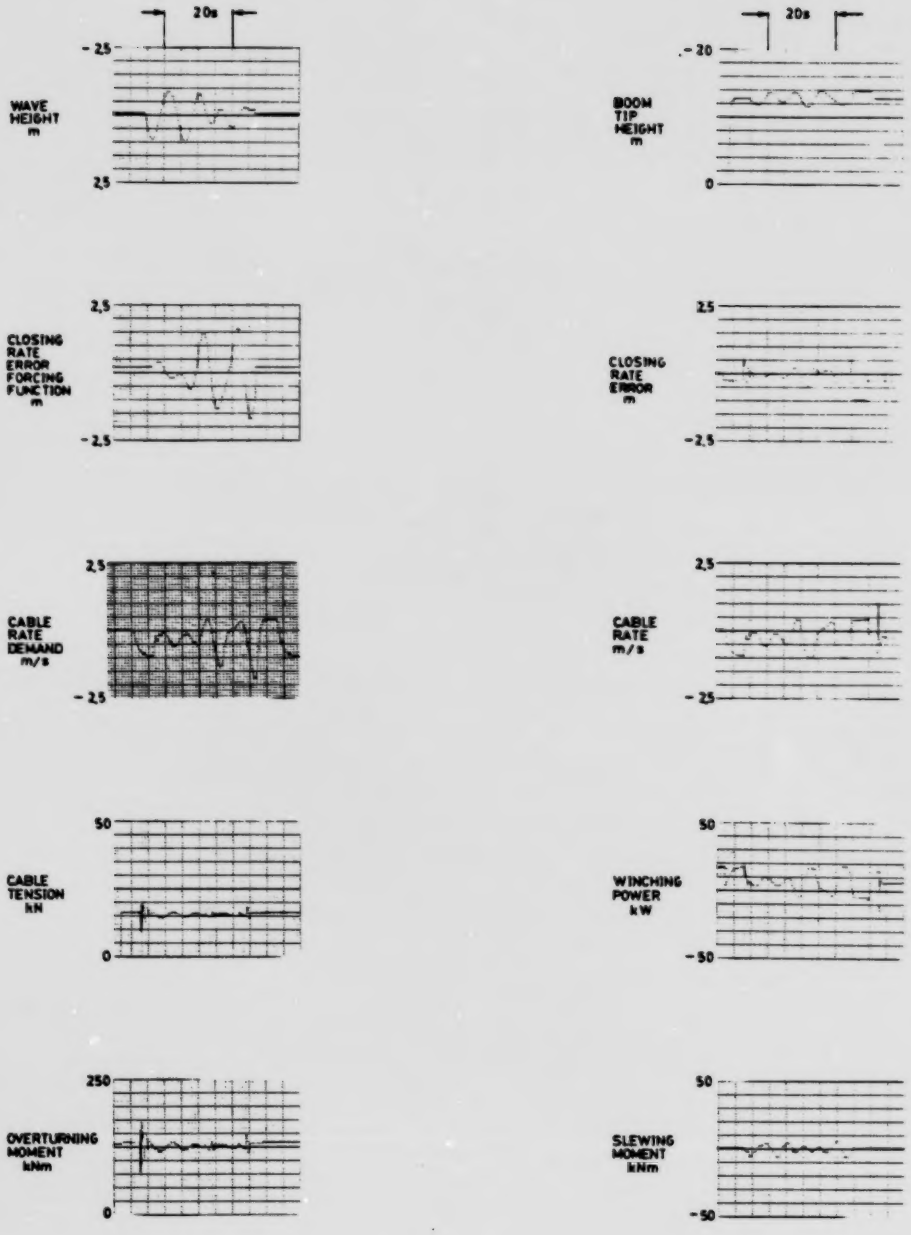

Figure 6.17 (a) Rate Control Performance - Sea State 5 - No Compensation

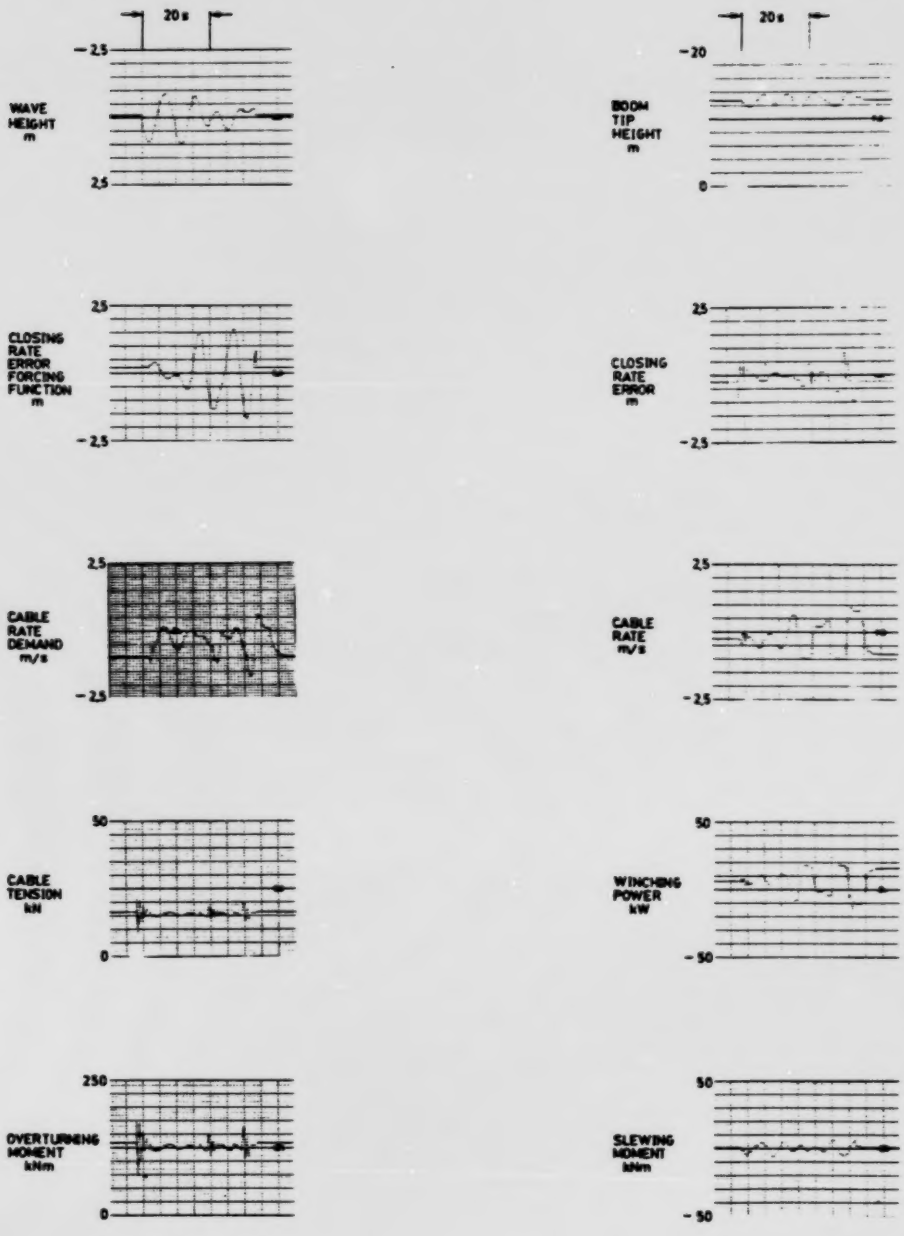

Figure 6.17 (b) Rate Control Performance - Sea State 5 - Level 1 Compensation

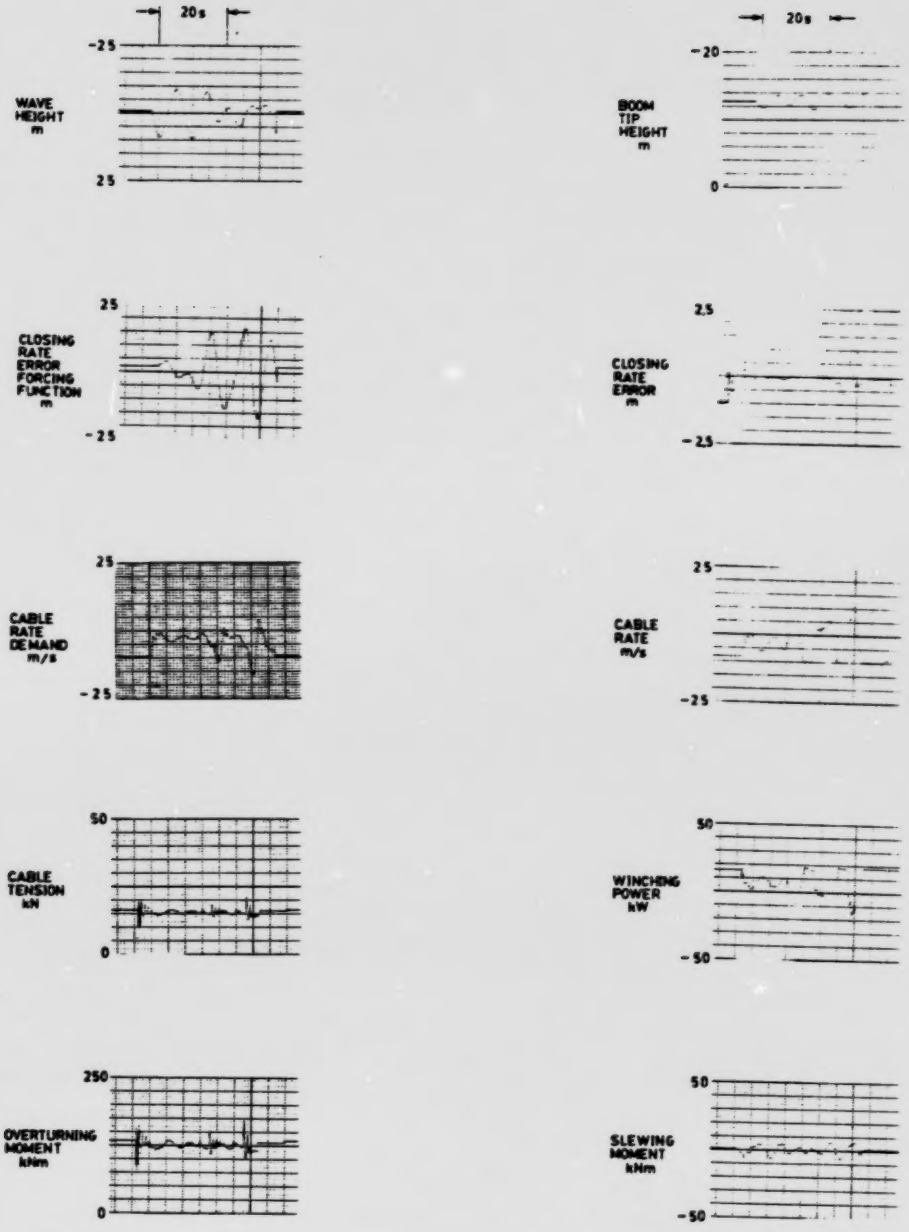

Figure 6.17 (c) Rate Control Performance - Sea State 5 - Level 2 Compensation

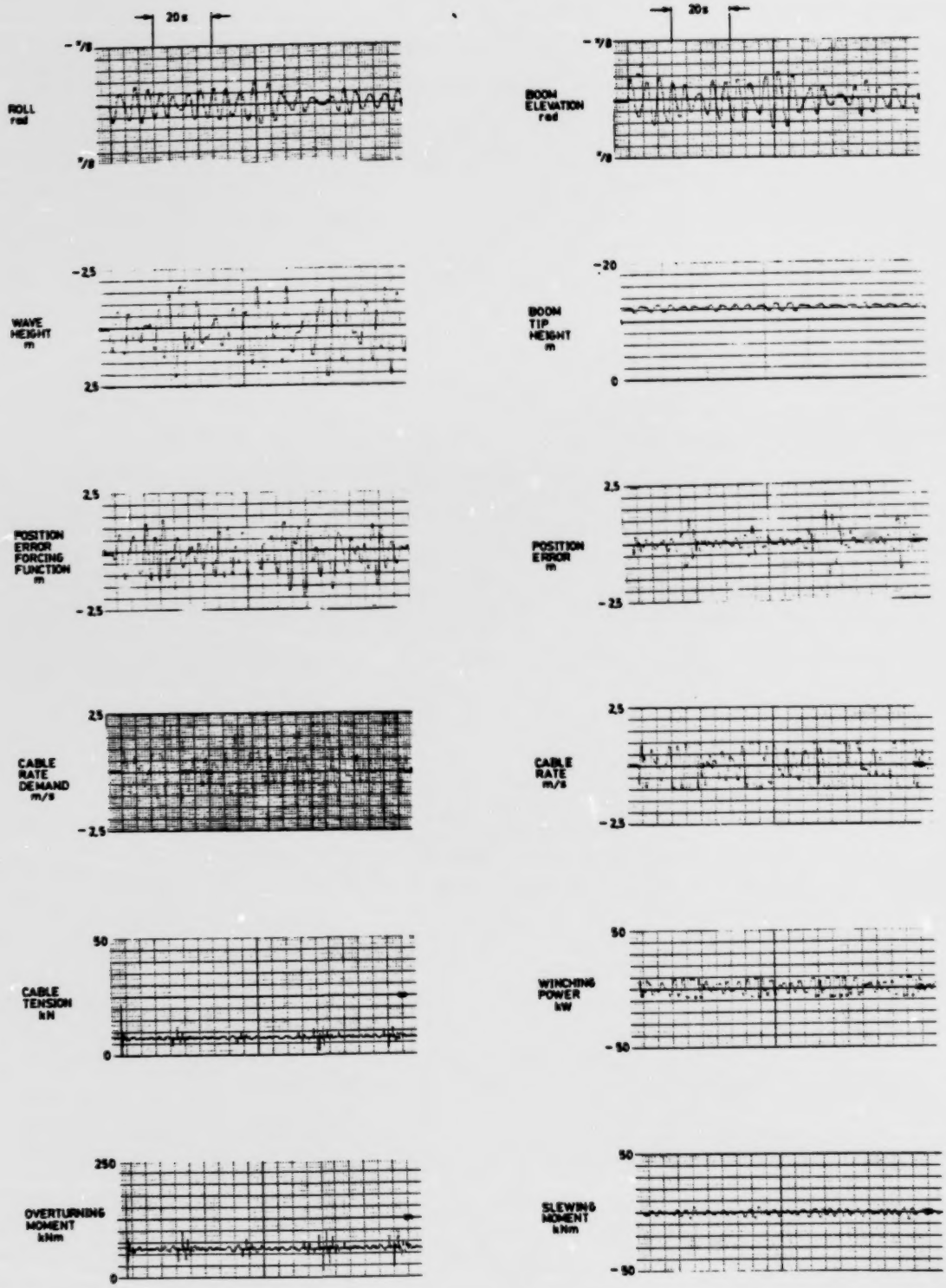

Figure 6.18 Position Control With Roll Compensation - Sea State 5

7. CONCLUSIONS

The objective of developing a simulation program capable of modelling an irregular sea, vessel response characteristics, and a human operator for the study of at-sea lifting operations, has been achieved.

Two levels of motion compensation have been studied during the evaluation phase of the project. The first of these, termed level 1, provided compensation by correcting for the motions of the vessel upon which the crane was mounted. The second, termed level 2, applied corrective action to remove the relative motion between the load lifting point and the deck of vessel 2.

Two methods of applying the compensation to a typical hydraulic crane with a telescopic cantilevered boom were considered. In one case, the winching rate commanded by the operator was modified by the compensating signals. In an alternate approach, boom elevation was modulated in response to the compensating signals leaving the entire capability of the winch available to the operator for controlling load height. The first method used calculated vertical speeds at the load lifting point on the crane and at the load deck on the second vessel as the feedback signals to the compensating controls, while for the second method, ship roll angle controlled boom elevation.

It was consistently found that level 1 compensation reduced the control errors of the human operator and that level 2 compensation offered even further improvement.

In addition to reducing tracking errors, compensation reduced operator workload, and load transients in the system.

The greatest contributor to performance degradation was the rate limit on the winch, or in broader terms, the physical limitations of the hoisting gear, encountered in higher sea states.

Also limiting the operator's performance was the resonant action of the load and cable combination, particularly at higher loading. This was not anticipated originally, and the reaction of an operator to motions of a frequency beyond his ability to apply corrective action, is to use less gain, or in other words, be more tolerant of errors.

Motion compensation improved performance on both accounts. By applying corrective action without the same lag as a human operator, the compensating controls reduced the number of encounters with the physical limitations of the hoisting gear, resulting in tighter setpoint control. By eliminating part or

all of the unwanted vessel motions, the compensating controls reduced the error forcing function so that the tracking of an error-tolerant operator was improved.

It is interesting to note that for the vessels chosen in this study, the smaller vessel exhibited displacements in heave closely following the wave amplitude, suggesting it might make the greatest contribution to the disturbance or error forcing function. However, the rotations of the larger vessel in the same sea states, caused it to contribute disturbances of the same magnitude as the smaller vessel by virtue of the location of the load lifting point remote from the vessel's centre of gravity. Thus the decision to opt for level 1 compensation, or to adopt the full level 2 compensation must be taken with a knowledge of the vessel seakeeping characteristics and load lifting point location.

The simulation also computes and displays the pendulous response of the load in the XY-plane to the ship's motion. No use has been made of this feature to date, but the potential is there for modelling and evaluating load stabilizing devices, an example of which would be a tag line system.

(This page intentionally left blank.)

REFERENCES

1. Olsen, H.
   Falkenberg, E.
   Robertsson, S.
   "Offshore Crane Operations - Failure Mechanisms and Dynamic Load Effects".
   Norwegian Maritime Research, No. 3, 1981.

2. Society of Automotive Engineers
   "Rating Lift Cranes on Fixed Platforms Operating in the Ocean Environment".
   SAE J1238, Society of Automotive Engineers

3. Gagne, R.E.
   "HYSTAN- A Standard Architecture for Hybrid Computer Models".
   DME Report LTR-AN-42, August 1980.

4. Gordon-Smith, M.
   "An Investigation into Certain Aspects of the Describing Function of a Human Operator Controlling a System of One Degree of Freedom".
   UTIAS no. 149

5. Stenhouse, Geo.A.
   Hilton, Robert J.
   "Method For Rating High Pedestal Cranes For Lifting from Supply Boats in Various Sea States".
   Lawrence-Allison & Associates Corp.
   Europec 78, paper no. 71

6. McRuer, D.T.
   Krendel, E.S.
   "Mathematical Models of Human Pilot Behaviour".
   AGARD-AG-188, January 1974

7. Sumney, D.C.
   Watson, T.C.
   "Comparison of Computed Response Amplitude Operators for Containership, Lighters and Barges".
   NCSC TM 342-82; February 1982

8. Schaner, D.S.
   "Crane Load Moment System For Offshore Crane Operations".
   European Offshore Petroleum Conference, Vol. II, paper 70

9. Kidera, E.H.
   "A Motion-Compensated Launch/Recovery Crane For Towing of Oceanographic Instruments".
   Ocean Engineering Division of ASTM, Nov. 1981

10. Stricker, P.A.
    "Active-Passive Motion Compensating Crane For Handling a Remote Unmanned Work System".
    OTC 3236, OTC Proceedings Vol. III, 1978

BIBLIOGRAPHY - With Brief Abstracts

Balfour, James A.D.
Owen, David G.

"Dynamic Behaviour of Platform Cranes".
OTC 3794, OTC Proceedings, Vol.II, 1980

For fixed base (platform mounted cranes) engaged in lifting operations with supply boats, various mathematical models are examined. Balfour and Owen conclude that a two degree-of freedom model of a crane can offer useful results for parametric studies but recommend a multi degree-of freedom model for detailed crane design.

Charrett, D.E.
Hyden, A.M.

"Dynamic Factors for Offshore Cranes".
OTC 2578, OTC Proceedings, Vol.II, 1976

For a luffing crane mounted on a non-moving platform, the authors derive the magnitude of the dynamic factor as a load is hoisted from a supply boat moving sinusoidally. Six crane configurations are analyzed and overturning moments on the slewing ring are determined as well.

Clarkson, John A.
Denny, Francis M.

"Offshore Crane Dynamics".
OTC 3793, OTC Proceedings, Vol.II, 1980

Account is taken of the inertia and stiffness properties of all components of the crane structure in this development of a full dynamic analysis of platform-mounted offshore cranes. The authors analyze the factors which affect dynamic amplification and note that factors in excess of 5 are not uncommon.

Gagne, R.E.

"HYSTAN- A Standard Architecture for Hybrid Computer Models".
DME Report LTR-AN-42, August 1980

This report describes the standard model architecture for the NRC hybrid computer software package.

Gordon-Smith, M.

"An Investigation Into Certain Aspects Of The Describing Function Of A Human Operator Controlling A System Of One Degree Of Freedom".
UTIAS no. 149

Mr. Gordon-Smith reports on an experimental investigation undertaken to examine the "remnant" portion of the mathematical model of a human operator. Of particular significance is his presentation of group mean fitted describing function parameters resulting from his experiments with a number of subjects in a rate control tracking task. His values provide a useful starting point for the model of the human operator in this report.

Kenny, M. Francis

"Operational Dynamics Of An Offshore Crane".
European Offshore Petroleum Conference, Vol. II, paper 69

A very detailed finite element model of a crane is used to determine the transient overloading factors for all its critical components in response to different lift-off velocities. A fixed-base pedestal crane lifting from a supply boat is the subject, and loading is confined to the vertical with crane stresses computed only in the topping plane.

Kidera, E.H.

"A Motion-Compensated Launch/Recovery Crane For Towing Of Oceanographic Instruments".
Ocean Engineering Div. of ASTM, Nov 1981

"A Motion-Compensated Launch/Recovery Crane".
Ocean Engineering, Vol. 10, No. 4, 1983

"At-Sea Handling and Motion Compensation".
Proceedings OCEANS'83, Vol. II: Technical Papers.

Kidera describes a launch/recovery system for overboarding, towing and retrieving a variety of depressor types. The system he discusses is a passive system operating on the bobbing boom principle. Hydraulic accumulators provide a soft spring, the spring rate (hence natural frequency) of which may be adjusted by varying the quantity of hydraulic oil in the system. The system had six months of operational experience and had performed satisfactorily in that period.

McRuer, D.T.
Krendel, E.S.

"Mathematical Models of Human Pilot Behaviour".
AGARD-AG-188, January 1974

McRuer and Krendel review the response characteristics of human pilots in control tasks and examine various mathematical models of their performance that have evolved over the years. The authors also discuss the limitations and shortcomings of these models, and provide an extensive bibliography on this and related topics.

Olsen, H.
Falkenberg, E.
Robertsson, S.

"Offshore Crane Operations - Failure Mechanisms and Dynamic Load Effects".
Norwegian Maritime Research, No. 3, 1981

The authors discuss the safety record of cranes engaged in lifting operations in the North Sea. They compare accident rates from the North Sea to those of typical land-based operations, showing a much higher accident rate for the offshore operations. Failure mechanisms are discussed and the authors point to load velocity at the moment of pick-up as a major contributor to many of the failure modes. In modelling cranes to study the dynamic response amplification, the authors caution against the use of a 1-degree of freedom model and recommend a finite element model.

Reid, L.D.

"The Measurement of Human Pilot Dynamics In A Pursuit-Plus-Disturbance Tracking Task".
UTIAS Report No. 138, April 1969

A controlled experiment with a number of subjects was undertaken to obtain human operator performance measurements in a pursuit-plus-disturbance tracking task. The data gathered during the experiment was then used to establish the parameters of a comparable continuous servo-analysis model. The parameters defined in this report were relevant to the human operator model engaged in a load-lifting task.

Schaner, David S.

"Crane Load Moment System For Offshore Crane Operations".
European Offshore Petroleum Conference, Vol. II, paper 70

Regulations requiring the use of safe-load indicating systems are reviewed and load rating parameters for pedestal mounted platform cranes are discussed. The author then describes the design of a microprocessor based safe-load system and the sensors he would recommend. He does not consider slewing moment in his work.

Society of Automotive Engineers

"A Recommended Method of Analytically Determining the Competence of Hydraulic Telescopic Cantilevered Crane Booms".
SAE J1078, Society of Automotive Engineers

This SAE information report establishes a standard analytical method for rating hydraulic telescopic cantilevered crane booms. The technique presented is applicable only to land based cranes. It could provide a useful starting point in developing a similar analysis for rating shipboard cranes.

Society of Automotive Engineers

"Rating Lift Cranes on Fixed Platforms Operating in the Ocean Environment". SAE J1238, Society of Automotive Engineers

The SAE recommended practice is described for establishing design dynamic loads on fixed base cranes engaged in lifting operations from vessels in various sea conditions. The practice assumes the supply boat motions follow the waves and the lifting crane is fixed. Dynamic stress amplification due to crane mass is not considered.

Stenhouse, Geo. A.
Hilton, Robert J.

"Method for Rating High Pedestal Cranes For Lifting From Supply Boats In Various Sea States".
Lawrence-Allison & Associates Corp.
Europec 78, paper no. 71

Multi degree-of-freedom analysis techniques are used to predict the dynamic loading on platform cranes (particularly high pedestal types) when lifting from supply boats. The analytical technique can also be used to generate fatigue spectra for the various crane components and to determine the impact effects which occur with derrick barge lifts.

Strengehagen, J.
Gran, S.

"Supply Boat Motion, Dynamic Response And Fatigue Of Offshore Cranes".
OTC 3795, OTC Proceedings, Vol.II, 1980

Strengehagen and Gran analyze the case of a non-moving crane (platform mounted) lifting loads from a supply boat. Using a statistical approach to model the vertical speed variation of a supply boat, the authors examine methods of calculating vibration and dynamic forces in a crane, and make the point that fatigue life can be strongly influenced by the loading history and boom dynamics. They conclude that fatigue process may be accelerated by transient and random vibrations, and that crane derating should be based on a reasonably representative dynamic model of the crane and ship motion.

Stricker, P.A.

"Active-Passive Motion Compensating Crane For Handling A Remote Unmanned Work System".
OTC 3236, OTC Proceedings, Vol.III, 1978

A combination of an active and passive compensating system for a ship-mounted boom is described from conception through analysis to sea trials. The bobbing boom, capable of deploying and retrieving unmanned work systems up to 10 tons, uses a gas-charged hydraulic accumulator and servo valve to control boom motion in response to boom tip acceleration measurements.

Summey, D.C.
Watson, T.C.

"Comparison of Computed Response Amplitude Operators for Containership, Lighters and Barges".
NCSC TM 342-82; February 1982

Using four container vessels, two discharge lighters and two barges, the Response Amplitude Operators (RAO's) are computed using two ship motion computer models for various sea states and loading conditions. The RAO data curves generated are used in the current study of crane dynamics.

Ward, Carley C.
Johnson, Frank R.

"Dynamic Loads On A Shipboard Crane Boom Due To Ship Motion".
OTC 3321, OTC Proceedings, Vol.IV, 1978

The authors address the problem of accounting for the inertial loading of a crane structure due to the translations and rotations of the vessel upon which it is mounted. In their digital program, they use vector analysis and rotating coordinate frames. Their intention is to combine this analysis with a structural analysis program to compute the dynamic stresses in a boom.

Watters, Allan J.
Moore, David J.
McGill, Iain S.

"Dynamics of Offshore Cranes".
OTC 3792, OTC Proceedings, Vol.II, 1980

Fixed offshore cranes engaged in off-loading and back loading supply boats in the North Sea are the subject of this paper. Watters et al compare various analog models of a crane boom to determine the relationship between the number of degrees of freedom modelled, and the fidelity of the model. The authors point out that the higher factors of safety being applied to hoisting ropes result in stiffer ropes, hence greater impact forces, and urge that these effects be fully investigated with a dynamic model.

Wyon, A.S.
Mackinnon, J.A.

"Dynamic Response of North Sea Cranes".
BSSM/RINA, Jt. Conference, Sept. 1975.

Messrs. Wyon et al. report on experimentally observed boom stresses, hook loads, and pedestal moments during lifts of a 5 ton test weight from a supply boat in rough weather. They then compare these results to standard drop tests and conclude load amplification factors of up to a factor of almost 3 must be considered.

Zwibel, Harry S.
Davis, Duane A.

"Cargo Transfer At Sea - The Pendulation of Loads Suspended from Shipboard Cranes".
Naval Civil Eng., Port Hueneme, Cal.,
December 1972

A ship motion analysis provides boom tip displacement operators as the forcing function in a load pendulation study. Pendulous action is the result of crane platform surge and pitch, and includes the effect of raising and lowering the load. No allowance was made for load damping in this analysis. The authors conclude some form of load restraining equipment must be used in even moderate seas and state that tests using a 100-ton floating crane confirm their analysis.

Auth. Anon.

"Relative Motion Compensation Sensing System Study for Cargo Transfer in Rough Sea".
Goodyear Aerospace Corp., Akron, Ohio; Naval Ship Systems Command, Dec. 1974

In a study for the U.S. Navy, conceptual designs were prepared for load stabilizing systems that would permit lifting in rough seas. This report sets out the prerequisites for the design of a relative motion sensing system. Various forms of sensor packages are examined (inertial, laser-based, FLIR, electromagnetic) and a sensing system design is proposed.

A P P E N D I X A

Analog Diagrams

SUMMING AMPLIFIER
$Y = (10X_1 + X_2)$

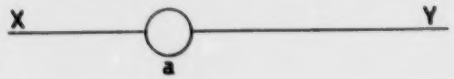

SERVO-SET POTENTIOMETER
$Y = aX$
$0 \leq a \leq 1$

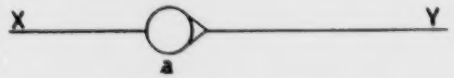

DIGITALLY CONTROLLED ATTENUATOR
$Y = aX$
$-1 \leq a \leq 1$

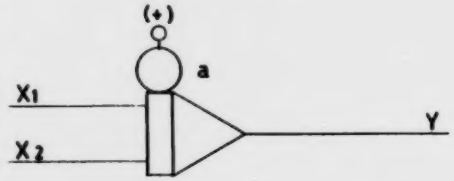

INTERGRATOR WITH INITIAL CONDITION
$Y = -a + \int (X_1 + X_2)\,dt$

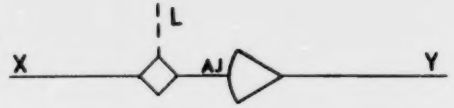

DIGITAL / ANALOG SWITCH
IF L=TRUE, Y=X
IF L=FALSE, Y=0

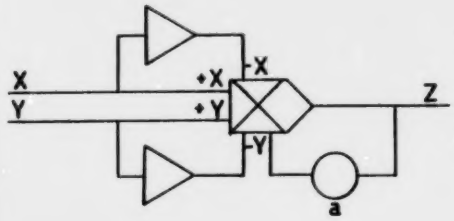

MULTIPLIER WITH POT FEEDBACK
$Z = \frac{-XY}{a}$

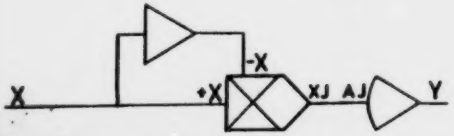

SQUARE
$Y = X^2$

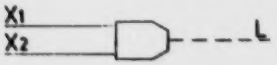

COMPARATOR
IF $X_1 + X_2 > 0$, THEN L = TRUE
, ELSE L = FALSE

DIGITAL TO ANALOG CONVERTER
$X = -D_1$, $-1 \leq D_1 \leq 1$

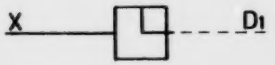

ANALOG TO DIGITAL CONVERTER
$D_1 = X$, $-1 \leq X \leq 1$

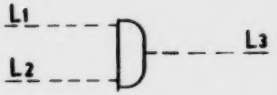

AND GATE
$L_3 = L_1 \bullet L_2$

LOGIC INVERTER
$L_1 = L_2$

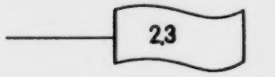

STRIP CHART RECORDER
NO. 2 CHANEL 3

FIGURE 1 -

ANALOG NOTATION

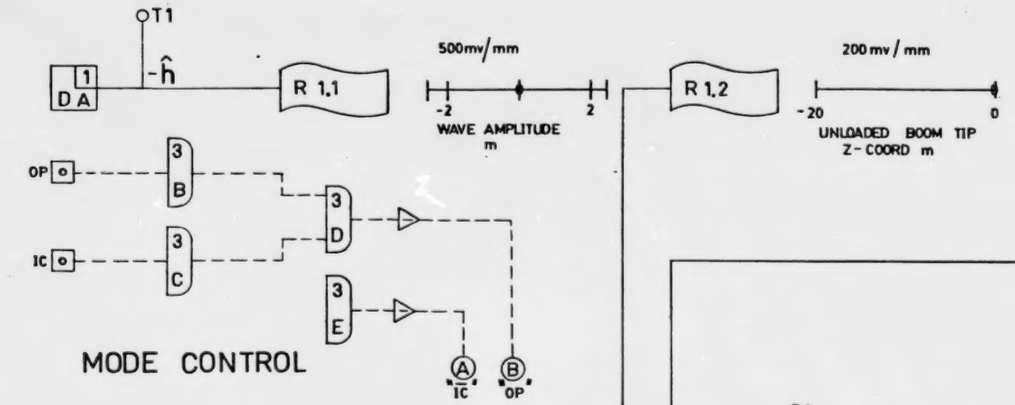

MODE CONTROL

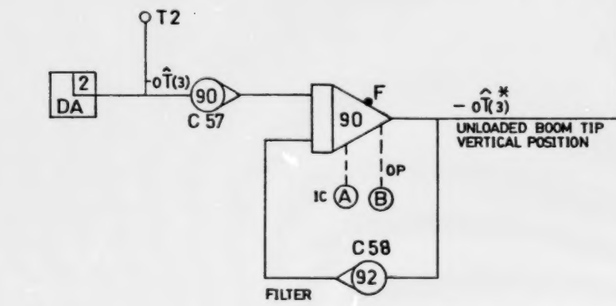

CLOCK CONTROL

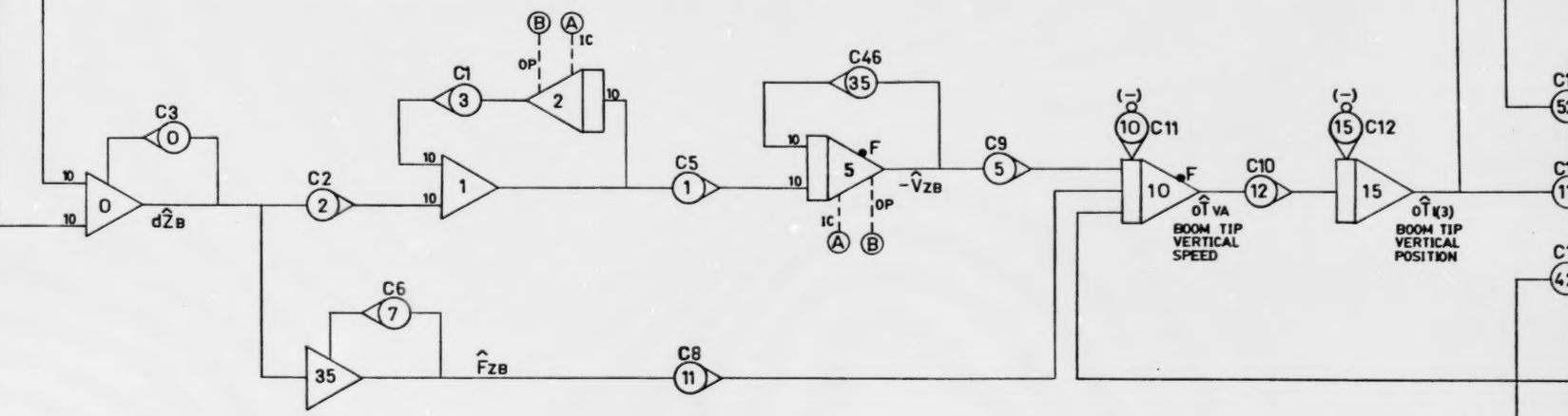

CRANE BOOM

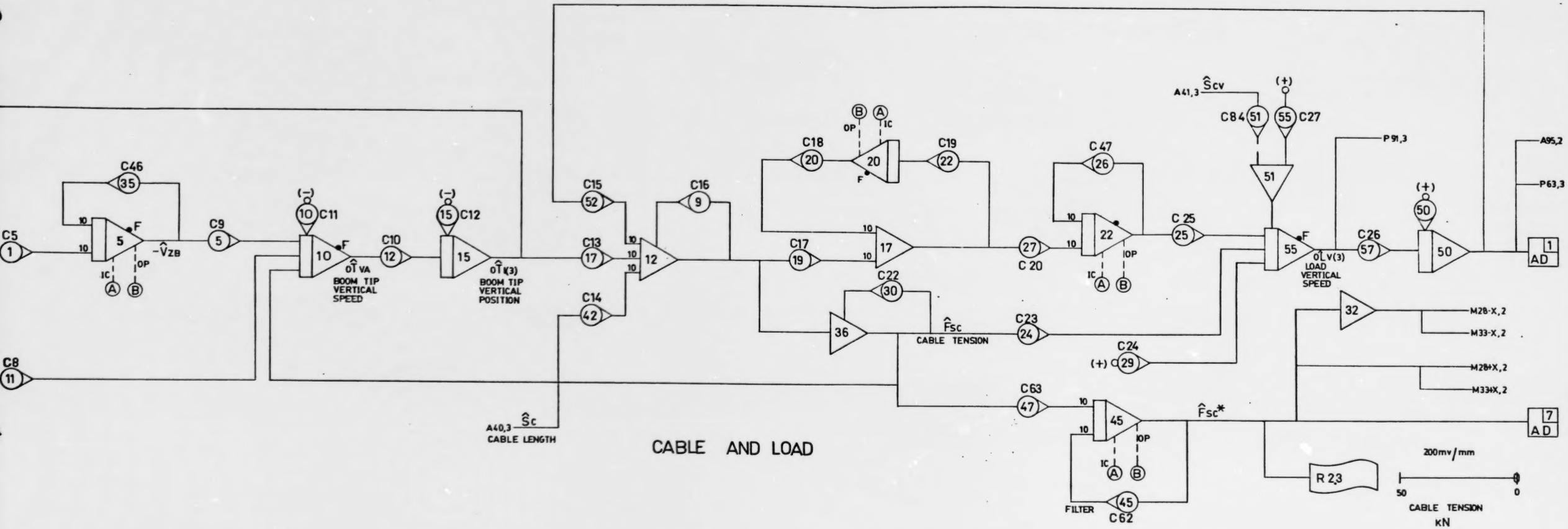

CABLE AND LOAD

FIGURE 2 - SHEET 1

CRANE BOOM
CABLE AND LOAD
CLOCK CONTROL
MODE CONTROL

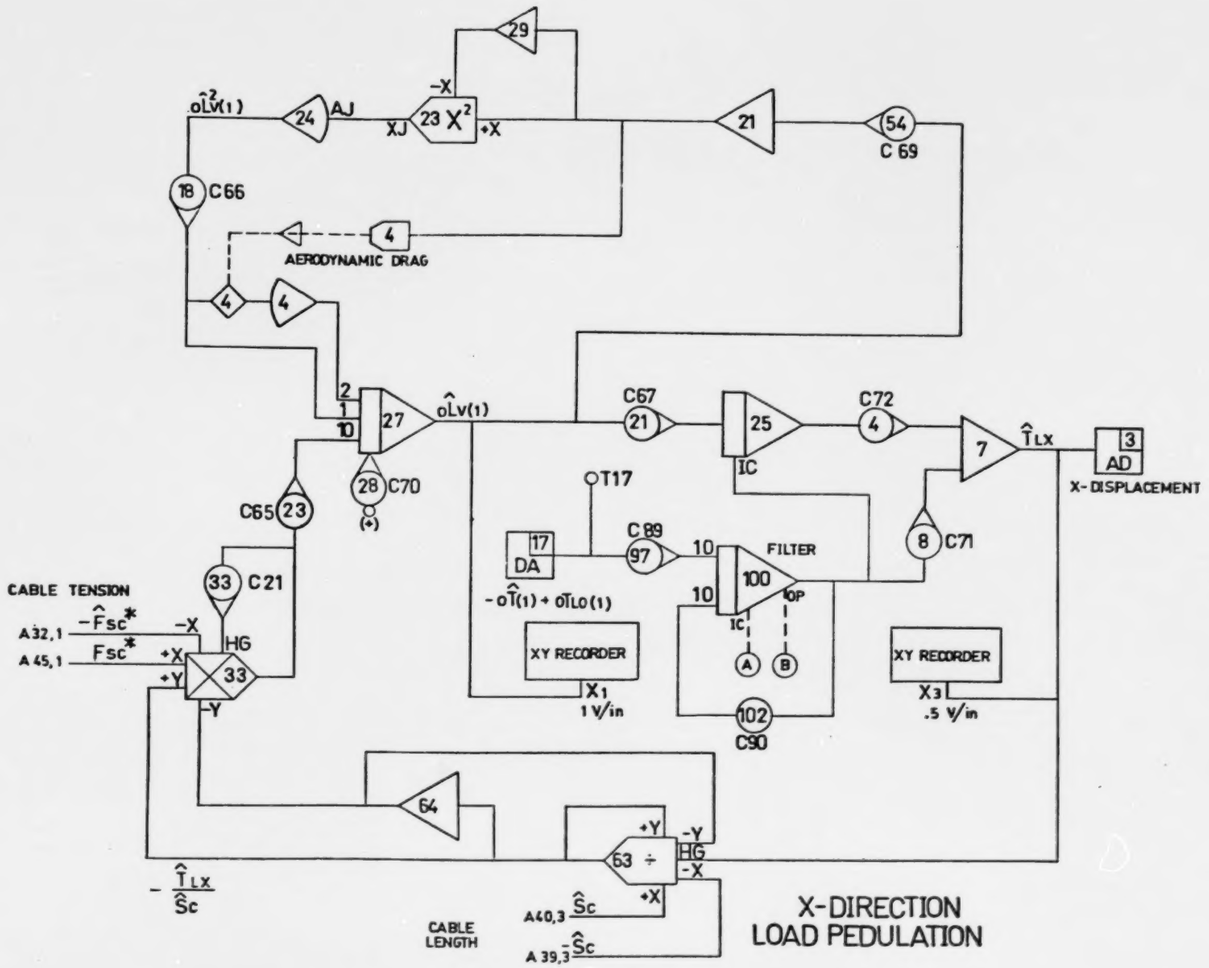
oL̂V(1)
24 AJ
XJ
23 X²
-X
+X
29
21
54
C 69
18 C66
4
AERODYNAMIC DRAG
4
4
2
1
10
27
ôLv(1)
C67
21
25
IC
C72
4
7
T̂LX
3
AD
X-DISPLACEMENT
28 C70
(+)
C65 23
T17
17
DA
-ôT̂(1) + ôTLO(1)
C89
97
10
FILTER
100
OP
IC
A
B
8 C71
XY RECORDER
X1
1 V/in
102
C90
XY RECORDER
X3
.5 V/in
CABLE TENSION
A32,1 -F̂sc*
A45,1 F̂sc*
-X
+X
+Y
-Y
HG
33
33 C21
64
63 ÷
HG
+Y
-Y
-X
+X
-T̂LX / Ŝc
CABLE LENGTH
A40,3 Ŝc
A39,3 -Ŝc
X-DIRECTION
LOAD PEDULATION

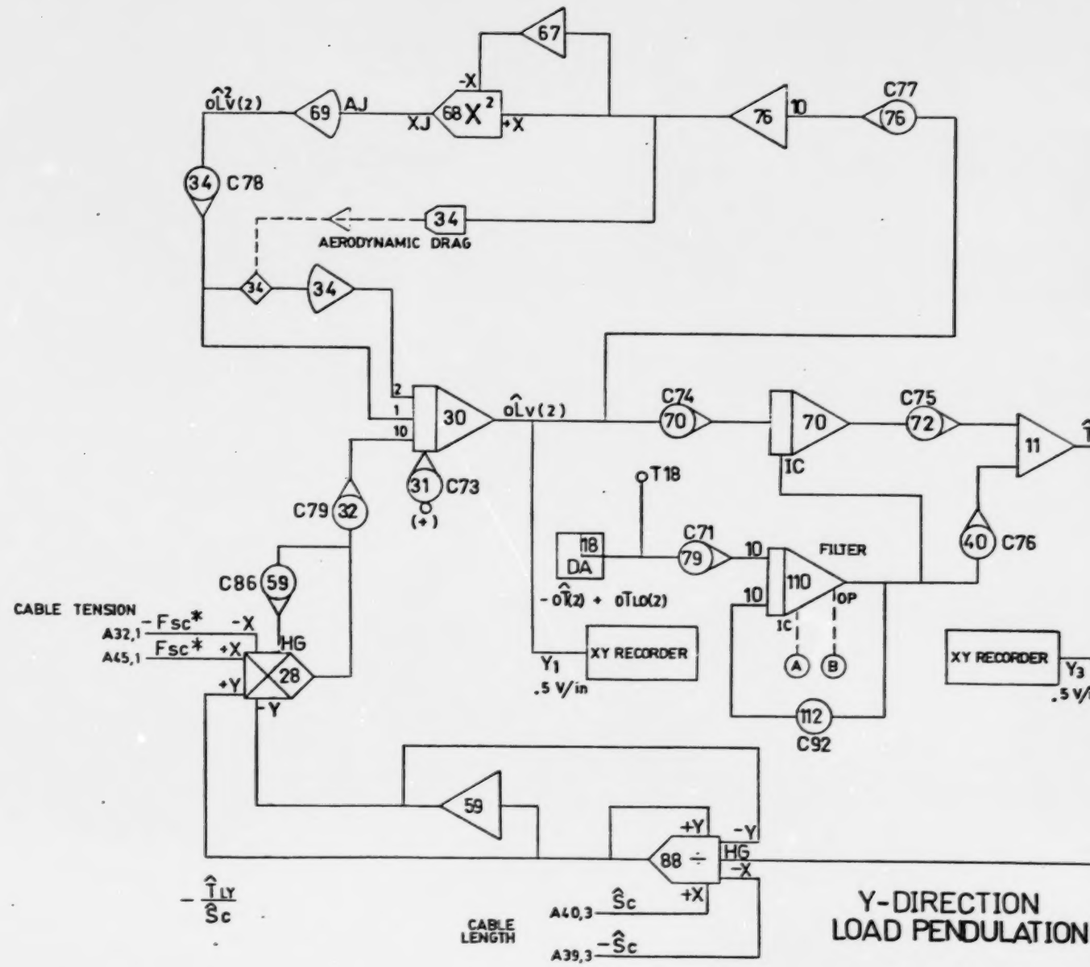
oL̂V(2)
69 AJ
XJ
68 X²
-X
+X
67
76
10
C77
76
34 C78
34
AERODYNAMIC DRAG
34
34
2
1
10
30
ôLv(2)
C74
70
70
IC
C75
72
11
31 C73
(+)
C79 32
T18
18
DA
-ôT̂(2) + ôTLO(2)
C71
79
10
FILTER
110
OP
IC
A
B
40 C76
XY RECORDER
Y1
.5 V/in
112
C92
XY RECORDER
Y3
.5 V/
C86 59
CABLE TENSION
A32,1 -F̂sc*
A45,1 F̂sc*
-X
+X
+Y
-Y
HG
28
59
88 ÷
HG
+Y
-Y
-X
+X
-T̂LY / Ŝc
CABLE LENGTH
A40,3 Ŝc
A39,3 -Ŝc
Y-DIRECTION
LOAD PENDULATION

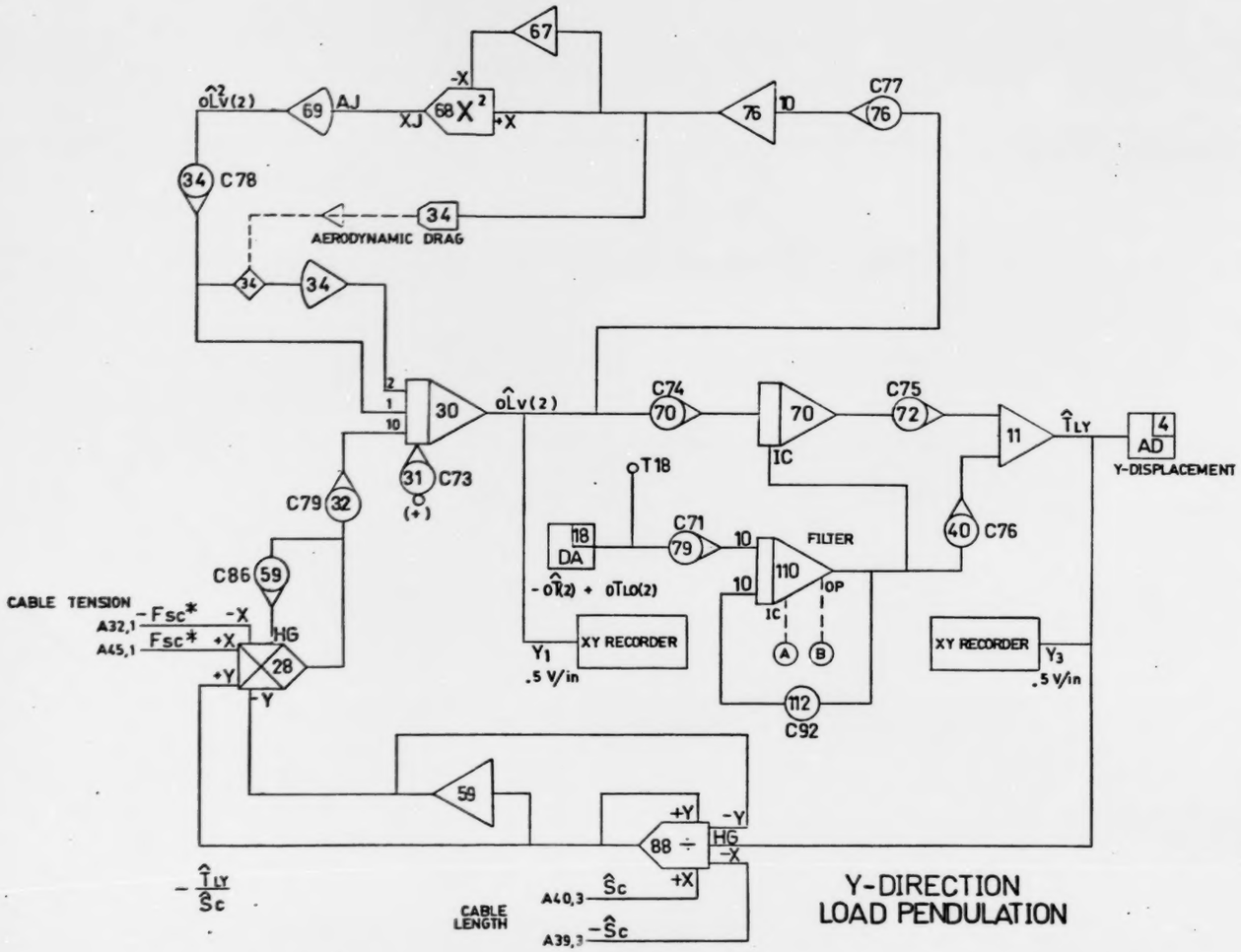

Y-DIRECTION
LOAD PENDULATION

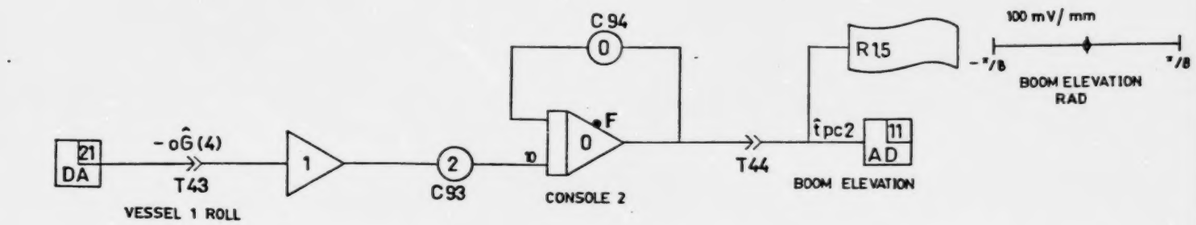

ROLL COMPENSATOR

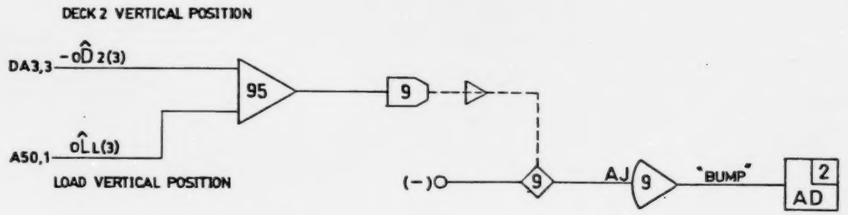

DECK CONTACT DETERMINANT

FIGURE 2 - SHEET 2

X-DIRECTION LOAD PENDULATION
Y-DIRECTION LOAD PENDULATION
ROLL COMPENSATOR
DECK CONTACT DETERMINANT

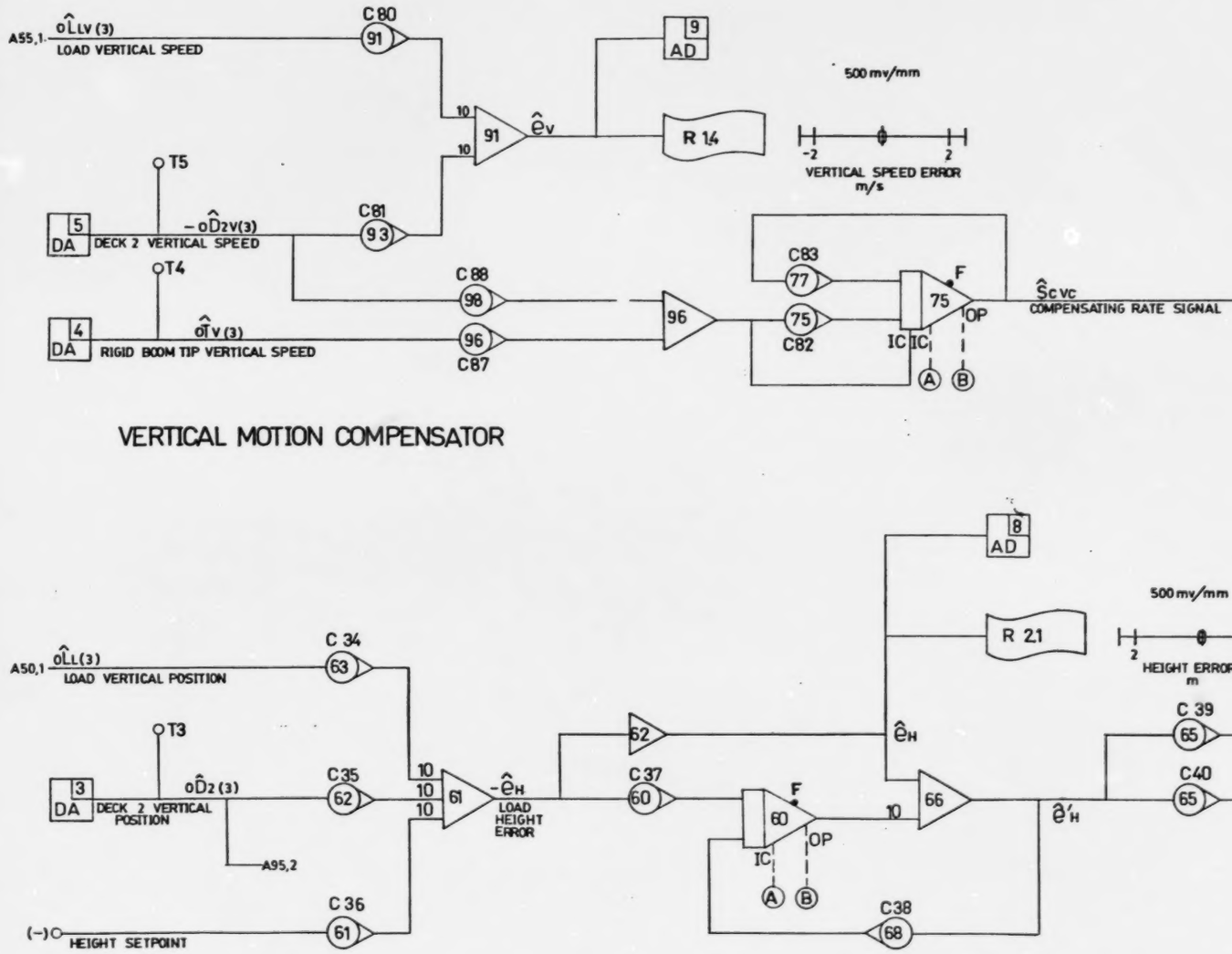
A55,1
oL̂LV(3)
LOAD VERTICAL SPEED
C80
91
10
10
91
ê_V
9
AD
500 mv/mm
R 14
-2
2
VERTICAL SPEED ERROR
m/s
T5
5
DA
DECK 2 VERTICAL SPEED
-oD̂2V(3)
C81
93
T4
4
DA
RIGID BOOM TIP VERTICAL SPEED
oT̂V(3)
C88
98
96
C87
96
C83
77
75
C82
75
F
OP
IC
IC
A
B
Ŝc vc
COMPENSATING RATE SIGNAL
VERTICAL MOTION COMPENSATOR
TENSION LIMITER
CABLE WINCHING RATE LIMIT
31
L31 ±
31
500 mv/mm
R 34
-2
2
OPERATOR RATE DMND
m/s
POWER LIMITER
Ŝ'cv
85
10
WINCH
A50,1
oL̂L(3)
LOAD VERTICAL POSITION
C34
63
T3
3
DA
DECK 2 VERTICAL POSITION
oD̂2(3)
C35
62
A95,2
C36
61
HEIGHT SETPOINT
10
10
10
61
-ê_H
LOAD HEIGHT ERROR
62
C37
60
60
F
IC
OP
A
B
10
66
C38
68
8
AD
500 mv/mm
R 21
2
-2
HEIGHT ERROR
m
ê_H
ê'_H
C39
65
C40
65
65
F
IC
OP
A
B
C41
67
10
71
ê_H'
C42
80
80
F
IC
OP
A
B
C51
82
115
C43
HUMAN OPERATOR GAIN
e_H*
HEIGHT CONTROL STRATEGY
HUMAN OPERATOR

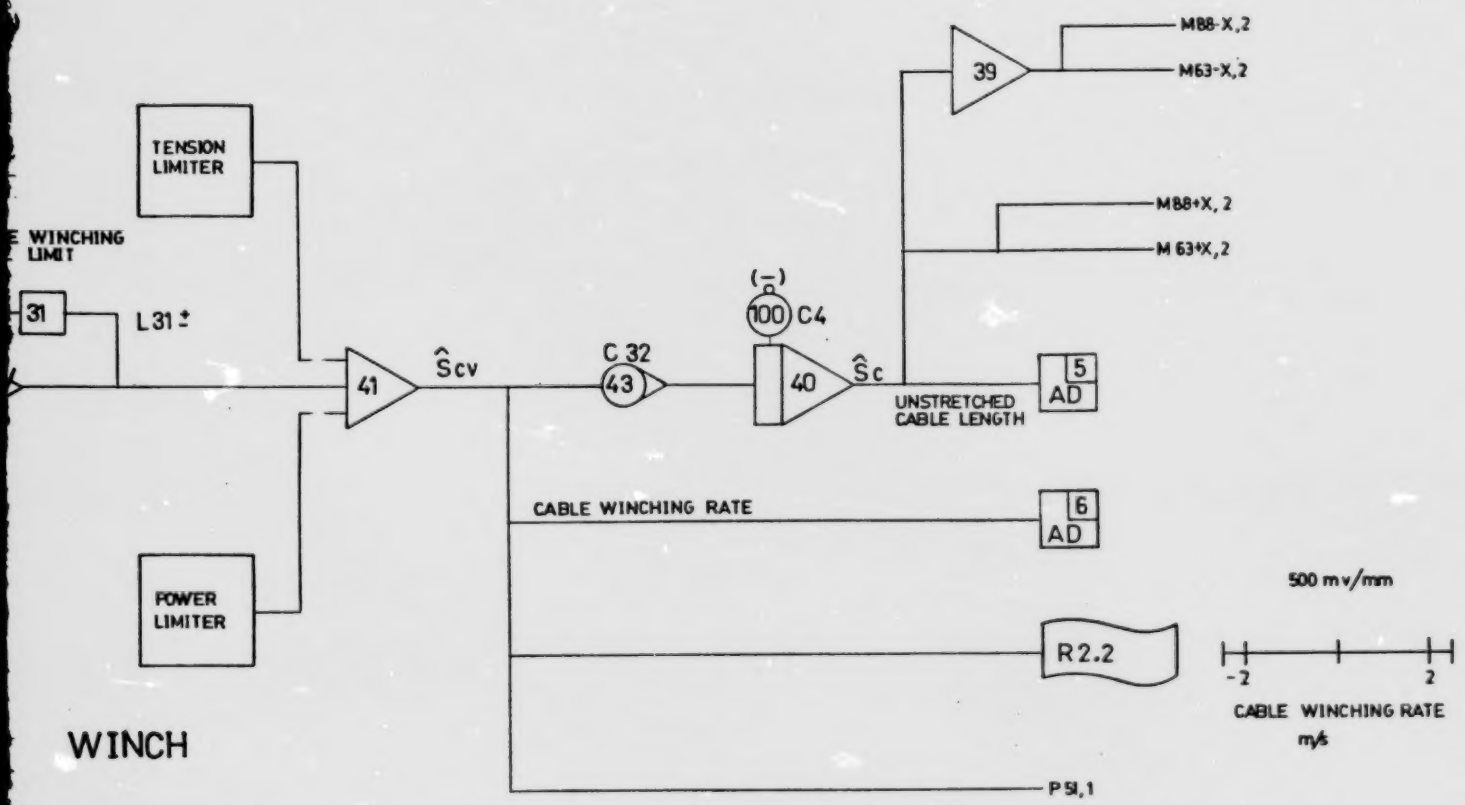

FIGURE 2 - SHEET 3

HUMAN OPERATOR
VERTICAL MOTION COMPENSATOR
WINCH

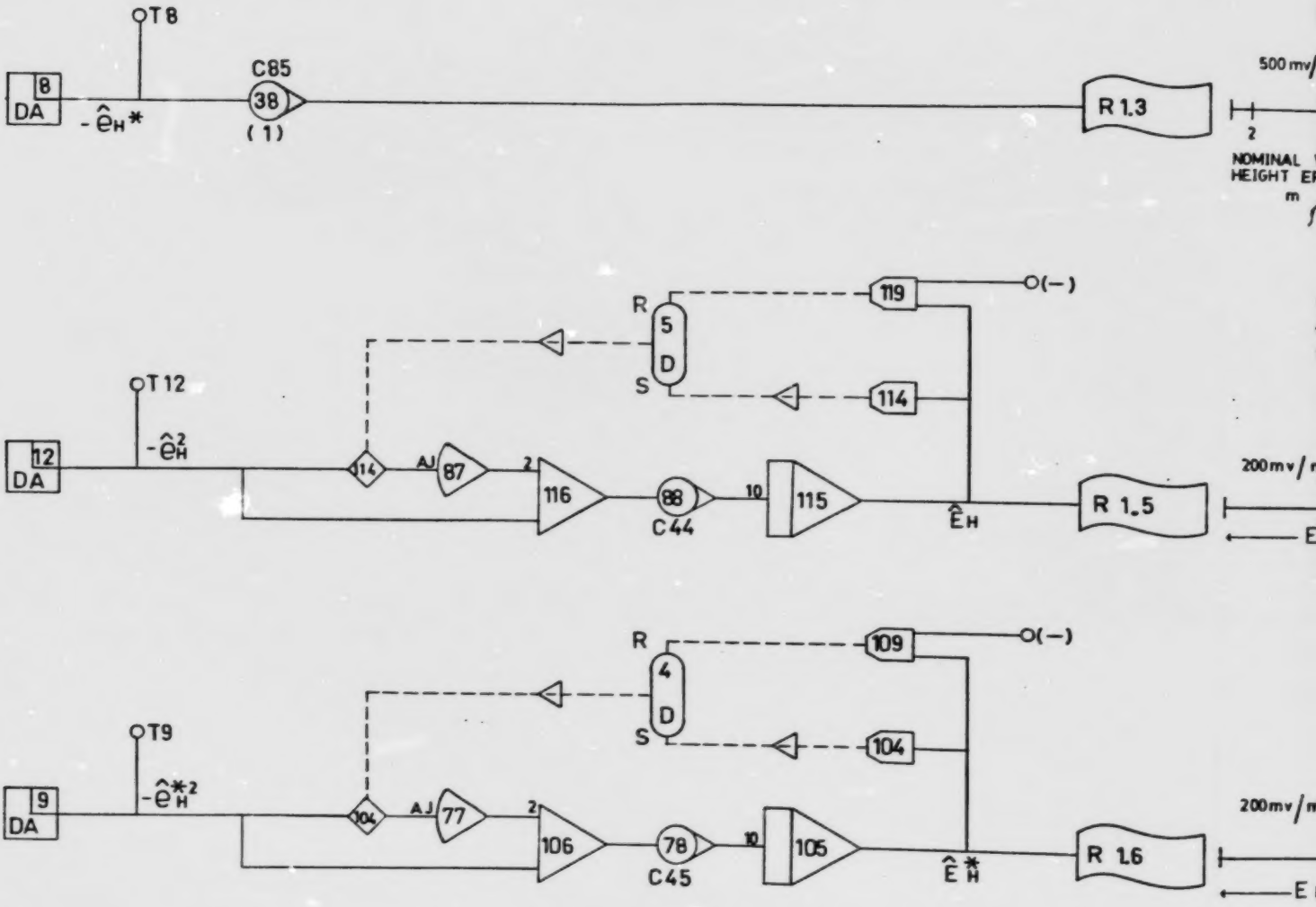

INTEGRATING RECORDERS

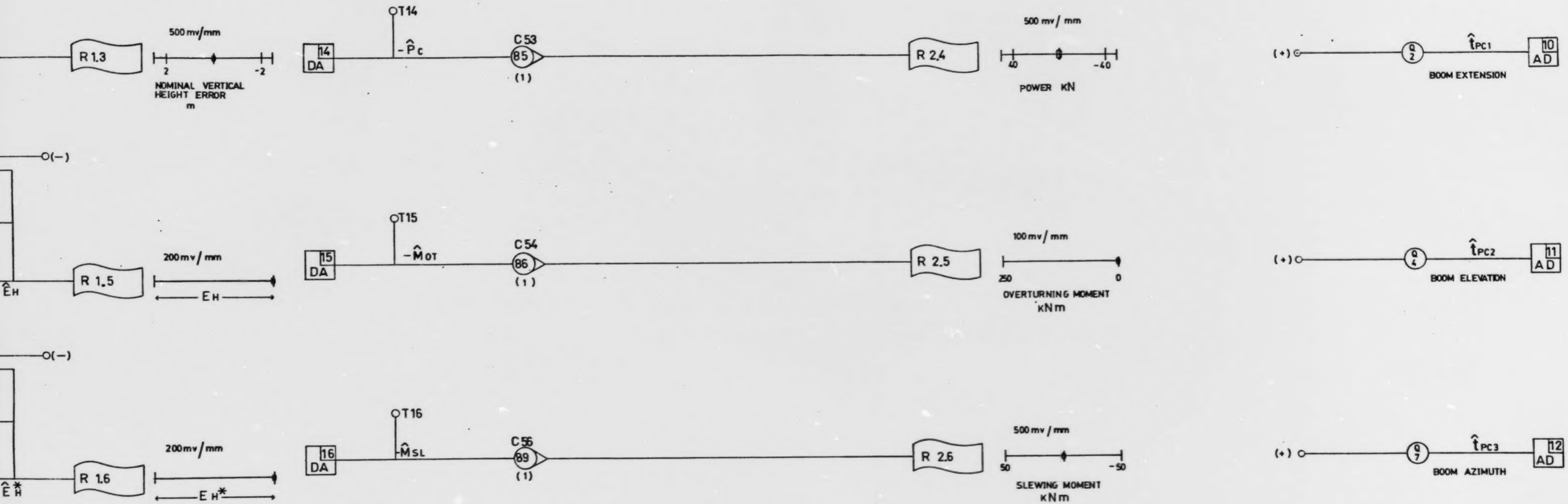

FIGURE 2 - SHEET 4

INTEGRATING RECORDERS
RECORDER OUTPUTS
MANUAL ACTUATOR INPUTS

A P P E N D I X B

Program Listings

```
      SUBROUTINE ADCSET
C
C  ASSIGNS ANALOG TO DIGITAL CHANNELS
C
C
      EQUIVALENCE (SAADC(1),SVOLL3)
      EQUIVALENCE (SAADC(2),SVbump)
      EQUIVALENCE (SAADC(3),SVTLx)
      EQUIVALENCE (SAADC(4),SVTLy)

      EQUIVALENCE (SAADC(5),SVSc)
      EQUIVALENCE (SAADC(6),SVScv)
      EQUIVALENCE (SAADC(7),SVFsc)
      EQUIVALENCE (SAADC(8),SVEH)

      EQUIVALENCE (SAADC(9),SVEV)
      EQUIVALENCE (SAADC(10),SVtpc1)
      EQUIVALENCE (SAADC(11),SVtpc2)
      EQUIVALENCE (SAADC(12),SVtpc3)
C
C  ASSIGN ADC CHANNELS

      IAADC(1)=1
      IAADC(2)=2
      IAADC(3)=3
      IAADC(4)=4
      IAADC(5)=5
      IAADC(6)=6
      IAADC(7)=7
      IAADC(8)=8
      IAADC(9)=9
      IAADC(10)=10
      IAADC(11)=11
      IAADC(12)=12

C
C  ESTABLISH NUMBER OF AD CONVERTERS
C
      NAADC=12
C
C
      RETURN
      END
```

```
      SUBROUTINE AREA
C                                                          23 October 85
C  Compute the area m0 under the energy spectrum, using the Descartes sums.
C
      REAL    RDrao(2,10,6)
      INTEGER IDnpt(6)
      DATA    pi/3.1415927/, step/.01/

C  Find the maximum frequency used in RAO description

      Fmax = 20.

C  Using a small step dw = .01 and Fmax as an upper limit compute the area
C under the Energy Spectrum assuming that ship influence on the wave is ignored

      RDm0 = .0
      save = RVgama
      RVgama = pi / 2.
      w = .0
   10 CONTINUE
      w = w + step
      RDm0 = RDm0 + ES(w) * step
      IF(w . LT . Fmax) goto 10
      RVgama = save

      RETURN
      END
```

```
      SUBROUTINE BOOM
C                                                          23 October 85 Rev. 2
      DIMENSION LVflag(50)
C
C  This subroutine computes the rigid Boom Tip Motion in an inertial
C  reference frame moving at constant velocity RVv1. Boom is assumed to be
C  inelastic.
C
      REAL    RVa(3,3),RCQC(3),RVCT(3),RVOT(3),RVder(6),RVader(3,3)
      REAL    RVOTv(3)
C
C  Call the subroutine CMPTA to compute the elements of matrix A, associated
C  with the rotation of G reference frame(body Fixed axes for Vessel 1).
C
      CALL    CMPTA
C
C  Call subroutine CMPTCT to compute the coordinates of point T in C refe-
C  rence system as a function of actuator positions.
C
      CALL    CMPTCT
C
C  Compute Boom Tip Motion
C
      DO 20 i = 1,3
        RVOT(i) = SHPMOT(i,RVtime)
        DO 10 j = 1,3
          RVOT(i) = RVOT(i) + RVa(i,j) * (RCQC(j) + RVCT(j))
10      CONTINUE
20    CONTINUE
      IF(LVflag(1)) THEN
                    DO  40  i = 1,3
                      RVOTv(i) = RVder(i)
                      DO  30  j = 1,3
                        RVOTv(i) = RVOTv(i) + RVader(i,j) * (RCQC(j) +
     @                  RVCT(j))
30                    CONTINUE
40                  CONTINUE
      ENDIF
C
C  *** WARNING !!! *** RVCT is considered to be constant in time
C                      (i.e. no relative motion between inelastic boom tip and
C                      crane base), otherwise a new term should be introduced
C                      into the above equation for speed computation.
C

      RETURN
      END
```

```
_DRB2: [USER2.TULAI.HYBRID]BUGSET.PRE;1                          1-APR-1986 2

C------------ BUGSET
C****BUGSET FOR STANDARD MODEL HYSTAN**********
C 30AUG80
C
C ******BUGSET SOURCE MUST GO THROUGH PREPROCESSOR*****
C ******WITH USER SUPPLIED SETUP RULES*****
C
C******MUST BE PREPROCESSED EACH TIME SETUP RULES CHANGED*******
      SUBROUTINE BUGSET
C
      COMMON/CBLOOK/NLOOK,ILDCAN(10),ILVARP(10),RLSCAL(10)
C LOOK ROUTINE VARIABLES ARE:
C     NLOOK=NUMBER OF LOOK ARRAY VARIABLES .LE.10
C        BUGOFF NAME OF NLOOK IS LN
C    ILDCAN=ARRAY OF DCA ADDRESSES TO BE USED AS OUTPUT DEVICES
C        BUGOFF NAME OF ILDCAN IS LD
C    ILVARP=ARRAY OF POINTERS TO RMODEL DATA BASE
C        BUGOFF NAME OF ILVARP IS LP
C    RLSCAL=ARRAY OF SCALE FACTORS FOR MODEL DATA
C        BUGOFF NAME OF RLSCAL IS LS
C
C INCLUDE FLAGS FOR OFFLINE MODEL
      LOGICAL LVFLAG(50)
C
C TELL BUGOFF ABOUT THE LOOK ARRAY VARIABLES
      CALL BUGINT(6HLN    ,NLOOK,2HIV)
      CALL BUGINT(6HLD    ,ILDCAN,2HIA)
      CALL BUGINT(6HLP    ,ILVARP,2HIA)
      CALL BUGINT(6HLS    ,RLSCAL,2HRA)
C INITIALIZE LOOK ROUTINE
      NLOOK=0
C POINT TO NONEXISTENT DCA'S ON CONSOLE
      DO 10 I=1,10
      ILDCAN(I)=100+I
  10  CONTINUE

C TELL BUGOFF ABOUT PROBLEM VARIABLES
      CALL BUGINT(6HRP    ,RPARM ,2HRA)
      CALL BUGINT(6HRS    ,RSCALE,2HRA)
      CALL BUGINT(6HRC    ,RCOEFF,2HRA)
      CALL BUGINT(6HID    ,IDATA ,2HIA)
      CALL BUGINT(6HIP    ,IPARM ,2HIA)
      CALL BUGINT(6HRD    ,RDATA ,2HRA)
      CALL BUGINT(6HRV    ,RMODEL,2HRA)
      CALL BUGINT(6HIV    ,IMODEL,2HIA)
      CALL BUGINT(6HLV    ,LMODEL,2HLA)
      CALL BUGINT(6HSV    ,SMODEL,2HRA)
      CALL BUGINT(6HISP1  ,IASPT1,2HIA)
      CALL BUGINT(6HSSP1  ,SASPT1,2HRA)
      CALL BUGINT(6HNA    ,NADEV ,2HIA)
      CALL BUGINT(6HSAD   ,SAADC ,2HRA)
      CALL BUGINT(6HSDA   ,SADAC ,2HRA)
      CALL BUGINT(6HIAD   ,IAADC ,2HIA)
      CALL BUGINT(6HIDA   ,IADAC ,2HIA)
      CALL BUGINT(6HSSP2  ,SASPT2,2HRA)
      CALL BUGINT(6HISP2  ,IASPT2,2HIA)
      RETURN
      END
```

```
      SUBROUTINE CALCUL

      REAL     RVa(3,3),RVCT(3),RVOT(3),RVOD2(3),RVOTv(3),RVOD2v(3)

C     Calculates parameters for display and monitoring purposes


C     Calculate cable force component in x-direction  - [N]
        RVFSCx = -(RVTLx / RVSc) * RVFSC

C     Calculate cable force component in y-direction - [N]
         RVFSCy = -(RVTLy / RVSc) * RVFSC

C     Calculate cable power - positive for lifting - [W]
        RVPc = -RVFSC * RVSCv

C     Calculate height disturbance error - boomtip and Deck2 - [m]
        RVEHS = -(RCHS - (RVOT(3) - RVOD2(3)))

C     Calculate square of height disturbance error - [m**2]
        RVEHS2 = RVEHS * RVEHS

C     Calculate longitudinal speed disturbance error - [m/s]
        RVEVXS = RVOTV(1) - RVOD2v(1)

C     Calculate lateral speed disturbance error - [m/s]
        RVEVYS = RVOTV(2) - RVOD2v(2)

C     Calculate vertical speed disturbance error - [m/s]
        RVEVS = RVOTV(3) - RVOD2v(3)

C     Calculate square of speed disturbance error - [(m/s)**2]
        RVEVS2 = RVEVS * RVEVS

C     Calculate square of actual height error - [m**2]
        RVEH2 = RVEH * RVEH

C     Calculate square of actual vertical speed error - [(m/s)**2]
        RVEV2 = RVEV * RVEV

C     Calculate the moments - [N*m]
C             Overturning moment RVMOT
C             Slewing     moment RVMSL
C       NOTE THE FOLLOWING EQUATIONS:
C             a(1,1) = RVa(1,1)
C             a(1,2) = RVa(2,1)
C             a(1,3) = RVa(3,1)
C             a(2,1) = RVa(1,2)
C             a(2,2) = RVa(2,2)
C             a(2,3) = RVa(3,2)
C             a(3,1) = RVa(1,3)
C             a(3,2) = RVa(2,3)
C             a(3,3) = RVa(3,3)
C             a(i,j) are direct EULER transformation coefficients
      RVFSCz = RVFSC
      FSCx = RVa(1,1) * RVFSCx + RVa(2,1) * RVFSCy + RVa(3,1) * RVFSCz
      FSCy = RVa(1,2) * RVFSCx + RVa(2,2) * RVFSCy + RVa(3,2) * RVFSCz
      FSCz = RVa(1,3) * RVFSCx + RVa(2,3) * RVFSCy + RVa(3,3) * RVFSCz
C     MFCx = RVCT(2)  * FSCz   - RVCT(3)  * FSCy
C     MFCy = RVCT(3)  * FSCx   - RVCT(1)  * FSCz
```

```
      RVMSL = RVCT(1)  * FSCy    - RVCT(2)  * FSCx

      CT12pr = SQRT(RVCT(1) * RVCT(1) + RVCT(2) * RVCT(2))
      RVMOT  = FSCz * CT12pr - RVCT(3)*(FSCy * RVCT(2) + FSCx * RVCT(1)
     @ ) / CT12pr


C
      RETURN
      END
```

```
      SUBROUTINE CFP
C                                                    08 September 85 Rev. 3
C
C  Subroutine CFP Computes Fourier Parameters.
C
      INTEGER a
C
      REAL    RDfre(9),RDfr(9),RDa(9,6),RDphas(9),RDrwa(9)
      REAL    random(9,2)
C
      DATA    pi/3.1415927/,a/0/
      DATA    random/.039,1.103,1.327,.3973,.50197,.55196,.59407,
     @               .62715,.75575,
     @               .9039,1.0103,1.1327,1.3973,.067632,.10411,.12093
     @               ,.12401,.065337/
C
C  Modify frequencies in RDfr array to allow for ship speed.
C
      sum = .0
      DO 5 i = 1,IDnfr
        RDfre(i) = FE(RDfr(i))
        RDrwa(i) = ES(RDfr(i))
        RDrwa(i) = SQRT(RDrwa(i) * 2)
        sum = sum + RDrwa(i)
5     CONTINUE
C
C  Adjust regular wave amplitude if their sum is bigger than 2.5 * Sign.Wave H.
C
      top = 2.75 * SQRT(RDm0)
      IF(sum .GE. top) THEN
                       DO 7 i = 1,IDnfr
                         RDrwa(i) = RDrwa(i) * top / (.8 * sum)
 7                     CONTINUE
      ENDIF
C
C  Compute the ship response to the regular waves at given frequencies of
C  encounter.
C
      DO 10 i = 1,6
        DO 10 j = 1,IDnfr
          RDa(j,i) = SHIPRP(RDfre(j),i) * RDrwa(j)
10    CONTINUE
C
C  Compute initial phase for each regular wave.
C
      DO 20 i = 1,IDnfr
C       RDphas(i) = random(i,a)
        RDphas(i) = RAN(a) * pi * 2.
20    CONTINUE
      a = a + 1
      RETURN
      END
```

```
_DRB2: [USER2. TULAI. HYBRID]CGRESP. PRE; 4                          1-APR-1986 ;

      SUBROUTINE CGRESP
C                                                        05 SEPT. 85 Rev. 1
C
C  Computes centre of gravity motions for both vessels
C
      REAL    RVOG(6), RVGH(6)
C
      DATA    pi/3. 1415927/
      CALL GETDAT(1)
      DO 10 i = 1,6
        RVOG(i) = SHPMOT(i, RVtime)
        IF(i . GE . 4) RVOG(i) = RVOG(i) * 180. / pi
10    CONTINUE
C
      CALL GETDAT(2)
      DO 20 i = 1,6
        RVGH(i) = SHPMOT(i, RVtime)
        IF(i . GE . 4) RVGH(i) = RVGH(i) * 180. / pi
20    CONTINUE
      RETURN
      END
```

```
      SUBROUTINE CMPTA
C                                                          12 August 85 Rev. 1
      DIMENSION  LVflag(50)
C
C  Subroutine CMPTA CoMPuTes the A matrix ' elements representing coordinate
C  transformation matrix by rotations.
C
      REAL     RVa(3,3),RVtime,sinphi,cosphi,sinth,costh,sinpsi,cospsi
      REAL     RVder(6),RVader(3,3)
C
C  Compute SIN and COS functions of angles used in ship motion
C
      sinphi = SIN(SHPMOT(4 , RVtime))
      cosphi = SQRT(1 - sinphi ** 2)
      sinth  = SIN(SHPMOT(5 , RVtime))
      costh  = SQRT(1 - sinth ** 2)
      sinpsi = SIN(SHPMOT(6 , RVtime))
      cospsi = SQRT(1 - sinpsi ** 2)
C
C  Compute A matrix' elements
C
      RVa(1,1) = sinpsi * sinphi * sinth + cospsi * costh
      RVa(1,2) = cospsi * sinphi * sinth - sinpsi * costh
      RVa(1,3) = cosphi * sinth
      RVa(2,1) = sinpsi * cosphi
      RVa(2,2) = cospsi * cosphi
      RVa(2,3) =-sinphi
      RVa(3,1) = sinpsi * sinphi * costh - cospsi * sinth
      RVa(3,2) = cospsi * sinphi * costh + sinpsi * sinth
      RVa(3,3) = cosphi * costh
C
C  Compute the derivative of these elements if LVflag(1) is .TRUE.
C
      IF(LVflag(1)) THEN
                  RVader(1,1) = RVder(6) * RVa(1,2) + RVder(4)
     @            * sinpsi * RVa(1,3) + RVder(5) * RVa(3,1)
                  RVader(1,2) =-RVder(6) * RVa(1,1) + RVder(4)
     @            * cospsi * RVa(1,3) + RVder(5) * RVa(3,2)
                  RVader(1,3) =-RVder(4) * sinphi * sinth + RVder(5)
     @            * RVa(3,3)
                  RVader(2,1) = RVder(6) * RVa(2,2) - RVder(4) *
     @            sinpsi * sinphi
                  RVader(2,2) =-RVder(6) * RVa(2,1) - RVder(4) *
     @            cospsi * sinphi
                  RVader(2,3) =-RVder(4) * cosphi
                  RVader(3,1) = RVder(6) * RVa(3,2) + RVder(4) *
     @            sinpsi * RVa(2,2) - RVder(5) * RVa(1,1)
                  RVader(3,2) =-RVder(6) * RVa(3,1) + RVder(4) *
     @            cospsi * RVa(2,2) - RVder(5) * RVa(1,2)
                  RVader(3,3) =-RVder(6) * sinpsi * costh - RVder(5)
     @            * cospsi * sinth
         ENDIF
         RETURN
         END
```

```
_DRB2: [USER2.TULAI.HYBRID]CMPTCT.PRE;3                          1-APR-1986 :

      SUBROUTINE CMPTCT
C                                                    23 October 85
C
C  Subroutine CMPTCT computes the Boom Tip Coordinates in C reference frame
C  for an inelastic boom.
C
      REAL    RVCT(3),RVtpc(3)
C
C  Go to CRANE1 subroutine to update CRANE1 parameters :
C                       r     - boom length
C                       alfa  - boom elevetion with respect to deck plane
C                       beta  - boom SLEW angle - BOOM FORE          angle 0
C                                               - BOOM OVER STBD     angle +
C                                               - BOOM OVER PORSIDE  angle -
C
      RVCT(1) = RVtpc(1) * COS(RVtpc(2)) * COS(RVtpc(3))
      RVCT(2) = RVtpc(1) * COS(RVtpc(2)) * SIN(RVtpc(3))
      RVCT(3) = RVtpc(1) * SIN(RVtpc(2))
C
      RETURN
      END
```

```
      SUBROUTINE CMPUTE
C
C  Computes problem constants outside of the high speed loop.
C
      REAL    RVOT(3),RCOT10(3),RCOL0(3),RCOTv0(3),RVOTv(3),RCOLv0(3)
      REAL    RCOD10(3),RVOD1(3),RCOD1v(3),RVOD1v(3),RCOD20(3),RCOT0(3)
      REAL    RVOD2(3),RCOD2v(3),RVOD2v(3),RCGC(3),RCOG(3),RCHD2(3)
C
C     Nominal height of boom tip above Deck2 (assumes 0 boom elevation) - m
            RCHS = RCGC(3) - (RCOG(3) + RCHD2(3))

C     Initial boom tip deformation w.r.t. unloaded position - [m]

            RCdzBO = RCmL * RCg / RCksB

c     Initial incremental cable stretch - [m]

            RCdzCO = RCmL * RCg / RCksC


C     Initial boom tip x-position when loaded - [m]
            RCOT10(1) = RVOT(1)

C     Initial boom tip y-position when loaded - [m]
            RCOT10(2) = RVOT(2)

C     Initial boom tip z-position when loaded [m]
            RCOT10(3) = RVOT(3) + RCdzBO

C     Initial boom tip x,y,z - directions position and  speed - [m/s]
      DO 10 i = 1,3
            RCOT0(i)   = RVOT(i)
            RCOTv0(i) = RVOTv(i)
 10   CONTINUE

C     Initial load speed in x-direction - [m/s]
            RCOLv0(1) = RVOTv(1)

C     Initial load speed in y-direction - [m/s]
            RCOLv0(2) = RVOTv(2)

C     Initial load speed in z-direction - [m/s]
            RCOLv0(3) = RVOTv(3)

C     Initial position of the 1-st ship's deck - [m]
            RCOD10(3) = RVOD1(3)

C     Initial speed of the 1-st ship's deck - [m/s]
            RCOD1v(3) = RVOD1v(3)

C     Initial position of the 2-nd ship's deck in x-direction
            RCOD20(1) = RVOD2(1)

C     Initial position of the 2-nd ship's deck in y-direction
            RCOD20(2) = RVOD2(2)

C     Initial position of the 2-nd ship's deck in z-direction
            RCOD20(3) = RVOD2(3)

C     Initial speed of the 2-nd ship's deck in x-direction
```

```
                RCOD2v(1) = RVOD2v(1)

C       Initial speed of the 2-nd ship's deck in y-direction
                RCOD2v(2) = RVOD2v(2)

C       Initial speed of the 2-nd ship's deck in z-direction
                RCOD2v(3) = RVOD2v(3)

C       Initial cable length - [m]
                RCScO = RCOD2O(3) + RCZSP - RCOT1O(3) - RCdzCO

C       Initial load position in z-direction - [m]
                RCOLO(3) = RCOT1O(3) + RCScO + RCdzCO


        RETURN
        END
```



```
        SUBROUTINE CRANE1
C                                                    08 September 85 Rev. 1
C  Subroutine CRANE1 defines initial crane actuator positions.
C  Crane is a hydraulically operated, telecopic boom type pedestal crane.
C
        REAL    RVtpc(3)
C
        DATA    pi/3.1415927/

C  Define initial boom length - [m]
        RVtpc(1) = 8.0
C  Define initial elevation - [rad]
        RVtpc(2) = 0.
C  Define initial slewing angle - [rad]
        RVtpc(3) = pi + pi / 2.

        RETURN
        END
```

```
      SUBROUTINE DACSET
C
C
C
C  ASSIGNS DIGITAL TO ANALOG CHANNELS
C
C
      EQUIVALENCE(SADAC(1),SVh)
      EQUIVALENCE(SADAC(2),SVOT3)
      EQUIVALENCE(SADAC(3),SVOD23)
      EQUIVALENCE(SADAC(4),SVOTv3)
      EQUIVALENCE(SADAC(5),SVOD2v)

      EQUIVALENCE(SADAC(6),SVFscx)
      EQUIVALENCE(SADAC(7),SVFscy)
      EQUIVALENCE(SADAC(8),SVEHS)
      EQUIVALENCE(SADAC(9),SVEHS2)
      EQUIVALENCE(SADAC(10),SVEVS)

      EQUIVALENCE(SADAC(11),SVEVS2)
      EQUIVALENCE(SADAC(12),SVEH2)
      EQUIVALENCE(SADAC(13),SVEV2)
      EQUIVALENCE(SADAC(14),SVPC)
      EQUIVALENCE(SADAC(15),SVMOT)

      EQUIVALENCE(SADAC(16),SVMSL)
      EQUIVALENCE(SADAC(17),SVOT1)
      EQUIVALENCE(SADAC(18),SVOT2)
      EQUIVALENCE(SADAC(19),SVD21v)
      EQUIVALENCE(SADAC(20),SVD22v)

      EQUIVALENCE(SADAC(21),SVROLL)
C

C  ESTABLISH DA POINTERS
      IADAC(1)=1
      IADAC(2)=2
      IADAC(3)=3
      IADAC(4)=4
      IADAC(5)=5
      IADAC(6)=6
      IADAC(7)=7
      IADAC(8)=8
      IADAC(9)=9
      IADAC(10)=10
      IADAC(11)=11
      IADAC(12)=12
      IADAC(13)=13
      IADAC(14)=14
      IADAC(15)=15
      IADAC(16)=16
      IADAC(17)=17
      IADAC(18)=18
      IADAC(19)=19
      IADAC(20)=20
      IADAC(21)=21

C
C
C  ESTABLISH NUMBER OF DA CONVERTERS
```

```
C
      NADAC=21
C
C
      RETURN
      END
```

```
      SUBROUTINE DATSET(k)
C                                                    30 OCTOBER 85
C
C   Subroutine DATSET gets the data for the first or second vessel
C   from the general set of data according to the parameter passed.
C
      REAL    RDfre1(9),RDfre2(9),RDfre(9)
      REAL    RDa1(9,6),RDa2(9,6),RDa(9,6)
      REAL    RDphs1(9),RDphs2(9),RDphas(9)
C
      IF(k . EQ . 2) GOTO 25
C
C  Copy the data for the first ship.
C
      DO  20  i = 1,IDnfr
        RDfre1(i) = RDfre(i)
        DO  15  j = 1,6
          RDa1  (i,j) = RDa  (i,j)
15      CONTINUE
        RDphs1(i) = RDphas(i)
20    CONTINUE
      RETURN
C
C  Copy the data for the second ship
C
25    DO  40  i = 1,IDnfr
        RDfre2(i) = RDfre (i)
        DO  30  j = 1,6
          RDa2  (i,j) = RDa   (i,j)
30      CONTINUE
        RDphs2(i) = RDphas(i)
40    CONTINUE
      RETURN
      END
```

```
_DRB2: [USER2. TULAI. HYBRID]DECK1. PRE;3                                  8-APR-1986

      SUBROUTINE DECK1
C                                                          12 August 85
C  Computes the coordinates of a point found on the first ship's deck
C  where the load has to be placed.
C
      DIMENSION LVflag(50)
C
      REAL      RVa(3,3),RCGD1(3),RVder(6),RVader(3,3)
      REAL      RVOD1(3),RVOD1v(3)
C
C  Compute elements of matrix A involved in G reference system rotation.
C
      CALL CMPTA
C
C  Compute D1 coordinates and speed.
C
      DO  20  i = 1,3
        RVOD1(i) = SHPMOT(i,RVtime)
        RVOD1v(i) = RVder(i)
        DO  10  j = 1,3
          RVOD1(i) = RVOD1(i) + RVa(i,j) * RCGD1(j)
          RVOD1v(i) = RVOD1v(i) + RVader(i,j) * RCGD1(j)
10      CONTINUE
20    CONTINUE
C
      RETURN
      END
```

```
      SUBROUTINE DECK2
C                                                    21 August 85 Rev. 2
C
C  Computes the coordinates and speed of a point D2 found on the second
C  ship's deck from where the load has to be picked up.
C
      REAL     RVa(3,3),RCHD2(3),RVOD2(3),RVOG(3),RCOG(3),RVtime
      REAL     RVder(6),RVader(3,3),RVOD2v(3)
C
      RVOG(1) = RCOG(1)
      RVOG(2) = RCOG(2)
      RVOG(3) = RCOG(3) + (RVv2 - RVv1) * RVtime
C
C  Compute elements of matrix A involved in H reference system rotation.
C
      CALL CMPTA
C
      DO 20 i = 1,3
        RVOD2(i) = RVOG(i) + SHPMOT(i,RVtime)
        RVOD2v(i) = RVder(i)
        DO 10 j = 1,3
          RVOD2(i) = RVOD2(i) + RVa(i,j) * RCHD2(j)
          RVOD2v(i) = RVOD2v(i) + RVader(i,j) * RCHD2(j)
10      CONTINUE
20    CONTINUE
C
      RETURN
      END
```

```
      FUNCTION ES(w)
C
C                                                    14 August 85 Rev. 1
C
C  The Energy Spectrum function implements the equation:
C                        S(WE)=S(W)/(1-(2wv/g)COS(psi))    where:
C
C
C                        S(w)=(a/w**5)exp(-b/w**4)
C
C                        a & b are constants for a given h
C
      REAL      a,b,s
      DATA      g/9.81/
C
C        Subroutine's parameters are:
C                 w - wave frequency
C               RVh - significant wave height - defined in subroutine PARGET
C            RVgama - the angle between the direction of ship motion
C                     and the direction of advance of waves - def. in PARGET
C               RVv - ship velocity           - defined in subroutine PARGET
C
      a=8.1 * 1.0E-3 * g ** 2                  ! [m ** 2 / s ** 2]
      b=3.11 / RVh ** 2                        ! []
C
C  Compute the energy function for the specific frequency
C
      s = (a/w ** 5) * EXP(-b / w ** 4)        ! [m ** 2 * s]
C
C  Compute the energy function for the case of a ship in motion.
C
      ES = s / (1 - (w * RVv * 2 / g) * COS(RVgama))
      RETURN
      END
```

```
_DRB2:[USER2.TULAI.HYBRID]ETCLOK.PRE;10                          1-APR-1986

      SUBROUTINE ETCLOK
C                                                    8 October 1985 Rev.2
C
C  DETERMINES ELAPSED TIME SINCE THE LAST CALL TO CLOCK AND
C  COMPUTES ELAPSED TIME SINCE BEGINNING OF RUN.
C  RESETS CLOCK TO ZERO AFTER EACH CALL TO ETCLOK
                                                     !  ******************
C  DETERMINE ANALOG MODE                             !  * SET CLOCK RATE *
      CALL GRAMI(ILOC)                               !  *                *
                                                     !  * TO 1000/s ON   *
C  IS ANALOG IN IC?  IF YES, RESET CLOCK TO 'ZERO'    !  *                *
      IF(ILOC.EQ.6) THEN                             !  * PATCH PANEL    *
                    RVtime = .0                      !  ******************
                    CALL GWTIMR(65000.,IER)
      ENDIF
C
C  READ CLOCK
      CALL GRTIMR(COUNT,IER)

C  CALCULATE ELAPSED TIME SINCE LAST CALL TO CLOCK (SEC)
      RVDTIM=(65000.-COUNT)/1000.

C  CALCULATE TOTAL ELAPSED TIME (SEC)
      RVTIME=RVTIME+RVDTIM

C  RESET CLOCK TO 'ZERO'
      CALL GWTIMR(65000.,IER)

      RETURN
      END
```

```
      FUNCTION FE(w)
C                                                        22 Sept. 85
C  Function for computing frequency of encounter WE for a given frequency w.
C
C  Subroutine's parameters are:
C                    w - wave frequency
C  Parameters given in COMMON :
C                RVgama - the angle between the direction of ship motion and
C                         the wave direction
C                   RVv - ship velocity
C
      DATA     g/9.81/
      FE = w * (1 - w * RVv * cos(RVgama) / g )
      RETURN
      END
```

```
      SUBROUTINE FRQSET
C                                                        85.09.04 REV 2
C
C  Subroutine FRQSET computes the set of discrete frequencies to be used
C  for irregular wave modeling.
C

      REAL    step(2),RCfrac(2,5),b,save,enpeak,RDfr(9),RDrwa(9)
C
      DATA    step/-0.005,0.005/,pi/3.1415927/
      DATA    RCfrac/.71,.82,.54,.63,.31,.45,.1,.22,.058,.075/
C
      b=3.11 / RVh ** 2

C  Compute the central frequency corresponding to the energy peak, known as
C  Characteristic Wave Frequency (CWF)

      cwf = (.8 * b) ** .25

C  M will mark the position of the central frequency in RDfr array

      m = IDnfls + 1

C Adjust gamma angle to avoid the impact over the enrgy spectrum

      save = RVgama
      RVgama = pi / 2.

C  Introduce CWF in the centre of frequencies array.

      RDfr(m) = cwf
      RDrwa(m) = ES(cwf)
      RDrwa(m) = SQRT(RDrwa(m) * 2.)

C  Compute the energy peak ENPEAK corresponding to CWF frequency

      enpeak = ES(cwf)

C  'psi' angle was set up to 90 degrees to eliminate all alterations of
C  S(w) function.

      DO 3 i = 1,2

C  When i = 1, compute the frequencies on left side of CWF (step=-0.005)
C  and for i = 2, compute the frequencies on right side of CWF.

      IF (i .EQ. 1) THEN
                      n = IDnfls
                    ELSE
                      n = IDnfrs
      ENDIF

      w = cwf
        DO 2 j = 1,n

C  Compute V1 as a fraction of the energy peak and find to which frequency
C  it corresponds.

          v1 = enpeak * RCfrac(i,j)
1         w = w + step(i)
```

```
            v2 = ES(w)
            IF(v2 . GT . v1) GOTO 1

c Introduce new found frequency into the Frequency Table.

            IF(i . EQ . 1) THEN
                             l = -j
                           ELSE
                             l = j
            ENDIF

            v3 = ES(w - step(i))
            ratio = (v1 - v2) / (v3 - v2)
            RDfr(l + m) = w + ratio * (-step(i))
  2       CONTINUE
  3     CONTINUE
        RVgama = save

        RETURN
        END
```

```
      SUBROUTINE GETDAT(k)
C
      REAL     RDfre1(9),RDfre2(9),RDfre(9)
      REAL     RDa1(9,6),RDa2(9,6),RDa(9,6)
      REAL     RDphs1(9),RDphs2(9),RDphas(9)
C
      IF(k .EQ. 2) GOTO 25
C
C  Copy the data of the first ship.
C
      DO  20  i = 1,IDnfr
        RDfre(i) = RDfre1(i)
        DO  15 j = 1,6
          RDa  (i,j) = RDa1 (i,j)
15      CONTINUE
        RDphas(i) = RDphs1(i)
20    CONTINUE
      RETURN
C
C  Copy the data of the second ship
C
25    DO  40  i = 1,IDnfr
        RDfre(i) = RDfre2(i)
        DO  30  J = 1,6
          RDa  (i,j) = RDa2  (i,j)
30      CONTINUE
        RDphas(i) = RDphs2(i)
40    CONTINUE
      RETURN
      END
```

```
_DRB2:[USER2.TULAI.HYBRID]INALG.PRE;45                    1-APR-1986 ;

      SUBROUTINE INALG
C
C
C  GETS ANALOG COMPUTER INPUTS
C
      REAL RSOL(3),RVtpc(3)
C
C  GET SCALED ANALOG DATA
      CALL QRRADR(SAADC,IAADC,NAADC,IER)
C
C  DESCALE PROBLEM VARIABLES

      RVOLL3 = SVOLL3 * RSOL(3)
      RVbump = SVbump
      RVTLx = SVTLx * RSTLx
      RVTLy = SVTLy * RSTLy

      RVSc = SVSc * RSSc
      RVScv = SVScv * RSScv
      RVFsc = SVFsc * RSFsc
      RVEH = SVEH * RSEH

      RVEV = SVEV * RSEV
      RVtpc(1) = SVtpc1 * RStpc1
      RVtpc(2) = SVtpc2 * RStpc2
      RVtpc(3) = SVtpc3 * RStpc3

      RETURN
      END
```

```
      SUBROUTINE MISION
C                                                          18 October 85 Rev.24
      DIMENSION  LVflag(50)
C
      REAL       RCOTO(3),RCOTv0(3),RVOT(3),RVOTv(3),RCOT10(3)
C
C  Call AREA to compute the Energy Spectrum surface m0 used in subroutine
C  CFP under the name RDm0
C
      LVflag(1) = .TRUE.
      CALL AREA
C
C  Get data for the first ship
C
      RVv=RVv1
      CALL FRQSET
      CALL RAODA(1)
      CALL CFP
C
C  Compute initial boom tip parameters (coordinates and velocity)
C
      RVtime = .0
      CALL CRANE1
      CALL BOOM
C
C  Compute  initial coordinates and speed for D1.
C
      CALL DECK1
C
C  Save the data in the first vessel's set of data.
C
      CALL DATSET(1)
C
C  Get data for the second ship.
C
      RVv = RVv2
      CALL RAODA(2)
      CALL CFP
      RVtime = .0
      CALL DECK2
      CALL DATSET(2)
      RETURN
      END
```



```
      SUBROUTINE MODEL
C                                                          18 October 85 Rev. 9
C
C  Defines the subroutines to be called and executed in the high-speed loop.
C
      DIMENSION  LVflag(50),RVOG(6),RVtpc(3),RCGC(3)

      DATA       pi/3.1415927/
C
C     If load has contacted Deck 2, halt simulation
C
      IF(RVbump .GT. .5) THEN
                         RVtime = .0
                         CALL GHOLD(1)
      ENDIF
C
C  Compute the wave amplitude if so required
C
      IF(LVflag(25)) CALL WAVE
C
C  Compute the Centre of Gravity motions if required.
C
      IF(LVflag(26)) CALL CGRESP


C
C  Calls the individual subroutines that comprise the MODEL.
C
C
C  Get data for the first vessel
C
      CALL GETDAT(1)
C
C  Compute the boom tip coordinates and speed
C
      CALL BOOM
C
C  Compute the roll if LVflag(29) is TRUE.
C
      IF(LVflag(29)) THEN
                      a = SHPMOT(6,RVtime)
                      RVOG(4) = (-SIN(a)*RCGC(1)+COS(a)*(RCGC(2)-
     @                RVtpc(1))) / RVtpc(1) / 10. * SHPMOT(4,RVtime)
      ENDIF
C     IF(LVflag(29)) then
C                     RVOG(4) = SHPMOT(4,RVtime)
C     ENDIF

C
C  Get data for the second vessel
C
      CALL GETDAT(2)
C
C  Compute D2 coordinates and speed
C
      CALL DECK2
C
C  Update the RVtime
C
```

```
C
C  Do some calculation
C
      CALL CALCUL
C
C  Read the time
C
      CALL ETCLOK

      RETURN
      END
```

_DRB2:[USER2.TULAI.HYBRID]OFLINE.PRE;7 3-APR-1986

```
      SUBROUTINE OFLINE
C                                                    29 Sept.85 Rev.2
C     Executes individual modules under ofline control
      DIMENSION LVflag(50)
      IF(LVflag(2)) CALL BOOM
      IF(LVflag(3)) CALL CFP
      IF(LVflag(4)) CALL CMPTA
      IF(LVflag(5)) CALL CMPTCT
      IF(LVflag(6)) CALL CMPUTE
      IF(LVflag(7)) CALL CRANE1
      IF(LVflag(8)) CALL DATSET
      IF(LVflag(9)) CALL DECK1
      IF(LVflag(10)) CALL DECK2
      IF(LVflag(11)) CALL ES
      IF(LVflag(12)) CALL FE
      IF(LVflag(13)) CALL FNGSET
      IF(LVflag(14)) CALL FRQSET
      IF(LVflag(15)) CALL GETDAT
      IF(LVflag(16)) CALL MISION
      IF(LVflag(17)) CALL MODEL
      IF(LVflag(18)) CALL PARGET
      IF(LVflag(19)) CALL POTSET
      IF(LVflag(20)) CALL RADDA
      IF(LVflag(21)) CALL SCLGET
      IF(LVflag(22)) CALL SHIPRP
      IF(LVflag(23)) CALL SHPMOT
      IF(LVflag(24)) CALL ETCLOK
      IF(LVflag(25)) CALL WAVE
      IF(LVflag(26)) CALL CGRESP
      IF(LVflag(27)) CALL INALG
      IF(LVflag(28)) CALL OUTALG

C     LVflag(29) used for allowing roll computation.

      RETURN
      END
```

```
      SUBROUTINE OUTALG

      REAL    RVOT(3),RVOTv(3),RVOD2(3),RVOD2v(3),RVOG(6)
      REAL    RSOT(3),RSOTv(3),RSOD2(3),RSOD2v(3),RCOT10(3)
C
C  OUTPUTS MODEL VARIABLES TO ANALOG
C
C  SCALE PROBLEM VARIABLES
C
      SVH = RVwh / RSh
      SVOT3 = RVOT(3) / RSOT(3)
      SVOTV3 = RVOTv(3) / RSOTv(3)
      SVOD23 = RVOD2(3) / RSOD2(3)
      SVOD2V = RVOD2v(3) / RSOD2v(3)

      SVFscx = RVFscx / (.1 * RSFsc)
      SVFscy = RVFscy / (.1 * RSFsc)
      SVEHS = RVEHS / RSEH
      SVEHS2 = RVEHS2 / RSEH2
      SVEVS = RVEVS / RSEV

      SVEVS2 = RVEVS2 / RSEV2
      SVEH2 = RVEH2 / RSEH2
      SVEV2 = RVEV2 / RSEV2
      SVPC = RVPC / RSPC
      SVMOT = RVMOT / RSMOT

      SVMSL = RVMSL / RSMSL
      SVOT1 = (RVOT(1) - RCOT10(1)) / RSTLX
      SVOT2 = (RVOT(2) - RCOT10(2)) / RSTLY
      SVD21v = RVOD2v(1) / RSOD2v(1)
      SVD22v = RVOD2v(2) / RSOD2v(2)

      SVROLL = RVOG(4) / RStpc2
C
      CALL GWRDAR(SADAC, IADAC, NADAC, IER)
      CALL GSTDA
C
      RETURN
      END
```

```
      SUBROUTINE PARGET
C
C
C  Defines fixed constants for simulation
C  Constants are grouped by the subroutine which first uses them
C
      REAL    RCGC(3),RCOG(3),RCHD2(3),RCGD1(3)
      DATA    pi/3.1415927/
C     FUNCTION ES
C
C  The Energy Spectrum is defined for the general case of a ship in
C  unaccelerated motion with a speed RVv [m/s] making an angle RVgama [rad]
C  with the wave direction, in a sea of Significant Wave Height RVh [m].
C  Significant Wave Height may be related to sea state as follows:
C
C                          SEA STATE        SIGNIF. WAVE HEIGHT [m]
C                             2                    .3
C                             3                   1.0
C                             4                  1.75
C                             5                  3.75
      RVh     = 3.75
      RVgama = pi
      RVv     = 2.5
      RVv1    = 2.5
      RVv2    = 2.5
C
C     SUBROUTINE FRQSET
C
C  The number of frequencies to be selected at the left and right of the
C  central frequency are constants of the run.
C
      IDnfls = 4
      IDnfrs = 4
C
C  There are three different types of Fourier parameters to be computed.
C  For each type, the number to be computed is equal to the total number of
C  frequencies, IDnfr, selected in FRQSET subroutine.
C
      IDnfr = 9

C       Crane base coordinates in G reference frame - [m]
            RCGC(1) = -70.00
            RCGC(2) = - 3.00
            RCGC(3) = -12.80

C       Point D1 coordinates (found on the first vessel) in G reference frame
            RCGD1(1) = -64.
            RCGD1(2) = .0
            RCGD1(3) = -12.8

C       Second ship's inertial frame coordinates in O reference frame - [m]
            RCOG(1) = -70.
            RCOG(2) = -11.
            RCOG(3) = -.34

C       Point D2 coordinates (found on the second vessel) in H referece frame
            RCHD2(1) = .0
            RCHD2(2) = .0
            RCHD2(3) = -.16
```

```
C       CRANE MODEL CONSTANTS

C         Boom mass - [kg]
                RCmB = 680.
C         Load mass - [kg]
                RCmL = 800.
C         Gravitational acceleration - [m / s ** 2]
                RCg = 9.81
C         Spring stiffness of boom - [N / m]
                RCksB = 150000.
C         Spring stiffness of cable - [N / m]
                RCksC = 225000.
C         Effective damping constant for boom - [N / (m / s)]
                RCkdB = 5636.
C         Effective damping constant for load - [N / (m / s)]
                RCkdC = 14000.
C         Initial Boom tip deformation w.r.t. unloaded position - [m]
C               RCdzBO = RCmL * RCg / RCksB
C         Initial cable length (hanging under the boom tip) - [m]
                RCScO = 2.
C         Initial incremental cable stretch - [m]
C               RCdzCO = RCmL * RCg / RCksC
C         Position differentiator gain Gdif
                RCGdif = 40.
C         Differentiator band width - [rad/s]
                RCC2 = 40.

C  **     WINCH MODEL
C         Maximum allowable tension - [N]
                RCMFsC = 40000.
C         Maximum allowable power at winch - [w]
                RCMPc = 40000.
C         Power limiter gain - [(m/s)/(N*(m/s))]
                RCGPmx = 1./8000.
C         Tension limiter gain - [(m/s)/N]
                RCGFmx = 1./8000.
C         Maximum winching rate - [m/s]
                RCMSCv = 1.
C         Compensator time constant - [s]
                RCTAUc = .7
C         Filter time constant
                RCTAUd = .75

C  **     HUMAN OPERATOR MODEL      **
C         Pilot gain [(m/s)/(m/s)]
                RCKp = 5.
C         Pure time delay - [s]
                RCTd = .128
C         General lag time constant of human pilot describing function - [s]
                RCTi = 1.
C         General lead time constant of human pilot describing function - [s]
                RCTl = .128
C         Lag time constant, in precision model of human op., descr. function -[s]
                RCTk1 = 10.
C         Lead time constant in precision model of human op., descr. function[s]
                RCTk  = 1. / .3
C         Lag time for first-order approximation to neuro-muscular dynamics-[s]
C               Tn = Tn1 + 2 * ZethaN / OhmegaN
                RCTn = 1. / 8.9 + 2 * .16 / 16.6
C         Controlled element gain
```

```
                RCkC = 3.

C         Desired Closing Speed - [m/s]
                RCVa = .4

C         Time constant for DA 1 filter - s
                RCTT3 = .25

C         Proportional gain for compensator no.1
                RCGC1 = 1.
C         Proportional gain for compensator no.2
                RCGC2 = 1.

C         Error signal gain
                RCKEI = 2.
C         Time constant for cable tension signal - s
                RCTff = 1. / 30.
C         Height in position control
                RCZSP = -5.


C       LOAD AERODYNAMICS
C         Aerodynamics constant Kcd, Kcd = .5 * ro * AE * CD
                ro = 1.29                          !  kg/m**3
                RCAE = 1.5                         !  m**2
                RCCD = 1.5                         !   -
                RCKCD = .5 * ro * RCAE * RCCD      !  kg/m

          RETURN
          END
```

```
_DRB2: [USER2.TULAI.HYBRID]POTSET.PRE;84                          8-APR-1986

      SUBROUTINE POTSET
C                                                    27 October 85 Rev 2

      REAL    RSOTv(3),RSOT(3),RSOT1(3),RSOT1v(3),RCOTv0(3)
      REAL    RCOT10(3),RSOL(3),RSOLv(3),RCOL0(3),RCOLv0(3)
      REAL    RSOD2v(3),RSOD2(3),RCHD2(3),RCQC(3),RCOQ(3)
C
C  To assign,compute and set potentiometers and static DCA's of the problem.
C
C        ASSIGN POTS OR DCA'S
C
C
C        COMPUTE VALUES OF POTS OR DCA'S
C
      SASPT1(01) = RCQdif * RSdzB / (RSVzB1 * 10.)
         IASPT1(01) = 3

      SASPT1(02) = RCQdif * RSY2BM / (RSVzB1 * 10.)
         IASPT1(02) = 2

      SASPT1(03) = -10. * RSdzB / RSOT(3)
         IASPT1(03) = 0

      SASPT1(04) = RCSc0 / RSSc
         IASPT1(04) = 100

      SASPT1(05) = RCC2 * RSVzB1 / (RSVzB * 100.)
         IASPT1(05) = 1

      SASPT1(06) = -1. / (RCksB * RSdzB / RSFsB )
         IASPT1(06) = 7

      SASPT1(07) = RSFsC / (RCmB * RSOTv(3) * 10.)
         IASPT1(07) = 13

      SASPT1(08) = -RSFsB / (RCmB * RSOTv(3) * 10.)
         IASPT1(08) = 11

      SASPT1(09) = RCkdB * RSVzB / (RCmB * RSOTv(3) * 10.)
         IASPT1(09) = 5

      SASPT1(10) = RSOT1v(3) / RSOT1(3)
         IASPT1(10) = 12

C  !!!  C011 and C012 are used for initial conditions.
      SASPT1(11) = -RCOTv0(3) / RSOTv(3)
         IASPT1(11) = 10

      SASPT1(12) = -RCOT10(3) / RSOT1(3)
         IASPT1(12) = 15

            G = 2.0
      SASPT1(16) = - 1. / G
         IASPT1(16) = 9

      SASPT1(13) = RSOT1(3) / (RSdzC * 10. * G)
         IASPT1(13) = 17

      SASPT1(14) = RSSc / (RSdzC * 10. * G)
         IASPT1(14) = 42
```

```
      SASPT1(15) = -RSOL(3) / (RSdzC * 10.  * G)
         IASPT1(15) = 52

      SASPT1(17) = RCGdif * RSdzC / (RSVzC1 * 10. )
         IASPT1(17) = 19

      SASPT1(18) = RCGdif * RSY2CM / (RSVzC1 * 10. )
         IASPT1(18) = 20

      SASPT1(19) = -RSVzC1 / (RSY2CM * 10. )
         IASPT1(19) = 22

      SASPT1(20) = RCC2 * RSVzC1 / (RSVzC * 100. )
         IASPT1(20) = 27

      SASPT1(21) = -1.  / (RSFSC / RSFSCX)
         IASPT1(21) = 33

      SASPT1(22) = -1 / (RCksC * RSdzC / RSFsC)
         IASPT1(22) = 30

      SASPT1(23) = -RSFsC / (RCmL * RSOLv(3) * 10. )
         IASPT1(23) = 24

      SASPT1(24) = RCg / (RSOLv(3) * 10)
         IASPT1(24) = 29

      SASPT1(25) = RCkdC * RSVzC / (RSOLv(3) * RCmL * 10. )
         IASPT1(25) = 25

      SASPT1(26) = RSOLv(3) / RSOL(3)
         IASPT1(26) = 57

C  !!!  C027 and C028 used for initial conditions

      SASPT1(27) = -RCOLv0(3) / RSOLv(3)
         IASPT1(27) = 55

      SASPT1(28) = RCOLO(3) / RSOL(3)
         IASPT1(28) = 50

      SASPT1(29) = RCMFsC / RSFsC
         IASPT1(29) = 6

      SASPT1(30) = -RCGPmx * RSPc / (10.  * RSScV)
         IASPT1(30) = 18

      SASPT1(31) = -RCGFmx * RSFsC / (10.  * RSScV)
         IASPT1(31) = 41

      SASPT1(32) = -RSScV / RSSc
         IASPT1(32) = 43

      SASPT1(33) = RCMPc / RSPc
         IASPT1(33) = 16

C     SASPT1(34) = -RSOLv(3) / RSeV / 10.
      SASPT1(34) = -RSOL(3) / RSeV / 10.
         IASPT1(34) = 63
```

```
C       SASPT1(35) = -RSOD2v(3) / RSeV / 10.
        SASPT1(35) = -RSOD2(3) / RSeV / 10.
           IASPT1(35) = 62

C       SASPT1(36) = -RCVa / RSeV / 10.
        SASPT1(36) = -RCZSP / RSeH / 10.
           IASPT1(36) = 61

        SASPT1(37) = 1. / (100. * (RCTd / 2.))
           IASPT1(37) = 60

        SASPT1(38) = 1. / (100. * (RCTd / 2.))
           IASPT1(38) = 68

        SASPT1(39) = RCT1 / (10. * RCTi)
           IASPT1(39) = 66

        SASPT1(40) = -1. / RCTi / 10.
           IASPT1(40) = 65

        SASPT1(41) = 1. / RCTi / 10.
           IASPT1(41) = 67

        SASPT1(42) = -1. / (10. * RCTn)
           IASPT1(42) = 80

        SASPT1(43) =  (RCkp * RSeV) / (RSScV * 10.)
           IASPT1(43) = 115

        SASPT1(44) = .2
           IASPT1(44) = 88

        SASPT1(45) = SASPT1(44)
           IASPT1(45) = 78

        SASPT1(46) = -SASPT1(5)
           IASPT1(46) = 35

        SASPT1(47) = -SASPT1(20)
           IASPT1(47) = 26

        SASPT1(48) = RCTk / RCTk1
           IASPT1(48) = 73

        SASPT1(49) = -1. / RCTk1
           IASPT1(49) = 70

        SASPT1(50) = 1. / RCTk1
           IASPT1(50) = 72

        SASPT1(51) = -1. / (10. * RCTn)
           IASPT1(51) = 82

        SASPT1(52) = 1.
           IASPT1(52) = 56

C       These pots are used as inverters
        SASPT1(53) = 1.
```

```
      IASPT1(53) = 85

   SASPT1(54) = 1.
      IASPT1(54) = 86

   SASPT1(55) =  (RCQC1 * RSOTv(3)) / (RSScV * 10.)
      IASPT1(55) = 97

   SASPT1(56) = 1.
      IASPT1(56) = 89

   SASPT1(57) = 1. / RCTT3 / 10.
      IASPT1(57) = 90

   SASPT1(58) = - SASPT1(57)
      IASPT1(58) = 92

   SASPT1(59) = -1. / RCKEI
      IASPT1(59) = 81

   SASPT1(60) = -1. / RCKEI
      IASPT1(60) = 70

   SASPT1(61) = (RCQC2 * RSeV) / (RSScV * 10.)
      IASPT1(61) = 95

   SASPT1(62) = - 1. / (100. * RCTff)
      IASPT1(62) = 45

   SASPT1(63) = - SASPT1(62)
      IASPT1(63) = 47

   SASPT1(64) = (RCQC(3) - RCQQ(3)) / RSOT(3)
      IASPT1(64) = 99

   SASPT1(65) = -RSFscx / (10. * RCmL * RSOLv(1))
      IASPT1(65) = 23

   SASPT1(66) = RSVLx**2 * RCKCD  / RCmL / RSOLv(1)
      IASPT1(66) = 18

   SASPT1(67) = RSOLv(1) / RSTLX
      IASPT1(67) = 21

   SASPT1(68) = RVV1 / RSVLx
      IASPT1(68) = 14

   SASPT1(69) = RSOLv(1) / RSVLx
      IASPT1(69) = 54

   SASPT1(70) = RCOLvO(1) / RSOLv(1)
      IASPT1(70) = 28

   SASPT1(71) = 1.
      IASPT1(71) = 08

   SASPT1(72) = 1.
      IASPT1(72) = 04

   SASPT1(73) = RCOLvO(2) / RSOLv(2)
```

```
      IASPT1(73) = 31

     SASPT1(74) = RSOLv(2) / RSTLY
      IASPT1(74) = 70

     SASPT1(75) = 1.
      IASPT1(75) = 72

     SASPT1(76) = 1.
      IASPT1(76) = 40

     SASPT1(77) = RSOLv(2) / RSVLy / 10.
      IASPT1(77) = 76

     SASPT1(78) = RSVLy ** 2 * RCKCD / RCmL / RSOLv(2)
      IASPT1(78) = 34

     SASPT1(79) = - RSFSCy / ( 10. * RSOLv(2) * RCmL)
      IASPT1(79) = 32

     SASPT1(80) = -RSOLv(3) / RSeV / 10.
      IASPT1(80) = 91

     SASPT1(81) = -RSOD2v(3) / RSeV / 10.
      IASPT1(81) = 93

     SASPT1(82) = -1. / RCTAUc / 10.
      IASPT1(82) = 75

     SASPT1(83) = -1. / RCTAUc / 10.
      IASPT1(83) = 77

     SASPT1(84) = -RSScV / RSOLv(3)
      IASPT1(84) = 51

     SASPT1(85) = 1.
      IASPT1(85) = 38

     SASPT1(86) = -1. / (RSFSC / RSFSCX)
      IASPT1(86) = 59

     SASPT1(87) = RSOTv(3) / RSScV / 10.
      IASPT1(87) = 96

     SASPT1(88) = -RSOD2v(3) / RSScV / 10.
      IASPT1(88) = 98

     SASPT1(89) = 1. / RCTAUd / 10.
      IASPT1(89) = 97

     SASPT1(90) = 1. / RCTAUd / 10.
      IASPT1(90) = 102

     SASPT1(91) = 1. / RCTAUd / 10.
      IASPT1(91) = 79

     SASPT1(92) = 1. / RCTAUd / 10.
      IASPT1(92) = 112

C       SET NUMBER OF POTS AND DCA'S USED.
```

```
      NASPT1 = 92

C       TO SET POTS AND DCA'S EXECUTE APPROPRIATE ROUTINES

      CALL GWRPTR (SASPT1,IASPT1,NASPT1,1,IER)
      TYPE *,'CONSOLE 1 POTS ARE SET'
      TYPE *,'THE ERROR FLAG IS IER = ',IER
      TYPE *,'SET L31 TO +/-',RCMSCV/RSSCV
      TYPE *,' '

      RETURN
      END
```

```
_DRB2:[USER2.TULAI.HYBRID]RAODA.PRE;1                          1-APR-1986

      SUBROUTINE RAODA(k)
C                                                    14 August 85 Rev. 1
C
C  Subroutine RAODA obtains data from a disk file,representing the ship
C  Response Amplitude Operators versus frequency of encounter for vessel (k).
C  These are given as :
C                        NAME            CODE          UNIT
C                        ****            ****          ****
C
C                        SURGE             1           (ft/ft)
C                        SWAY              2           (ft/ft)
C                        HEAVE             3           (ft/ft)
C                        ROLL              4           (rad/ft)
C                        PITCH             5           (rad/ft)
C                        YAW               6           (rad/ft)
C
C  **  Conversion to metric is done for the last three parameters  **
C
      REAL      RDrao(2,10,6)
C
      INTEGER   IDnpt(6)
C
      CHARACTER txrao(100)
C
  100 FORMAT(100A1)
C
      DATA      mnp/10/
C
C  Open disk file and read data.
C
      IF(k .EQ. 1) THEN
                     OPEN(UNIT=k,NAME='RAO1DA.DAT',TYPE='OLD')
                   ELSE
                     OPEN(UNIT=k,NAME='RAO2DA.DAT',TYPE='OLD')
      ENDIF
      READ(k,100) txrao
C
C  Read discrete curves description in the order given above
C
      DO  20  i = 1,6
        READ(k,*) npoint
        IDnpt(i) = npoint
C
C  'npoint' contains the number of points describing a RAO,which is supposed
C  to have less than 10 points.If not so,modify the value of 'mnp' variable
C  (Maximum Number of Points)given in DATA instruction.
C
        IF(npoint .GT. mnp) THEN
                     TYPE *,'Too many points describing RAO No. ',i
                     STOP
        ENDIF
C
C  Get the data into the matrix RDrao(2,10,6) used to keep RAO description.
C
        READ(k,*) ((RDrao(l,j,i),l=1,2),j=1,npoint)
C
C  The RAO for the first three ship motions are nondimensional so there is
C  no requirement for unit conversion as in the case of the last three
C  motions where a conversion from imperial to metric is required.
C  In addition a descaling factor is to be considered.
```

_DRB2: [USER2. TULAI. HYBRID]RAODA. PRE; 1

```
          IF(i . GT . 3) THEN
                              DO  10  j = 1,npoint
                                RDrao(2, j, i) = RDrao(2, j, i) * 3.280839 E-2
                              CONTINUE
   10
            ENDIF
   20     CONTINUE
C
          WRITE(*,100) txrao
          CLOSE(k)
          RETURN
          END
```

```
      SUBROUTINE SCLGET

C  Routine to define simulation scale factors
C  Defines scale factors for analog-to-digital and digital-to-analog
C  conversions, for calculating pot settings, and for scaling the
C  resetting integrators.

      REAL    RSOT(3),RSOTv(3),RSOL(3),RSOLv(3)
      REAL    RSOT1(3),RSOT1v(3),RSOD2v(3),RSOD2(3)
      DATA    pi/3.1415927/
C
C
C     SEA STATE SCALE FACTORS
C       Maximum wave height - [m]
            RSh = 2.

C     BOOM SCALE FACTORS
C       Maximum Boom Tip X coordinate in O inertial reference frame - [m]
            RSOT(1) = 100.
C       Maximum Boom Tip Y coordinate in O inertial reference frame - [m]
            RSOT(2) = 25.
C       Maximum Boom Tip Z coordinate in O inertial reference frame - [m]
            RSOT(3) = 20.

C       Maximum absolute unloaded boom tip speed in Z-direction
            RSOTv(3) = 10.

C       Maximum loaded boom tip z-coordinate - [m]
            RSOTL(3) = 20.
C       Maximum loaded boom tip speed - [m/s]
            RSOTLv(3) = 10.
C       Maximum Boom tip vertical speed wrt unloaded boom tip position[m/s]
            RSVzB = 5.
C       Scale factor equal to RSVzB
            RSVzB1 = RSVzB

C       Maximum Boom Spring stretch - [m]
            RSdzB = 1.
C       Scale factor equal to RSdzB
            RSY2BM = RSdzB

C       Maximum force in boom spring - [N]
            RSFsB = 50000.
C       Maximum Damping Force in the Boom spring - [N]
            RSFdB = 50000.

C       Maximum boom length - [m]
            RStpc1 = 10.
C       Maximum boom elevation angle - [rad]
            RStpc2 = pi / 2.
C       Maximum slewing angle - [rad]
            RStpc3 = 2 * pi

C     CABLE SCALE FACTORS
C       Maximum cable length (as it comes from the actuator) - [m]
            RSSc = 20.
C       Maximum cable rate - [m/s]
            RSScV = 2.
C       Maximum cable stretch - [m]
```

```
              RSdzC = 1.
C         Scale factor equal to RSdzC
              RSY2CM = RSdzC

C         Maximum tension in the cable in X-direction - [N]
              RSFSCx = 5000.
C         Maximum tension in the cable in Y-direction - [N]
              RSFSCy = 5000.
C         Maximum tension in the cable - [N]
              RSFsC = 50000.

C         Maximum damping force in the cable - [N]
              RSFdC = 50000.
C         Maximum winch /cable power - [w]
              RSPc = 40000.

C       LOAD SCALE FACTORS
C         Maximum X-coordinate of load in O inertial reference frame - [m]
              RSOL(1) = 100.
C         Maximum Y-coordinate of load in O inertial reference frame - [m]
              RSOL(2) = 25.
C         Maximum Z-coordinate of load in O inertial reference frame - [m]
              RSOL(3) = 20.


C         Maximum load speed in x-direction in O reference frame - [m/s]
              RSOLv(1) = 5.
C         Maximum load speed in y-direction in O reference frame - [m/s]
              RSOLv(2) = 5.
C         Maximum load speed in z-direction in O reference frame - [m/s]
              RSOLv(3) = 10.

C         Maximum load vertical speed wrt unloaded boom tip position- [m/s]
              RSVzC = 5.
C         Scale factor equal to RSVzC
              RSVzC1 = RSVzC

C         Max difference in x-dir'n between boom tip T and load L - [m]
              RSTLx = 5.
C         Max difference in y-dir'n between boom tip T and load L - [m]
              RSTLy = 5.

C         Maximum load aerodynamic speed in x-direction - [m/s]
              RSVLx = 5.
C         Maximum load aerodynamic speed in y-direction - [m/s]
              RSVLy = 5.

C       DECK2 SCALE FACTORS
C         Maximum absolute position of the second ship's Deck - [m]
              RSOD2(3) = 20.

C         Maximum x-velocity of Deck2 - [m/s]
              RSOD2v(1) = 5.
C         Maximum y-velocity of Deck2 - [m/s]
              RSOD2v(2) = 5.
C         Maximum z-velocity of Deck2 - [m/s]
              RSOD2v(3) = 5.
```

```
C       PERFORMANCE MONITORING SCALE FACTORS
C         Maximum vertical speed error - [m/s]
              RSEV = 2.
C         Maximum vertical (speed error)**2 - [(m/s)**2]
              RSEV2 = 4.
C         Maximum vertical position error - [m]
              RSEH = 2.
C         Maximum vertical (position error)**2 - [m**2]
              RSEH2 = 4.
C         Maximum integrand of square of rate error - [ m*m / s ]
              RSEI = .5
C         Maximum overturning  moment of the crane - [N*m]
              RSMOT = 500000.
C         Maximum slewing moment of the crane - [N*m]
              RSMSL = 40000.

        RETURN
        END
```

```
      FUNCTION SHIPRP(W, M)
C
C  Function SHIPRP computes the ship response to a wave having a given frequency
C  of encounter (RDfre) and a given height (RDrwa)
C
      REAL     RDrao(2, 10, 6)
C
      INTEGER IDnpt(6)
C
C  Function parameters are :
C              W - frequency of encounters
C              M - the motion code (1<= M <=6)
      npoint = IDnpt(M)
C
C  Ensure W is within RAO range
C
      IF(W. LT. RDrao(1, 1, M). OR. W. GT. RDrao(1, npoint, M)) THEN
              TYPE *, 'Frequency of encounter out of RAO''s range w=', w
              STOP
      ENDIF
C
C  Find RAO(W) using interpolation.
C
      DO 10 i = 2, npoint
        IF(W. LT. RDrao(1, i, M)) GOTO 20
10    CONTINUE
C
C  Consider the case W = RDrao(1, npoint, M)
C
      SHIPRP = RDrao(2, npoint, M)
      RETURN
C
C  Consider the case RDrao(1, 1, M) <= W < RDrao(1, npoint, M)
C
20    slope = (RDrao(2, i, M) - RDrao(2, i-1, M)) /
     c        (RDrao(1, i, M) - RDrao(1, i-1, M))
      i = i - 1
30    SHIPRP = RDrao(2, i, M) + slope * (W - RDrao(1, i, M))
      RETURN
      END
```

```
_DRB2:[USER2.TULAI.HYBRID]SHPMOT.PRE;2                          1-APR-1986 ;

      FUNCTION  SHPMOT(N,T)
C                                                        21 August 85 Rev. 3
      DIMENSION  LVflag(50)
C  Function SHPMOT computes one of the six possible ship motions at
C  a given moment of time.
C
      REAL     RDa(9,6),RDfre(9),RDphas(9),RVder(6)
C  Function parameters are:
C              N - integer value between 1 and 6 to define ship motion
C                  of interest :
C                                1     ROLL
C                                2     PITCH
C                                3     YAW
C                                4     SURGE
C                                5     SWAY
C                                6     HEAVE
C              T - the moment of time when the motion should be computed - [S]
C
      SHPMOT = .0
      RVder(N) = .0
C
C  Compute the Fourier series
C
      DO 10 i = 1,IDnfr
        factor = RDfre(i) * T + RDphas(i)
        SHPMOT = SHPMOT + RDa(i,N) * SIN(factor)
C
C  Compute the derivative of the ship response to the sea action.
C
        RVder(N) = RVder(N) + RDfre(i) * RDa(i,N) *
     @COS(factor)
10    CONTINUE
      RETURN
      END
```

```
      SUBROUTINE WAVE
C                                                    29 August 85 Rev. 1
C  Computes the wave amplitude
C
      REAL     RDfr(9),RDrwa(9),RDphas(9)
      RVwh = .0
      DO  10 i = 1,IDnfr
        factor = RDfr(i) * RVtime + RDphas(i)
        RVwh = RVwh + RDrwa(i) * SIN(factor)
10    CONTINUE

      RETURN
      END
```

```
_DRB2: [USER2.TULAI.HYBRID]CRELIB.COM;4                    1-APR-1986 2(

$ !
$   DEL HYMODEL.OLB;*
$ !
$   LIBRARY/CREATE HYMODEL.OLB
$ !
$        UPDATE BUGSET
$        UPDATE ADCSET
$        UPDATE AREA
$        UPDATE BOOM
$        UPDATE CALCUL
$        UPDATE CFP
$        UPDATE CGRESP
$        UPDATE CMPTA
$        UPDATE CMPTCT
$        UPDATE CMPUTE
$        UPDATE CRANE1
$        UPDATE DACSET
$        UPDATE DATSET
$        UPDATE DECK1
$        UPDATE DECK2
$        UPDATE ES
$        UPDATE ETCLOK
$        UPDATE FE
$        UPDATE FNGSET
$        UPDATE FRQSET
$        UPDATE GETDAT
$        UPDATE INALG
$        UPDATE MISION
$        UPDATE MODEL
$        UPDATE OFLINE
$        UPDATE OUTALG
$        UPDATE PARGET
$        UPDATE POTSET
$        UPDATE RAODA
$        UPDATE SCLGET
$        UPDATE SHIPRP
$        UPDATE SHPMOT
$        UPDATE WAVE
```

```
_DRB2: [USER2. TULAI. HYBRID]LIST. COM;3                    11-MAR-1986 15:

$ !Command procedure to list the variables
$ !in the variable data base
$ !
$ !  Use:  @LIST
$ !
$   RUN [FTS]VARLIS
       HYMODEL. DAT
       HYMODEL. LIS
$   PRINT/NOFLAG_PAGE/HEADER HYMODEL. LIS
$ ! DELETE HYMODEL. LIS. *
$ EXIT
```

```
_DRB2: [USER2. TULAI. HYBRID]START. COM;2                    15-JAN-1986 1

!PROCEDURE TO CREATE A STANDARD VARIABLE DATA BASE
$ RUN [FTS]VARSET
    HYMODEL. RUL
    HYMODEL. DAT
$ ASSIGN/USER_MODE TT SYS$INPUT
$ EXIT
```

```
! ROUTINE TO MOVE ALL THE MODULES OF A MODEL
! TO THE HYBRID VERSION OF THE STANDARD MODEL
!
!    USE:   @SWITCH
!
$ COPY *. PRE [TULAI. HYBRID]*. PRE
$ COPY *. DAT [TULAI. HYBRID]*. DAT
$ RENAME [TULAI. HYBRID]DIGMODEL. DAT [TULAI. HYBRID]HYMODEL. DAT
$ COPY DIGMODEL. OLB [TULAI. HYBRID]HYMODEL. OLB
$ COPY *. FOR [TULAI. HYBRID]*. FOR
$ SET DEFAULT [TULAI. HYBRID]
$ TIDY
$ EXIT
```

_DRB2: [USER2. TULAI. HYBRID]TIDY. COM; 3 15-JAN-1986 14:

```
! TIDY.COM
! Routine to clean up the files
!
$   PU
$   DELETE *.OBJ.*
$   EXIT
```

```
_DRB2: [USER2. TULAI. HYBRID]TRY. COM; 5                                    25-FEB-1986 16:

!TRY. COM
!A procedure to preprocess, compile, link and
!execute a user's hybrid module using the
!standard model architecture
!                                  reg May83 Updated 7Dec83
!      Use:  @TRY MODULE
!
!The string  'MODULE' is used with the files and extensions
!listed below to create or access the user's files.
!
!If  P1  is blank, user asked to try again
!
!The following naming convention is assumed and used
!        HYMODEL. RUL -- preprocessor rules to be used -- created by user
!        HYMODEL. DAT -- model variables and rules -- created by START
!        'MODULE'. PRE -- module source-file -- created by user
!        HYMODEL. LIS -- list of model variables -- created by LIST
!        'MODULE'. FOR -- Fortran file created by preprocessor
!        'MODULE'. OBJ -- object file of compiled module
!        HYMODEL. OLB -- library of previous modules -- maintained by UPDATE
!        HYMAIN. EXE -- executable image of whole model
!
$!SET NOVERIFY
$        IF P1. NES. "" THEN GOTO DONE
$        WRITE SYS$OUTPUT "Include module name and try again"
$EXIT
$DONE:   CURMODULE:=='P1'
$!Establish the right file state
$        CLOSE HYINPUT
$        DELETE HYCMDS. DAT. *
$        WRITE SYS$OUTPUT "Preprocessing ''CURMODULE'  "
$!Create the dialogue file
$        OPEN/WRITE HYINPUT HYCMDS. DAT
$        WRITE HYINPUT "HYMODEL. DAT"
$        WRITE HYINPUT "''CURMODULE'. PRE"
$        WRITE HYINPUT "''CURMODULE'. FOR"
$        CLOSE HYINPUT
$!Start the preprocessing
$        OPEN/READ HYINPUT HYCMDS. DAT
$        ASSIGN/USER_MODE HYINPUT SYS$INPUT
$        RUN [FTS]VARTRY
$!Compile the module
$        WRITE SYS$OUTPUT "Compiling ''CURMODULE' "
$        FORTRAN 'CURMODULE'. FOR
$!Link everything together
$        WRITE SYS$OUTPUT "Linking whole model together"
$        LINK [ROLAND. HYBRID]RHYMAIN. BAK, []'CURMODULE'. OBJ, HYMODEL/LIB, -
            [ROLAND. HYBRID]HYLIB/LIB, HYSTUB/LIB, -
            SYS$INPUT: /OPTION
            HYBRID/SHARE
$        ASSIGN/USER_MODE TT:  SYS$INPUT:
$!Now run the image
$        WRITE SYS$OUTPUT "Here we GO!!"
$        WRITE SYS$OUTPUT ""
$        RUN RHYMAIN
$        EXIT
```

```
!UPDATE. COM
!A procedure to preprocess and compile a module
! and update the model library which may contain
! previous versions of the module as well as other
! previously debugged modules.
!
!     Use: @UPDATE MODULE
!
!The string  'MODULE' is used with the files and extensions
!listed below to create or access the user's files.
!
!
!The following naming convention is assumed and used
!       HYMODEL. DAT -- model variables and rules created by START
!       'MODULE'. PRE -- module source-file created by user
!       'MODULE'. FOR -- Fortran file created by preprocessor
!       'MODULE'. OBJ -- object file for compiled module
!       HYMODEL. OLB -- library of previous modules, maintained by UPDATE
!
$SET NOVERIFY
$       IF P1. NES. "" THEN GOTO DONE
$       WRITE SYS$OUTPUT "Include module name and try again"
$EXIT
$DONE:  CURMODULE: =='P1'
!Establish the right file state
$       CLOSE HYINPUT
$       DELETE HYCMDS. DAT. *
$       WRITE SYS$OUTPUT "Preprocessing ''CURMODULE'  "
!Create the dialogue file
$       OPEN/WRITE HYINPUT HYCMDS. DAT
$       WRITE HYINPUT "HYMODEL. DAT"
$       WRITE HYINPUT "''CURMODULE'. PRE"
$       WRITE HYINPUT "''CURMODULE'. FOR"
$       CLOSE HYINPUT
!Start the preprocessing
$       OPEN/READ HYINPUT HYCMDS. DAT
$       ASSIGN/USER_MODE HYINPUT SYS$INPUT:
$       RUN [FTS]VARPRE
$!Compile the module
$       WRITE SYS$OUTPUT "Compiling ''CURMODULE' "
$       FORTRAN 'CURMODULE'. FOR
$!Add the module to the library
$       LIBRARY HYMODEL. OLB 'CURMODULE'. OBJ
$       ASSIGN/USER_MODE TT: SYS$INPUT:
$       WRITE SYS$OUTPUT "Module ''CURMODULE' added to model library"
$       EXIT
```

_DRB2: [USER2. TULAI. HYBRID]RAO1DA. DAT; 15 3-APR-1986 2

** SHIP RAO FOR C4S1A IN LIGHT LOADING CONDITION AND QUARTERING SEA 5. 3. 86 **

8
. 0, . 6, . 375, . 6, . 5, . 4, . 7, . 21, . 82, . 03, 1. , . 07, 1. 3, . 0, 20. , . 0

9
. 0, . 64, . 4, . 64, . 56, . 54, . 7, . 3, 1. , . 04, 1. 1, . 0, 1. 3, . 03, 1. 5, . 0, 20. , . 0

8
. 0, . 95, . 35, . 95, . 5, . 75, . 66, . 5, . 82, . 16, 1. , . 23, 1. 35, . 0, 20. , . 0

8
. 0, . 0, . 3, . 0, . 58, 4. 3, . 68, 2. 2, 1. , . 2, 1. 2, . 3, 1. 35, . 0, 20. , . 0

9
. 0, . 0, . 2, . 0, . 72, . 75, 1. , . 22, 1. 1, . 25, 1. 35, . 0, 1. 4, . 1, 1. 5, . 0, 20. , . 0

7
. 0, . 0, . 2, . 0, . 6, . 3, . 7, . 3, 1. , . 08, 1. 25, . 0, 20. , . 0

```
_DRB2: [USER2. TULAI. HYBRID]RAO2DA. DAT; 6                    3-APR-1986 2C

** SHIP RAO FOR LCU-1610 IN LIGHT LOADING CONDITION AND QUARTERING SEA 9. 3. 86 **
4
. 0, 1. 6, . 21, . 78, 1. 3, . 0, 20. , . 0
7
. 0, 1. 5, . 25, . 7, . 4, . 56, . 64, . 48, 1. 1, . 15, 1. 5, . 0, 20. , . 0
10
. 0, 1. , . 32, 1. , . 5, . 96, . 75, . 91, 1. 16, . 75, 1. 32, . 4, 1. 5, . 1, 2. 25, . 32, 2. 8, . 0, 20. , . 0
5
. 0, . 0, . 5, . 17, 1. 0, . 35, 1. 75, . 0, 20. , . 0
9
. 0, . 0, . 3, . 3, 1. 65, 2. 57, 1. 83, . 3, 2. 25, . 85, 2. 66, . 2, 2. 75, . 25, 3. 1, . 0, 20. , . 0
8
. 0, 1. 4, . 21, . 55, . 4, . 47, . 63, . 45, 1. , . 5, 1. 5, . 22, 2. 25, . 0, 20. , . 0
```

```
      DIMENSION XDATA(20),YDATA(20)
C                                                    22 October 85 Rev.1
      DIMENSION ISTR1(8),ISTR2(11),ISTR3(18)
      REAL RDRAO(2,10,6)
      CHARACTER TXRAO(100)
      DATA ISTR1/86,69,83,83,69,76,32,49/
      DATA ISTR2/83,85,82,71,69,32,91,109,47,109,93/
      DATA ISTR3/82,65,68,73,65,78,83,32,80,69,82,32,83,69,67,79,
     @ 78,68/
      OPEN(UNIT=1,NAME='RAO1DA.DAT',TYPE='OLD')
      READ(1,100)TXRAO
      N = 1
      DO 10 J = 1,N
        DO 5 K = 1,20
          XDATA(K) = .0
          YDATA(K) = .0
    5   CONTINUE
        READ(1,*)NPOINT
        XDATA(1)=NPOINT
        YDATA(1)=NPOINT
        READ(1,*)(XDATA(I+1),YDATA(I+1),I=1,NPOINT)
   10 CONTINUE
      CALL OUTPUT('HPPLOT','PLOT.DAT',8)
      CALL INITT(960)
      CALL BINITT
      CALL SLIMX(250,900)
      CALL CHECK(XDATA,YDATA)
      CALL DSPLAY(XDATA,YDATA)
      CALL MOVABS(180,740)
      CALL HLABEL(11,ISTR2)
      CALL MOVABS(518,740)
      CALL HLABEL(8,ISTR1)
      CALL MOVABS(600,60)
      CALL HLABEL(18,ISTR3)
      CALL FINITT(0,0)
      CALL TRNSLT(IERR)
      IF(IERR.NE.0)WRITE(6,200)IERR
      STOP
  200 FORMAT(5X,I10)
  100 FORMAT(100A1)
  300 FORMAT('$>')
  400 FORMAT(I1)
      END
```

Program variables in HY file

Var	Type	Mode	Equivalence	
IDNFLS	V	INTEGER	IDATA	8
IDNFR	V	INTEGER	IDATA	7
IDNFRS	V	INTEGER	IDATA	9
IDNPT	A	INTEGER	IDATA	1
LVFLAG	A	LOGICAL	LMODEL	1
NAADC	V	INTEGER	NADEV	1
NADAC	V	INTEGER	NADEV	2
NASPT1	V	INTEGER	NADEV	3
RCAE	V	REAL	RCOEFF	83
RCC2	V	REAL	RCOEFF	62
RCCD	V	REAL	RCOEFF	84
RCDZBO	V	REAL	RCOEFF	35
RCDZCO	V	REAL	RCOEFF	39
RCFRAC	A	REAL	RCOEFF	45
RCG	V	REAL	RCOEFF	37
RCGC	A	REAL	RCOEFF	1
RCGC1	V	REAL	RCOEFF	78
RCGC2	V	REAL	RCOEFF	79
RCGD1	A	REAL	RCOEFF	42
RCGDIF	V	REAL	RCOEFF	61
RCGFMX	V	REAL	RCOEFF	66
RCGPMX	V	REAL	RCOEFF	65
RCHD2	A	REAL	RCOEFF	32
RCHS	V	REAL	RCOEFF	4
RCKC	V	REAL	RCOEFF	75
RCKCD	V	REAL	RCOEFF	85
RCKDB	V	REAL	RCOEFF	59
RCKDC	V	REAL	RCOEFF	60
RCKEI	V	REAL	RCOEFF	80
RCKP	V	REAL	RCOEFF	68
RCKSB	V	REAL	RCOEFF	38
RCKSC	V	REAL	RCOEFF	40
RCMB	V	REAL	RCOEFF	58
RCMFSC	V	REAL	RCOEFF	63
RCML	V	REAL	RCOEFF	36
RCMPC	V	REAL	RCOEFF	64
RCMSCV	V	REAL	RCOEFF	67
RCOD10	A	REAL	RCOEFF	17
RCOD1V	A	REAL	RCOEFF	20
RCOD20	A	REAL	RCOEFF	23
RCOD2V	A	REAL	RCOEFF	26
RCOLO	A	REAL	RCOEFF	8
RCOLVO	A	REAL	RCOEFF	14
RCOQ	A	REAL	RCOEFF	29
RCOTO	A	REAL	RCOEFF	55
RCOTLO	A	REAL	RCOEFF	5
RCOTVO	A	REAL	RCOEFF	11
RCSCO	V	REAL	RCOEFF	41
RCTAUC	V	REAL	RCOEFF	86
RCTAUD	V	REAL	RCOEFF	87
RCTD	V	REAL	RCOEFF	69
RCTFF	V	REAL	RCOEFF	81
RCTI	V	REAL	RCOEFF	70
RCTK	V	REAL	RCOEFF	73
RCTK1	V	REAL	RCOEFF	72
RCTL	V	REAL	RCOEFF	71

RCTN	V	REAL	RCOEFF	74
RCTT3	V	REAL	RCOEFF	77
RCVA	V	REAL	RCOEFF	76
RCZSP	V	REAL	RCOEFF	82
RDA	A	REAL	RDATA	140
RDA1	A	REAL	RDATA	230
RDA2	A	REAL	RDATA	284
RDFR	A	REAL	RDATA	131
RDFRE	A	REAL	RDATA	122
RDFRE1	A	REAL	RDATA	212
RDFRE2	A	REAL	RDATA	221
RDMO	V	REAL	RDATA	121
RDPHAS	A	REAL	RDATA	194
RDPHS1	A	REAL	RDATA	338
RDPHS2	A	REAL	RDATA	347
RDRAO	A	REAL	RDATA	1
RDRWA	A	REAL	RDATA	203
RSD21V	V	REAL	RSCALE	34
RSD22V	V	REAL	RSCALE	35
RSDZB	V	REAL	RSCALE	45
RSDZC	V	REAL	RSCALE	50
RSEH	V	REAL	RSCALE	9
RSEH2	V	REAL	RSCALE	27
RSEI	V	REAL	RSCALE	60
RSEV	V	REAL	RSCALE	10
RSEV2	V	REAL	RSCALE	28
RSFDB	V	REAL	RSCALE	58
RSFDC	V	REAL	RSCALE	59
RSFSB	V	REAL	RSCALE	49
RSFSC	V	REAL	RSCALE	8
RSFSCX	V	REAL	RSCALE	54
RSFSCY	V	REAL	RSCALE	57
RSH	V	REAL	RSCALE	26
RSMOT	V	REAL	RSCALE	30
RSMSL	V	REAL	RSCALE	31
RSOD2	A	REAL	RSCALE	20
RSOD2V	A	REAL	RSCALE	23
RSOL	A	REAL	RSCALE	1
RSOLV	A	REAL	RSCALE	42
RSOT	A	REAL	RSCALE	14
RSOT1	V	REAL	RSCALE	32
RSOT2	V	REAL	RSCALE	33
RSOTL	A	REAL	RSCALE	36
RSOTLV	A	REAL	RSCALE	39
RSOTV	A	REAL	RSCALE	17
RSPC	V	REAL	RSCALE	29
RSSC	V	REAL	RSCALE	6
RSSCV	V	REAL	RSCALE	7
RSTLX	V	REAL	RSCALE	4
RSTLY	V	REAL	RSCALE	5
RSTPC1	V	REAL	RSCALE	11
RSTPC2	V	REAL	RSCALE	12
RSTPC3	V	REAL	RSCALE	13
RSVLX	V	REAL	RSCALE	55
RSVLY	V	REAL	RSCALE	56
RSVZB	V	REAL	RSCALE	48
RSVZB1	V	REAL	RSCALE	46
RSVZC	V	REAL	RSCALE	53
RSVZC1	V	REAL	RSCALE	51
RSY2BM	V	REAL	RSCALE	47

RSY2CM	V	REAL	RSCALE	52
RVA	A	REAL	RMODEL	2
RVADER	A	REAL	RMODEL	23
RVBUMP	V	REAL	RMODEL	93
RVCT	A	REAL	RMODEL	11
RVDER	A	REAL	RMODEL	17
RVDTIM	V	REAL	RMODEL	91
RVEH	V	REAL	RMODEL	57
RVEH2	V	REAL	RMODEL	56
RVEHS	V	REAL	RMODEL	50
RVEHS2	V	REAL	RMODEL	51
RVEV	V	REAL	RMODEL	59
RVEV2	V	REAL	RMODEL	58
RVEVS	V	REAL	RMODEL	54
RVEVS2	V	REAL	RMODEL	55
RVEVXS	V	REAL	RMODEL	52
RVEVYS	V	REAL	RMODEL	53
RVFSC	V	REAL	RMODEL	45
RVFSCX	V	REAL	RMODEL	42
RVFSCY	V	REAL	RMODEL	46
RVFSCZ	V	REAL	RMODEL	60
RVGAMA	V	REAL	RMODEL	1
RVH	V	REAL	RMODEL	89
RVMOT	V	REAL	RMODEL	62
RVMSL	V	REAL	RMODEL	61
RVOD1	A	REAL	RMODEL	78
RVOD1V	A	REAL	RMODEL	81
RVOD2	A	REAL	RMODEL	36
RVOD2V	A	REAL	RMODEL	39
RVOG	A	REAL	RMODEL	63
RVOLL3	V	REAL	RMODEL	92
RVOG	A	REAL	RMODEL	84
RVOT	A	REAL	RMODEL	14
RVOTV	A	REAL	RMODEL	32
RVPC	V	REAL	RMODEL	48
RVQH	A	REAL	RMODEL	69
RVSC	V	REAL	RMODEL	44
RVSCV	V	REAL	RMODEL	49
RVTIME	V	REAL	RMODEL	35
RVTLX	V	REAL	RMODEL	43
RVTLY	V	REAL	RMODEL	47
RVTPC	A	REAL	RMODEL	75
RVV	V	REAL	RMODEL	90
RVV1	V	REAL	RMODEL	88
RVV2	V	REAL	RMODEL	87
RVWH	V	REAL	RMODEL	94
SVBUMP	V	REAL	SAADC	2
SVD21V	V	REAL	SADAC	19
SVD22V	V	REAL	SADAC	20
SVEH	V	REAL	SAADC	8
SVEH2	V	REAL	SADAC	12
SVEHS	V	REAL	SADAC	8
SVEHS2	V	REAL	SADAC	9
SVEV	V	REAL	SAADC	9
SVEV2	V	REAL	SADAC	13
SVEVS	V	REAL	SADAC	10
SVEVS2	V	REAL	SADAC	11
SVFSC	V	REAL	SAADC	7
SVFSCX	V	REAL	SADAC	6
SVFSCY	V	REAL	SADAC	7

SVH	V	REAL	SADAC	1
SVMOT	V	REAL	SADAC	15
SVMSL	V	REAL	SADAC	16
SVOD23	V	REAL	SADAC	3
SVOD2V	V	REAL	SADAC	5
SVOLL3	V	REAL	SAADC	1
SVOM	V	REAL	SMODEL	1
SVOT1	V	REAL	SADAC	17
SVOT2	V	REAL	SADAC	18
SVOT3	V	REAL	SADAC	2
SVOTV3	V	REAL	SADAC	4
SVPC	V	REAL	SADAC	14
SVROLL	V	REAL	SADAC	21
SVSC	V	REAL	SAADC	5
SVSCV	V	REAL	SAADC	6
SVSM	V	REAL	SMODEL	2
SVTLX	V	REAL	SAADC	3
SVTLY	V	REAL	SAADC	4
SVTPC1	V	REAL	SAADC	10
SVTPC2	V	REAL	SAADC	11
SVTPC3	V	REAL	SAADC	12

Equivalences to NADEV

NAADC	1
NADAC	2
NASPT1	3

Equivalences to SMODEL

SVOM	1
SVSM	2

Equivalences to LMODEL

LVFLAG	1

Equivalences to RMODEL

RVGAMA	1
RVA	2
RVCT	11
RVOT	14
RVDER	17
RVADER	23
RVOTV	32
RVTIME	35
RVOD2	36
RVOD2V	39
RVFSCX	42
RVTLX	43
RVSC	44
RVFSC	45
RVFSCY	46
RVTLY	47
RVPC	48
RVSCV	49
RVEHS	50
RVEHS2	51

RVEVXS	52
RVEVYS	53
RVEVS	54
RVEVS2	55
RVEH2	56
RVEH	57
RVEV2	58
RVEV	59
RVFSCZ	60
RVMSL	61
RVMOT	62
RVOG	63
RVGH	69
RVTPC	75
RVOD1	78
RVOD1V	81
RVOG	84
RVV2	87
RVV1	88
RVH	89
RVV	90
RVDTIM	91
RVOLL3	92
RVBUMP	93
RVWH	94

Equivalences to RDATA

RDRAO	1
RDMO	121
RDFRE	122
RDFR	131
RDA	140
RDPHAS	194
RDRWA	203
RDFRE1	212
RDFRE2	221
RDA1	230
RDA2	284
RDPHS1	338
RDPHS2	347

Equivalences to RCOEFF

RCGC	1
RCHS	4
RCOTLO	5
RCOLO	8
RCOTVO	11
RCOLVO	14
RCOD1O	17
RCOD1V	20
RCOD2O	23
RCOD2V	26
RCOG	29
RCHD2	32
RCDZBO	35
RCML	36
RCG	37
RCKSB	38

RCDZCO	39
RCKSC	40
RCSCO	41
RCGD1	42
RCFRAC	45
RCOTO	55
RCMB	58
RCKDB	59
RCKDC	60
RCGDIF	61
RCC2	62
RCMFSC	63
RCMPC	64
RCGPMX	65
RCGFMX	66
RCMSCV	67
RCKP	68
RCTD	69
RCTI	70
RCTL	71
RCTK1	72
RCTK	73
RCTN	74
RCKC	75
RCVA	76
RCTT3	77
RCGC1	78
RCGC2	79
RCKEI	80
RCTFF	81
RCZSP	82
RCAE	83
RCCD	84
RCKCD	85
RCTAUC	86
RCTAUD	87

Equivalences to RSCALE

RSOL	1
RSTLX	4
RSTLY	5
RSSC	6
RSSCV	7
RSFSC	8
RSEH	9
RSEV	10
RSTPC1	11
RSTPC2	12
RSTPC3	13
RSOT	14
RSOTV	17
RSOD2	20
RSOD2V	23
RSH	26
RSEH2	27
RSEV2	28
RSPC	29
RSMOT	30
RSMSL	31

RSOT1	32
RSOT2	33
RSD21V	34
RSD22V	35
RSOTL	36
RSOTLV	39
RSOLV	42
RSDZB	45
RSVZB1	46
RSY2BM	47
RSVZB	48
RSFSB	49
RSDZC	50
RSVZC1	51
RSY2CM	52
RSVZC	53
RSFSCX	54
RSVLX	55
RSVLY	56
RSFSCY	57
RSFDB	58
RSFDC	59
RSEI	60

Equivalences to IDATA

IDNPT	1
IDNFR	7
IDNFLS	8
IDNFRS	9

Library and Information Centre / Centre de documentation (GSLA)
RECEIVED - REÇU LE
JUL 18 1986
Transport Canada / Transports Canada